Insights from NMR metabolomics into plant responses to environmental stress

Ph.D. thesis

Anna Mascellani Bergo

Insights from NMR metabolomics into plant responses to environmental stress

Ph.D. thesis

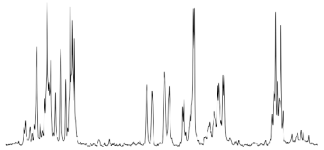

Anna Mascellani Bergo

1st edition

Insights from NMR metabolomics into plant responses to environmental stress

Czech University of Life Sciences Prague, Kamýcká 129, 165 00 Praha – Suchdol, Czech Republic
ISBN: 978-80-213-3291-1

Cover design and layout: Anna Leidenfrost | www.anna-leidenfrost.de
Illustrations: Anna Leidenfrost | www.anna-leidenfrost.de
Graphics: Anna Mascellani Bergo

Printing and binding: Tribun EU s.r.o., Cejl 892/32, 602 00 Brno, Czech Republic

This research was conducted under the "Zemědělská chemie" study program with the auspices of Czech University of Life Sciences Prague, Prague, Czech Republic. The research was funded by METROFOOD-CZ research infrastructure project (MEYS Grant No: LM2018100) including access to its facilities, and by the European Regional Development Fund-Project (grant number CZ.02.1.01/0.0/0.0/16_019/0000845).

CZECH UNIVERSITY OF LIFE SCIENCES PRAGUE
Faculty of Agrobiology, Food and Natural Resources
Department of Food Science

Insights from NMR metabolomics into plant responses to environmental stress

Ph.D. thesis

Author: **Anna Mascellani Bergo**

Supervisor: **Jaroslav Havlik, Ph.D.**

Co-supervisors: **Kirsten Leiss, Ph.D.,**
Petr Marsik, Ph.D.

Prague 2023

To all those who have guided, encouraged and inspired me on this journey.

Anna Mascellani Bergo

Insights from NMR metabolomics into plant responses to environmental stress

Ph.D. thesis, Czech University of Life Sciences Prague, Prague, Czech Republic (2023)

Declaration
I declare that given Ph.D. thesis is solely my own work unless otherwise referenced or acknowledged.

Prague, August 20, 2023

.....
Anna Mascellani Bergo

Abstract

Nuclear magnetic resonance (NMR) spectroscopy is a valuable approach for quantifying plant metabolites and monitoring metabolic changes. Using this technique, significant plant metabolite changes emerge, with the advantages of a non-destructive, high-throughput and reproducible method that excels in structure elucidation. A curated set of 30–60 molecules with high physiological relevance can outperform datasets based on mass spectrometry, which often contain thousands of provisionally identified features, when it comes to classification and biological interpretation. This thesis is based on a comprehensive and original literature review and three original scientific papers with robust design and clear output for agricultural practice, where NMR has been used to tent metabolic changes associated with biotic and abiotic stress.

In the last two decades, NMR metabolomics was limitedly chosen for assessing plant responses to biotic stress, although resistance mechanisms are detectable and clear.

Our research has shown that polyketides in gerbera are biomarkers of resistance to powdery mildew. Gerberinside emerged as the key compound involved in resistance detection; when its level was low, higher levels of gerberin and parasorboside contributed to the resistance. Furthermore, a new compound probably involved in resistance, 5-hydroxyhexanoic acid 3-*O*-*β*-D-glucoside, was described.

Maize overcomes the stress caused by the accumulation of carbamazepine with notable metabolic changes at the early phenological stage, including decreased photosynthesis and water potential, increased carotenoid levels, decreased carbohydrate levels (glucose and fructose) and *γ*-aminobutyric acid in roots, as well as increased maleic acid and phenylpropanoid (chlorogenic acid and its isomer, 5-*O*-caffeoylquinic acid) levels in aboveground biomass, whereas older plants adapt and only display minor effects.

Salinity stress affects the expression of key sugar metabolism and transport genes, as well as the soluble carbohydrate content of ripe fig fruits. A general increase in the transcript levels of genes involved in the transport of soluble carbohydrates was observed. *Alkaline-neutral* and *Acid Invertases* transcripts, related to the synthesis of glucose and fructose, were up-regulated in ripe fruits of NaCl-stressed plants without a change in the content of glucose and fructose. The increases in sucrose and sorbitol contents were likely the result of the up-regulation of the transcription of sucrose synthase- and sorbitol dehydrogenase-encoding genes.

The thesis concludes by pointing out the peculiarities of NMR-based metabolomics in plant science and presenting prospects for the technique.

Abstrakt

Spektroskopie nukleární magnetická rezonance (NMR) je cenným přístupem pro identifikaci a kvantifikaci metabolitů a sledování metabolických změn v rostlinách, přičemž jejími výhodami jsou nedestruktivita, vysoká výkonost a reprodukovatelnost. Technika navíc umožnuje i určení struktury. Dobře vybraný soubor 30-60 molekul s vysokou relevancí pro fyziologii rostlin může v klasifikaci a významu pro biologickou interpretaci předčit data pocházející z hmotnostní spektrometrie, které obsahují až tisíce sloučenin, ovšem často nepřesně identifikovaných. Práce krom literárního přehledu obsahuje i tři originální vědecké práce s robustním designem a jasným výstupem pro praxi popisující využití NMR ke stanovení metabolických změn souvisejících s biotickým a abiotickým stresem.

V posledních dvou dekádách byla NMR metabolomika ke studiu rostlinného stresu využívána jen velmi omezeně, přestože se jedná o metodu poskytující jasné odpovědi a vhled do souvislostí.

Náš výzkum ukázal, že polyketidy jsou látky v gerberách s jasným vlivem na odolnosti vůči padlí a jsou využitelné i jako biomarkery rezistence. Jedním z těchto biomarkerů byl gerberinsid, pokud ho rostlina neměla dostatek, mohly účinek doplňovat vyšší hladiny gerberinu a parasorbosidu. Byla izolována a popsána nová sloučenina, která se pravděpodobně podílí na rezistenci, kyselina 5-hydroxyhexanová 3-*O*-β-D-glukosid.

Zjistili jsme, že kukuřice reaguje v rané fenologické fázi na stres způsobený akumulací farmaceutika karbamazepinu metabolickými změnami, včetně snížení fotosyntézy a vodního potenciálu, zvýšení karotenoidů, snížení sacharidů (glukózy a fruktózy) a kyseliny γ-aminomáselné v kořenech a zvýšení kyseliny maleinové a fenylpropanoidů (kyseliny chlorogenové a jejího izomeru, kyseliny 5-*O*-kafeoylchinové) v nadzemní biomase; zatímco starší rostliny vykazují pouze mírné reakce.

Stres způsobený zasolením ovlivňuje expresi klíčových genů pro metabolismus a transport cukrů a také obsah rozpustných sacharidů v plodech fíků. Bylo pozorováno celkové zvýšení hladin transkriptů genů podílejících se na transportu rozpustných sacharidů. Transkripty *Alkalicko-neutrálních* a *Kyselých Invertáz*, které souvisejí se syntézou glukózy a fruktózy, byly ve zralých plodech rostlin stresovaných roztokem NaCl upregulovány, aniž by se změnil obsah glukózy a fruktózy. Obsah sacharózy a sorbitolu se pravděpodobně zvýšil důsledkem zvýšené regulace transkripce genů kódujících sacharózu syntázu a sorbitol dehydrogenázu.

V závěru práce jsou diskutovány důvody omezeného použití NMR ve výzkumu rostlin a jsou představeny perspektivy této techniky.

Table of content

CHAPTER 1

General introduction

Environmental stress and plant metabolome

Environmental stress is the deviation in environmental conditions from species' optima. Stress is defined as an external factor with unfavourable effects on the plant in relation to plant survival, plant reproduction, primary assimilation processes generally related to growth, biomass or crop yield and quality (Taiz and Zeiger, 1991). Plant species have acquired different abilities to overcome stresses. Two types of environmental stresses are encountered by plants, namely abiotic and biotic stress. Abiotic factors or stressors include extremely high and low levels of light, radiation such as UV-B and UV-A, high and low temperatures, drought, flooding, submergence, chemical factors such as heavy metals, metalloids, pH and fertilisers, pollution and gaseous pollutants (ozone, sulphur dioxide), soil type and composition, salinity due to excessive Na^+, deficiency or excess of macro- and micro-nutrients as well as non-essential nutrients, mechanical factors and other less frequently occurring stressors such as breaking of dormancy (Chen and Soltis, 2020). The impacts of abiotic stress on plant growth and development are evident among the emerging ecological impacts of climate change (Ahuja et al., 2010; Nicotra et al., 2010; Gray and Brady, 2016; Pereira, 2016). Biotic stress in plants is caused by living organisms including nematodes, bacteria, viruses, fungi, weeds, arachnids and insects negatively impacting plant reproduction, growth, morphology and yield (Chen and Soltis, 2020).

The concept of stress is closely associated to how plants adapt to an unfavourable environment. Phenotypic and genotypic variations are essential for plants to respond to environmental changes, compete for resources, withstand stresses and evolve over time. Both variations are present and important because they play distinct but interconnected roles (Taiz and Zeiger, 1991). Genotypic variation refers to the genetic diversity and differences among individuals within a species. It arises from factors such as genetic mutations, recombination during sexual reproduction and the random assortment of genes during gamete formation. Genotypic variation contributes to the resilience and adaptability of plant populations by providing a range of genetic traits which can confer advantages in the context of unfavourable environments (Taiz and Zeiger, 1991; Kalisz and Kramer, 2008; Forsman, 2014). Phenotypic variation can be broadly defined as the variation in the appearance of the organism, including a range of morphological, phenological, developmental and biochemical traits that are expressed within and among individual taxa. It provides a range of traits that can confer advantages under different stresses because it allows plants to respond to and thrive in different environments (Taiz and Zeiger, 1991; Kalisz and Kramer, 2008; Forsman,

2014). One genotype can have different phenotypes because it is influenced by environmental factors. Genetic variation is subject to evolution through selection, whereas phenotypic variation resulting from environmental factors is not heritable and therefore cannot be adapted through selection. Adaptations to environmental stress, whether phenotypic or genetic, involve a series of integrated events at genetic, protein and metabolic levels (Figure 1). The plant responses differ based on the phylogenetic allocation, habitat, perennial or seasonal growth, location and previous stress exposure. The principles and means by which plants respond and adapt to unfavourable conditions have been investigated separately, often focusing solely on the cellular, biochemical or molecular level. However, it is important to recognise the interconnected nature of these processes. Furthermore, it should be noted that in nature, multiple stresses often occur simultaneously, adding to the complexity of plant adaptation processes.

Generally, primary and secondary (also known as specialised) metabolites are found in plants. Primary metabolites are involved in several vital life processes across all species and crucial for plant growth and development (Verpoorte et al., 2007; Kumar et al., 2017). They include classes of metabolites such as amino acids, sugars and fatty acids involved in vital functions such as energy production via photosynthesis or osmoprotection in plants under abiotic stress (Verpoorte et al., 2007; Shulaev et al., 2008). Secondary metabolites are typically present in a taxonomically restricted set of plants, although some of them are widely diffused, such as phenolics. They play an essential role in mutualistic interactions, involving the attraction of beneficial organisms such as pollinators, or antagonistic interactions, serving as deterrents against herbivores and pathogens (Pichersky and Gang, 2000; Sirikantaramas et al., 2008). Furthermore, these specialised compounds aid in the adaptation to abiotic stressors such as increased UV-radiation (Ramakrishna and Ravishankar, 2011). Secondary metabolites include nitrogen-containing compounds, terpenes, thiols and phenolic compounds (Wink, 2003; Jamwal et al., 2018; Khare et al., 2020; Li et al., 2020; Yadav et al., 2021). With metabolites being the final metabolic product, metabolomics plays a crucial role in capturing the impact of upstream metabolic regulation, including genes, transcripts and proteins.

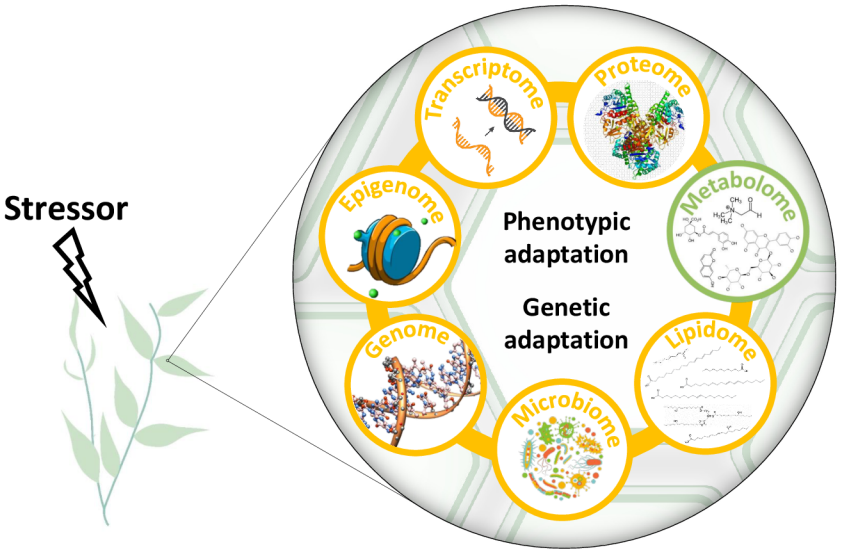

Figure 1 | Schematic representation of the levels where biological changes can occur in plants under environmental stress. One of them (green colour) is the metabolome which is the focus of this Ph.D. thesis.

What is metabolomics

The total set of metabolites in a living organism was first described as "metabolome" by Oliver et al. (1998) in a review article on yeast functional genomics by analogy to genome, transcriptome and proteome. The definition of metabolomics as a comprehensive and quantitative analysis of all metabolites in a living system was given a couple of years later in 2002 in a review article on plant metabolomes (Fiehn, 2002). Earlier, in 1999, Nicholson et al. (1999) referred to "the quantitative measurement of the dynamic multiparametric metabolic response of living systems to pathological stimuli or genetic modification" as "metabonomics" in an application of ^{1}H NMR. In practice, the terms metabolomics and metabonomics are often used interchangeably, and the analytical as well as modelling procedures are the same (Vignoli et al., 2019). Prior to the terminologies established by the European scientific community in the early 2000s, the first steps towards metabolomics took place in the 1960s. During this time, gas chromatography (GC) and GC coupled with mass spectrometry (MS) were developed to quantify metabolites. The development of LC-MS (liquid chromatography coupled to mass spectrometry) systems took approximately 10 years longer than that of GC-MS. Another factor contributing to the advancement and spread of metabolomics was the development of nuclear magnetic resonance (NMR) spectroscopy by the late

1940s and early 1950s. Metabolomics has taken off with chemometrics, a term coined in 1972 by Svante Wold (Wold, 1972). Chemometrics is the discipline which relates measurements performed on a chemical system or process to the state of the system via mathematical or statistical methods (Wold, 1972).
Metabolomics allows the simultaneous detection of a wide range of compounds (Kim et al., 2010), and multiple analytical methods can be applied for metabolomics. Advanced analytical tools, such as GC-MS, LC-MS and NMR, are those most commonly applied in plant science (Patel et al., 2021; Katam et al., 2022). However, other MS-based analytical techniques have sped-up precise metabolic profiling in plants, such as capillary electrophoresis-mass spectrometry (CE-MS), Fourier transform ion cyclotron resonance-mass spectrometry (FTICR-MS), matrix-assisted laser desorption/ionisation (MALDI) and ion mobility spectrometry (IMS) (Patel et al., 2021). Mass spectrometry imaging (MSI) is an attractive technique exploring the metabolic differences directly on living tissues for the comprehensive understanding of how multicellular organisms function (Boughton et al., 2016; Heyman and Dubery, 2016; Dueñas et al., 2019). Another group of analytical methods applied in metabolomics includes vibrational spectroscopy. Among these methods, Fourier-transform infrared spectroscopy (FT-IR) has been extensively applied in metabolomics compared to Raman spectroscopy or near infrared (NIR) spectroscopy (Dunn et al., 2005; Lima et al., 2021).
Depending on the objectives of their studies, researchers have the possibility to select appropriate analytical methodologies for the compounds of interest and flexibility to accordingly choose the metabolomics approach. Overall, there are two approaches for analysing NMR-based metabolomics data: targeted and untargeted. A non-targeted approach aims at a global profiling of the metabolome and is typically employed in hypothesis-generating studies such as biomarker discovery. On the contrary, a targeted approach refers to the quantitative measurement of a select group of metabolites to investigate specific metabolic pathways or to validate biomarkers identified using non-targeted metabolic profiling. Thus, non-targeted metabolomics often provides more information than targeted metabolomics, but targeted metabolomics typically is more quantitative, although it requires *a priori* knowledge (Li et al., 2022).

Metabolomics by NMR spectroscopy

The emphasis of this Ph.D. thesis is on the application of ^{1}H NMR spectroscopy, alternatively known as magnetic resonance spectroscopy (MRS). It is a spectroscopic method based on the measurement of local magnetic fields around atomic nuclei. The basic idea underlying NMR is that if an external magnetic field is applied to nuclei with spin, energy is transferred from the base energy level to a higher energy level. The energy transfer occurs at a wavelength that corresponds to radio frequencies ranging from 4 to 900 MHz, depending on the magnet strength. When the spin returns to its base level, energy at the same frequency is emitted and recorded by sensitive radio receivers. The fact that an NMR signal originates from a tiny fraction of active nuclei is triggering, even if it is the reason of its low sensitivity when compared to other analytical instruments. According to Boltzmann's distribution, for a given external magnetic field of 11.7T (500 MHz), the signal is determined by the population difference between the base energy level and the higher energy level, which is 0.004% of the active nuclei, corresponding to approximately 40 active nuclei per 1 million. The signal corresponding to this transfer is measured and processed to provide an NMR spectrum for the selected nucleus. The intramolecular magnetic field around an atom in a molecule alters the resonance frequency according to the chemical environment, allowing access to detailed specific functional groups in a molecule (Keeler, 2010). Proton and carbon-^{13} NMR spectroscopy are the two most used forms of NMR; however, it may be used with any kind nuclei with a spin, such as phosphorus-^{31}, nitrogen-^{15} and fluorine-^{19}, which have applications in plant science. Protons are primarily used in the application of NMR spectroscopy for metabolomics due to the higher natural isotope abundance compared to carbon-^{13}. The aim to generate identifiable signals from as many metabolites as possible nicely fits with the fact that molecules of biological interest contain hydrogen. The technique has advantages and limitations when compared to other major applied analytical methods for metabolomics (Table 1). According to previous studies, NMR spectroscopy can identify and quantify compounds quickly and reproducibly, with little sample preparation (Allwood et al., 2008; Verpoorte et al., 2008; Kim et al., 2010). In comparison with most common analytical metabolomics techniques, NMR is characterised by its high reproducibility. Throughout the years, chromatographic methods and mass spectrometry have shown to be affected by intra- and inter-day variability and inconsistency in reproducing the same results in another laboratory. On the contrary, NMR is a versatile method that is excellent for large-scale plant metabolomics studies involving numerous laboratories (Ward et

al., 2010a). Unlike chromatographic methods, NMR does not require continual calibration curves for each compound to be quantified but instead can rely on in-house databases (Verpoorte et al., 2007). Also, NMR is non-destructive and well-suited for high-throughput methodology, including the possibility of automation (Vignoli et al., 2019). A 3-minute analysis can provide quantitative data. Despite the limited number of compounds detected in an extract and the lower sensitivity, the major metabolic trends can be determined (Verpoorte et al., 2007). Further, NMR can be well integrated into other spectroscopic or spectrometric techniques to identify metabolites and elucidate their structures (Wolfender et al., 2003; Kim et al., 2010) and is an environmentally friendly method (Mielko et al., 2021). However, it is challenging to equal and outperform MS in terms of sensitivity. Nonetheless, technologies based on cryogenically cooled probes, as well as micro- and superconducting coil probes, have recently been developed, which substantially lowered the detection limit. However, they are not yet widely used and affordable. Another option to increase sensitivity is to combine NMR analysis with an in-line chromatographic separation technique which fractionates and concentrates the mixture before recording, leading to the identification of numerous molecules. The disparity with MS may decrease with the increased use of in-line chromatographic separation steps in NMR, despite the fact that using a smaller number of samples is a strength of MS (Krishnan et al., 2005).

Table 1 | Advantages and disadvantages of major analytical techniques used in MS and NMR metabolomics (Krishnan et al., 2005; Mielko et al., 2021; Patel et al., 2021; Katam et al., 2022).

Analytical method	Advantages	Disadvantages
NMR	• Precise quantification and high reproducibility • Minimal sample preparation required • Chromatographic separation is not required • Provides detailed information about the structure of metabolites • Application with liquid and solid samples • No instrument cleaning • Green analytical method • Suitable for inter-laboratory studies • Low costs per sample • Non destructive	• High investment costs • Low sensitivity • A considerable amount (50-100 mg) of biological material is required. • Inadequate bioinformatics platform • Automation in spectral analysis is limited • Number of detectable metabolites (30-60)
GC-MS	• Suitable for the identification of thermally stable and volatile compounds • Large commercial and public libraries • Identification of low molecular weight metabolites (~500 Daltons) • Identification of volatile metabolites or small molecules upon derivatization • Several separation mechanisms and conditions are available • Potential large number of detectable metabolites (300-3000) • Molecular formula is known • Possibility of high mass resolution, ionisation methods and ion fragmentation (alternative structure info by MS/MS)	• Quantification only with calibration curves • Sample pre-processing and derivatization • Many metabolites are thermally unstable or non-volatile • Instrument cleaning • Use of high amount of carrier gasses • High running costs • High costs per sample • Chromatographic separation is required • Destructive
LC-MS	• No derivatization • Several separation mechanisms and conditions are available • Molecular formula is known • Potential large number of detectable metabolites (300-1000) • Possibility of high mass resolution, ionisation methods and ion fragmentation (alternative structure info by MS/MS)	• Quantification only with calibration curves • Few commercial and public libraries • presence of insource fragmentation and adduct ions • Instrument cleaning • High running costs • Use of high amount of solvents • High costs per sample • Chromatographic separation is required • Destructive • Long sample preparation

CHAPTER 2

Scientific hypothesis and objectives

The central theme of this thesis is the use of ^{1}H NMR-based metabolomics to analyse metabolic changes in plants under various environmental stresses. The objectives of each chapter consist of a series of self-contained studies with independent hypotheses addressing biotic and abiotic stress responses in different plants (Figure 2).

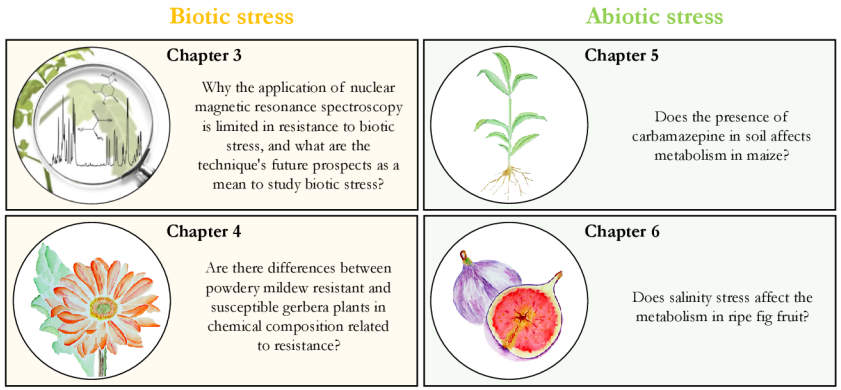

Figure 2 | Schematic outline and research questions pursued in this Ph.D. thesis to assess environmental stress responses in plants using ^{1}H NMR-based metabolomics.

This dissertation consists of seven chapters. **Chapter 1** provides an overview of the plant strategies for coping with stress conditions and highlights the role of metabolomics in detecting metabolic changes. This chapter also presents an outline of analytical techniques enabling such investigations, including the use of NMR spectroscopy; additionally, it offers a general introduction into NMR spectroscopy, comparing its advantages and disadvantages to those of the widely used mass spectrometry. In **Chapter 2**, the research questions pursued throughout this Ph.D. thesis are summarised. **Chapters 3–6** comprise the main chapters of the thesis, constituting my original scientific contributions to research in metabolomics and environmental stress. These chapters delve into the use of ^{1}H NMR to assess chemical changes in plants exposed to biotic and abiotic stress. **Chapters 3** and **4** focus on biotic stresses. I first present an overview of the potential applications of ^{1}H NMR-based metabolomics to study biochemical processes relating plant resistance to biotic stress, post-infection stress responses and plant-host interactions in **Chapter 3**. Additionally, I discuss the advancements required for moving the method forward. **Chapter 3** is focused on biotic stresses because a higher structural diversity of secondary metabolites is involved in responses

to biotic stresses, including alkaloids, terpenoids and saponins, which better demonstrates the power of ^{1}H NMR metabolomics. Moreover, during this work, I felt the need to provide a solid overview of which metabolites have already been annotated in previous works. This review supports the need for shared databases to fully exploit the potentials of NMR metabolomics. In **Chapter 4**, an NMR screening tool for powdery mildew resistance in gerbera was developed, identifying metabolites of constitutive host plant resistance to this pathogen. **Chapters 5** and **6** are dedicated to abiotic stresses. In **Chapter 5**, NMR spectroscopy was used to study the influence on maize metabolism of carbamazepine present in soil due to used of surface waste water and sewage sludge. In **Chapter 6**, we investigated how soil salinity influences fig fruit carbohydrate metabolism and associated gene regulation. Finally, the major results of this Ph.D. thesis are discussed, and the implications of this work on further studies are presented in **Chapter 7**.

The framework of the thesis (**Chapters 3–6**) is based on an array of scientific papers that I either wrote myself or significantly contributed to. My rights to reproduce them as chapters of the thesis are guaranteed by the copyright policies of the publications where the work has been published.

CHAPTER 3

NMR-based plant metabolomics: a way forward towards assessment of plant metabolites for constitutive and inducible defences to biotic stress

Based on a late-stage draft of a manuscript to be submitted to a scientific journal with impact factor.

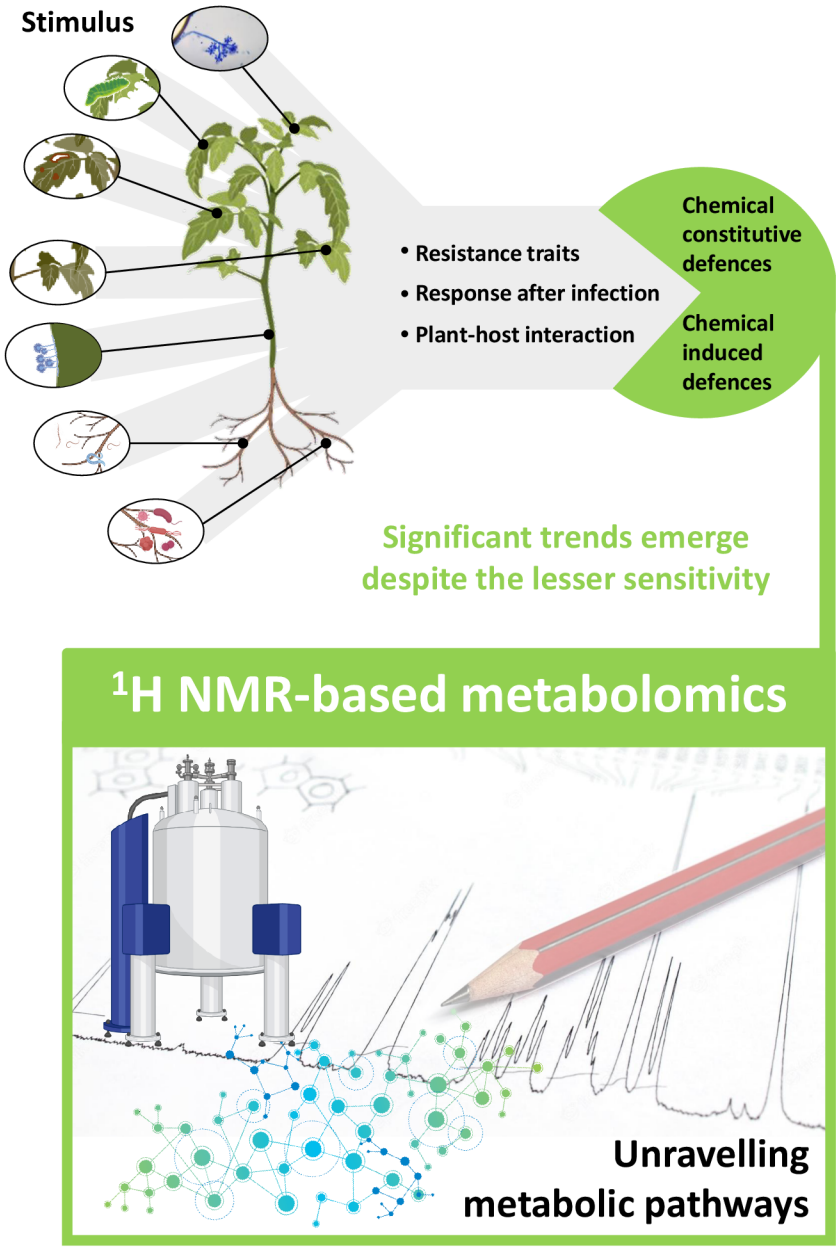

Abstract

Metabolomics is a key tool in plant research to bridge the gap between genotype and phenotype. Insights into the dynamics of metabolic processes involved in the regulation of plant defence mechanisms, including amino acids, carbohydrates, fatty acids, glucosinolates, acyl sugars, phenylpropanoids, terpenoids, saponins and other secondary metabolites, were provided through the application of NMR spectroscopy in 20 years, leading to the understanding of host-plant interactions and their regulations. This work reviews the status and future potential of ^{1}H NMR-based plant metabolomics to address the biochemical processes related to plant resistance to biotic stress, post- infection stress responses and host-plant interactions. The approach is openly and critically evaluated to give newcomers a clear idea of the challenges and benefits of applying NMR in plant metabolomics research. Combining NMR-based metabolomics with other omics approaches can provide a systemic picture of plant metabolism and its regulation, enabling a more efficient crop production, the identification of mechanisms of pathogenesis and the development of strategies for plant disease control.

Keywords: NMR metabolomics; biotic stress; host plant resistance.

Author contribution: I contributed to the current study by conducting the systematic review of the literature. I extracted the important information for each included study and drafted the original manuscript.

Introduction

The use of "omics" techniques (genomics, transcriptomics, proteomics and metabolomics) and their combination in multi-omics investigations have gained popularity in recent decades, expanding our understanding of biological systems at the molecular level. These include metabolomics and the related field of metabonomics, which focuses on using modern techniques to study the totality of metabolites in a given biological system and links chemical patterns to biology (Vignoli et al., 2019). The plant metabolome can be conventionally divided into two classes of metabolites, primary and specialised (comparatively termed secondary) ones, although it is becoming increasingly clear that there is much overlap. Primary metabolites are involved in several vital life processes across all species and crucial for plant growth and development (Verpoorte et al., 2007; Kumar et al., 2017). They include classes of metabolites such as amino acids, sugars and fatty acids involved in vital functions such as glycolysis or osmolytes and osmoprotectants in plants under biotic stress (Verpoorte et al., 2007; Shulaev et al., 2008). Secondary metabolites are typically present in a taxonomically restricted set of plants, although some of them are widely diffused, such as phenolics, and play an essential role in plant survival under various environmental stresses (Ramakrishna and Ravishankar, 2011). Secondary metabolites include nitrogen-containing compounds, terpenes, thiols and phenolic compounds (Wink, 2003; Jamwal et al., 2018; Khare et al., 2020; Li et al., 2020; Yadav et al., 2021). In this context, metabolomics plays a critical role in reflecting the effects of upstream regulation, including genes, transcripts and proteins.

Metabolomics is applied in plant science for various purposes such as phenotyping and diagnostic analysis of plants. Metabolomics studies have provided greater insight into crop biology regarding fruit maturation, quality, yield and nutritional value assessment (Kumar et al., 2017; Litvinov et al., 2021). No less important is the application of metabolomics in plant interactions with the environment (often referred to as environmental metabolomics) and other organisms (Shulaev et al., 2008; Lankadurai et al., 2013; Maag et al., 2015; Chen et al., 2019; Litvinov et al., 2021). To date, increasing attention has been paid to the identification, quantification and characterisation of the remarkable diversity of low-molecular-weight compounds produced by plants for their protection as bioindicators of biochemical events associated with biotic stress (caused by nematodes, bacteria, phytoplasmas, viruses, fungi, weeds, arachnids and insects). Such biological processes usually involve more than one compound, a crucial investigative factor in the diversity of physiological interactions resulting from additional,

if not synergistic, effects.

Even though metabolic alterations driven by biotic stress may be evaluated using a variety of analytical approaches, nuclear magnetic resonance (NMR) spectroscopy offers certain indisputable benefits. This review is focused on the achievements over the last 20 years and the potential of ^{1}H NMR-based metabolomics to study biochemical processes relating plant resistance to biotic stress, post-infection stress responses and plant-host interactions. In its simplest terms, the purpose of this review is to provide a guide for how ^{1}H NMR can and should be used for ecometabolomics. It is also intended to provide a roadmap for future improvements in this rapidly developing field, both regarding technical aspects and defining the metabolite function.

Potential of ^{1}H NMR in plant research

Although multiple analytical techniques can be used to assess simultaneous metabolic changes associated with biotic stress (Patel et al., 2021), NMR spectroscopy has some undeniable advantages, particularly in acquiring high-resolution spectra in a short time and regarding the highly reproducible quantification of compounds with simple and rapid sample preparation (Allwood et al., 2008; Verpoorte et al., 2008; Kim et al., 2010) (Figure 3). Because of the low instrumental variation, technical replicates are not needed (Martins et al., 2018). Moreover, NMR is a versatile tool ideal for large-scale plant metabolomics data collection where multiple laboratories are involved (Ward et al., 2010a). Unlike chromatographic techniques, NMR can rely on internal databases and does not require continuous calibration curves for each compound to be quantified (Verpoorte et al., 2007). It is a highly suitable non-destructive analysis for high-throughput methods, reproducible and inexpensive, including the possibility of automation. Quantitative data may be obtained within as little as 3 minutes (typically 10 minutes) as compared to 30 minutes, on average, for other metabolomic methods. Significant trends emerge despite the lesser sensitivity and limited number of compounds detected in an extract (Verpoorte et al., 2007). Moreover, no other analytical technique achieves the same performance regarding structure elucidation, and it can be easily integrated with other spectroscopic or spectrometric techniques (Wolfender et al., 2003; Kim et al., 2010). The choice of NMR or another metabolomics platform, such as LC-MS or GC-MS (Patel et al., 2021), depends

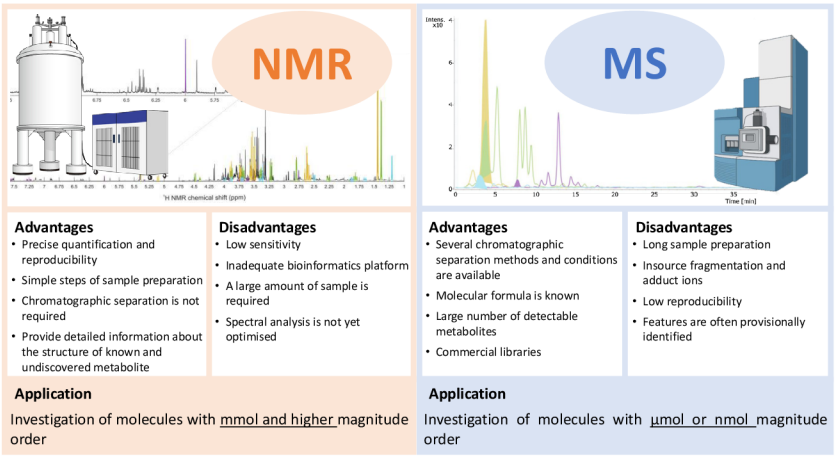

Figure 3 | Summary of advantages, disadvantages, and application of MS- and NMR-based analytical techniques used in metabolomics. NMR and MS spectra represent gerberine (yellow), parasorboside (green), 5-hydroxyhexanoic acid 3-*O*-*β*-D-glucoside (light blue) and gerberinside (purple) in *Gerbera hybrida* (Mascellani et al., 2022). NMR, nuclear magnetic resonance spectroscopy; MS, mass spectrometry. Created with BioRender.com.

on the biological question to be answered. Compared to the other mainstream techniques, the most common drawback of using an NMR-based approach is the low sensitivity (Kim et al., 2010, 2011; Patel et al., 2021). In the field of plant stress metabolomics, the application of NMR is strongly inadvisable when the aim is to study targeted metabolites at low concentration levels (e.g., µmol or nmol magnitude order), such as phytohormones (with the exception of salicylic acid (Choi et al., 2004a)), or volatiles. Therefore, NMR should be preferred for untargeted metabolomics approaches because it gives a good first overview over the compounds involved in plant biotic stress. Possibly, low-concentration metabolites may be missed, although the indication of a range of compounds and the related pathways involved is clear. It is highly suitable for the study of primary metabolites, including amino acids, organic acids and carbohydrates. Another important area for the application of ^{1}H NMR is the study of secondary metabolites in the order of mmols (the limit is dependent on the number of chemically equivalent protons, signal multiplicity and the matrix), including phenylpropanoids, such as chlorogenic acid derivatives, feruloyl derivatives, flavonoids, such as kaempferol or quercetin, glucosinolates, acyl sugars, saponins, alkaloids, polyketides or carotenoids. Table 2 provides an overview of these specific metabolites other than amino acids, carbohydrates and simple organic acids, that have been

identified in plant extracts using ^{1}H NMR spectroscopy. Usually, these metabolites are known for their antifeedant or antimicrobial activity (Wahyuni et al., 2021; Fernandes et al., 2022). The undeniable advantage is the high confidence in metabolite annotation and the possibility to clearly distinguish glycosylated and free forms of secondary metabolites (Table 2), which could be of great interest for the understanding of plant-host interactions. The amount of the available sample could be the only real limitation factor which makes an MS-based approach necessary.

Table 2 | List of metabolites annotated in the 67 reviewed studies, others than those included in the spectral reference libraries 400MHz − 800MHz version 9 of the Chenomx NMR Suite (Chenomx Inc., Edmonton, Canada). These libraries are often used for annotation and is accessible to a wide user community, although not specific to plants. Selection criteria of the literature search were described in Supplementary Table S1.

Chemical superclass	Compound name and references
Indoles	**indole-3-acetic acid** (Abdel-Farid et al., 2009; Simoh et al., 2009; Isha et al., 2019, 2020).
Acyl sugars	**acyl sugars** (Mirnezhad et al., 2010; de Falco et al., 2019).
Saccharides and glycosylic portion	**stachyose** (Leiss et al., 2009a; Cuperlovic-Culf et al., 2016), **rhamnose in rutin** (López-Gresa et al., 2010), **rhamnose in flavonoid** (Choi et al., 2006), **raffinose** (Leiss et al., 2009a), **D-fructofuranose** (Capitani et al., 2013), **D-fructopyranose** (Capitani et al., 2013).
Fatty acids	**hexanoic acid** (Jones et al., 2011), **linoleic acid** (Jones et al., 2011), ***γ*-linoleic acid** (Jones et al., 2011), ***α*-linolenic acid** (Choi et al., 2006; Figueiredo et al., 2008; Leiss et al., 2009b), **fatty acids** (Choi et al., 2006; Mirnezhad et al., 2010; de Falco et al., 2019; Vasmatkar et al., 2019), **steroids** (Choi et al., 2006), **lipid** (Liu et al., 2010; Benheim et al., 2014; Kumar et al., 2016).
Sterols	**phytosterol** (Kumar et al., 2016), ***β*-sitosterol** (Isha et al., 2020).
Carotenoids	***β*-cryptoxanthin** (Isha et al., 2019, 2020).
Tocopherols	***α*-tocopherol** (Isha et al., 2020).
Flavonoids	**flavone derivative** (Leiss et al., 2009b), **kaempferol** (Choi et al., 2006; Widarto et al., 2006; Simoh et al., 2009; Isha et al., 2019, 2020), **kaempferol glycoside** (Leiss et al., 2009b), **kaempferol analogues** (Abdel-Farid et al., 2009), **quercetin** (Choi et al., 2006; Simoh et al., 2009; Benheim et al., 2014; Vasmatkar et al., 2019), **quercetin-3-*O*-glucoside** (Figueiredo et al., 2008; Lima et al., 2010; Ali et al., 2012), **quercetin analogies** (Abdel-Farid et al., 2009), **myricetin** (Ali et al., 2012), **luteolin** (Leiss et al., 2013; Kumar et al., 2016), **rutin** (López-Gresa et al., 2010, 2012; Tomita et al., 2017), **(-)-epicatechin** (Ali et al., 2012; Isha et al., 2020; Pereira et al., 2021), **afzelin** (Sciubba et al., 2020), **kaempferitrin** (Sciubba et al., 2020), **genistein** (Kumar et al., 2016), **flavonoid glucoside** (Leiss et al., 2009a).
Phenolic compounds and precursors	**gallic acid derivatives** (Choi et al., 2004b), **salicylate** (Maravi et al., 2022), **syringic acid** (Ali et al., 2012), **salicin** (Kumar et al., 2016),

Table 2 | Continued.

Chemical superclass	Compound name and references
	4-nitrophenol (Kumar et al., 2016), **shikimic acid** (Figueiredo et al., 2008; Lima et al., 2010; Capitani et al., 2013), **quinic acid** (Capitani et al., 2013; Leiss et al., 2013; Chin et al., 2014; Sciubba et al., 2020).
Phenylpropanoids and precursors	**sinapoyl malate** (Widarto et al., 2006; Abdel-Farid et al., 2009; Simoh et al., 2009), **coumaroyl malate** (Widarto et al., 2006; Abdel-Farid et al., 2009; Simoh et al., 2009), **caffeoyl malate** (Widarto et al., 2006; Abdel-Farid et al., 2009), **feruloyl malate** (Widarto et al., 2006; Abdel-Farid et al., 2009), **5-hydroxyferuloyl malate** (Abdel-Farid et al., 2009), **malic acid conjugated with phenylpropanoids** (Abdel-Farid et al., 2009), **sinapic acid** (Leiss et al., 2013), **caffeic acid** (Figueiredo et al., 2008; Lima et al., 2010; López-Gresa et al., 2010; Srivastava et al., 2012; Benheim et al., 2014; Afifah et al., 2019, 2020; Isha et al., 2019, 2020; Sciubba et al., 2020), **ferulic acid** (López-Gresa et al., 2010), **ferulic acid glucoside** (López-Gresa et al., 2010), **gentisic acid glucoside** (López-Gresa et al., 2010), **3-*O*-caffeoylquinic acid** (Choi et al., 2006; Leiss et al., 2009b, 2009a; Plischke et al., 2012; Capitani et al., 2013; de Falco et al., 2019), **4-*O*-caffeoylquinic acid** (Choi et al., 2006; Plischke et al., 2012), **chlorogenic acid (5-*O*-caffeoylquinic acid)** (Choi et al., 2004b, 2006; Leiss et al., 2009b, 2009a; López-Gresa et al., 2010; Plischke et al., 2012; de Falco et al., 2019; Sabino et al., 2019; Sciubba et al., 2020), **neochlorogenic acid** (Liu et al., 2022), ***trans*-caffeoyl derivatives** (Ali et al., 2012), ***trans*-feruloyl derivatives** (Ali et al., 2012), ***trans*-caftaric acid** (Ali et al., 2012), ***trans*-fertaric acid** (Ali et al., 2012), **caffeoyl esters of polyhydroxy compounds** (López-Gresa et al., 2012), ***p*-coumaric acid** (Maravi et al., 2022), **5-*O*-feruloyl quinic acid** (Leiss et al., 2009b, 2009a), ***trans*-cinnamic acid** (Ali et al., 2012).
Furano lactones	**limonin** (Slisz et al., 2012; Chin et al., 2014), **limonin glucoside** (Slisz et al., 2012; Chin et al., 2014, 2020)
Glucosinolates	**neoglucobrassicin** (Abdel-Farid et al., 2009), **progoitrin** (Abdel-Farid et al., 2009; Simoh et al., 2009), **gluconapin** (Widarto et al., 2006)
Alkaloids	**synephrine** (Slisz et al., 2012; Chin et al., 2014, 2020), **nicotine** (Choi et al., 2006), **vindoline** (Choi et al., 2004b), ***α*-chaconine** (Plischke et al., 2012), ***α*-solanine** (Plischke et al., 2012), **catharanthine** (Choi et al., 2004b), **stemmadenine** (Choi et al., 2004b), **tabersonine** (Choi et al., 2004b)
Terpenoids	**cembratriene-4,6-diol** (Choi et al., 2006), **capsidiol** (Choi et al., 2006), **2-oxopolomic acid** (Hall et al., 2018), **maslinic acid** (Hall et al., 2018), ***cis-p*-coumaroyltormentic acid** (Hall et al., 2018), ***trans-p*-coumaroyltormentic acid** (Hall et al., 2018), **benzoyl ingenol-laurate** (Krstić et al., 2016), ***α*-amyrin decadienoate** (Krstić et al., 2016), ***β*-amyrin decadienoate** (Krstić et al., 2016), ***cis*-1,4-polyisoprene** (Krstić et al., 2016), **24-methylenecycloartanol** (Krstić et al., 2016).
Quinones	**quinone** (Kumar et al., 2016), **jacaranone** (Leiss et al., 2009a).
Saponins	**astragaloside** (Gao et al., 2021).
Polyketides	**gerberine** (Mascellani et al., 2022), **gerberinside** (Mascellani et al., 2022), **parasorboside** (Mascellani et al., 2022),

Table 2 | Continued.

Chemical superclass	Compound name and references
	5-hydroxyhexanoic acid 3-*O*-*β*-D-glucoside (Mascellani et al., 2022).
Others	**orotate** (Kumar et al., 2016), **guanidinoacetate** (Kumar et al., 2016), **nicotinate** (Kumar et al., 2016), **glycine betaine** (Sekiyama et al., 2017; Vasmatkar et al., 2019), **proline betaine (stachydrine)** (Chin et al., 2014, 2020; Ramsey et al., 2020), **2,3 butanediol** (Isha et al., 2020), **dopamine** (Machado et al., 2012), **octopine** (Simoh et al., 2009).

An invaluable tool in the assessment of constitutive and induced defences in plants for biotic stress

Generally, NMR spectroscopy is a valuable approach for identifying and quantifying plant metabolites. The use of ^{1}H NMR for plant metabolomics has been established since 2003 (Bailey et al., 2003) and has been accounting for one third of all metabolomics studies (Katam et al., 2022), although it is an emerging field in omics science. The first reported application to assess biotic stress consisted of metabolic profiling in *Catharanthus roseus* leaves infected with phytoplasma in 2004 (Choi et al., 2004b). A publication using NMR to investigate metabolites involved in constitutive resistance to a *Fusarium* head blight in wheat followed in 2007 (Browne and Brindle, 2007). Since then, NMR has been applied to a range of biochemical processes related to plant resistance to biotic stress, post-infection stress responses, and plant-host interactions, with a total of 67 studies over the last two decades. Part of this review is a systematic review of the literature between 2003 and 2022, finding 67 relevant studies (Figure 4). Studies were included if ^{1}H NMR spectroscopy was used as the analytical technique for metabolomics studies in plants to investigate biochemical processes related to plant resistance to biotic stress, post-infection stress responses, and plant-host interactions; the inclusion criteria are provided in Supplementary Table S1. Of these studies, 76.2% focused on induced chemical changes after bacterial (19.4%), fungal (25.4%) and viral infections (10.4%) as well as insect (13.4%) and nematode attacks (7.4%). Of the remaining studies, 23.8% focused on constitutive chemical defences towards bacteria (2.9%), fungi (8.9%), insects (8.9%) and nematodes (7.4%).

Over the last 5 years, the average publication number was 5.8 studies per year

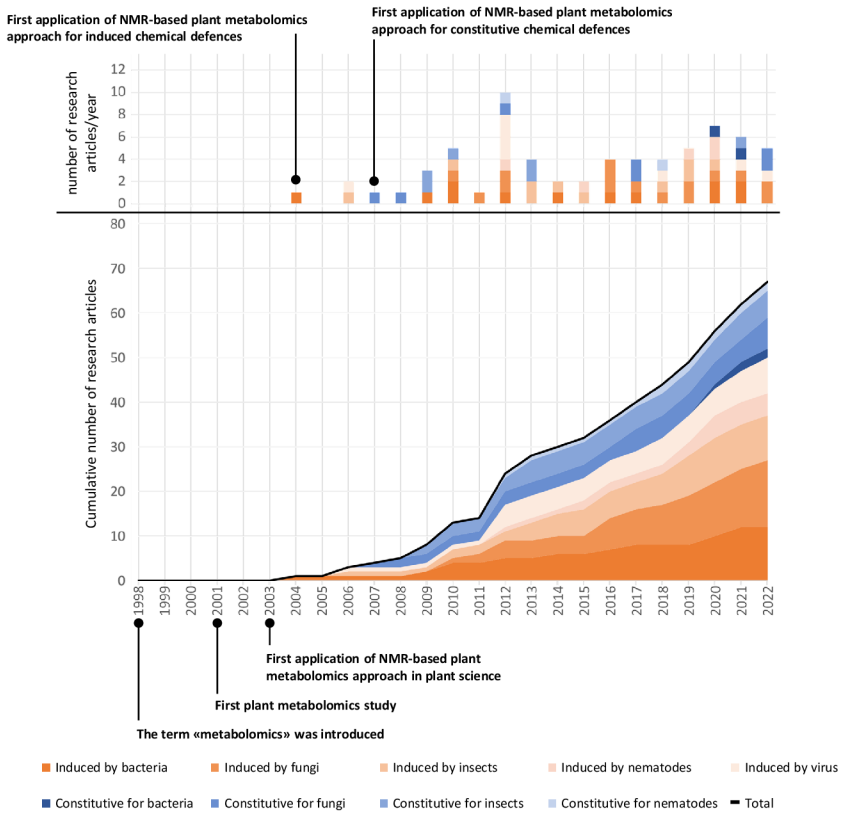

Figure 4 | Historical overview of the application of ^{1}H NMR-based plant metabolomics in research articles about plant responses to biotic stress. The number of publications was determined by using the keywords "NMR", "plant", "metabolomics", "biotic stress" and related synonyms from Scopus (https://www.scopus.com) and Web of Science (https://www.webofknowledge.com). At the time of the search, there were no articles for 2023.

(median: 6 studies/year), suggesting a stagnant application, not fully developed. This may be due to the instrument's limited availability in laboratories (Edison et al., 2021), underlined by the fact that the majority of publications are from the teams which applied the approach for the first time. Another reason could be that the method's capabilities are often underused and unknown to the scientific community and that the studies cover only amino acids and some well-databased compounds, leaving the majority of signals unidentified. An interesting experimental design involves the search for associations between NMR profiles with

bioassays or the simultaneous use of other analytical techniques. Most of the studies are limited to the exclusive use of ^{1}H NMR, with only few including toxicity tests of selected compounds (Machado et al., 2019; Sabino et al., 2019), the monitoring of diseases and physiological parameters (Slisz et al., 2012; Baldacci-Cresp et al., 2015; Krstić et al., 2016; Afifah et al., 2019; Gao et al., 2021) and additional complementary analytical techniques to quantify a fraction of metabolites (López-Gresa et al., 2010; Ward et al., 2010b; Machado et al., 2012; Hall et al., 2018; Jlilat et al., 2021). Multi-omics combination with transcriptomics (quantitative real-time PCR and RNA sequencing), proteomics (LC-MS proteomics with gene onthology enrichment analysis) and metabolomics with the use of other analytical techniques (FT-IR, GC-MS and LC-MS) was limited to five studies (Jones et al., 2011; Kumar et al., 2016; Copley et al., 2017; Su et al., 2018; Vasmatkar et al., 2019).

Chemical induced defences

The interaction between plants and their phytophagous enemies has resulted in a complex network of defences and counter-defences over millions of years (Santamaria et al., 2013). Generally, plant defences can be characterised as constitutive (permanent) or induced (temporary) (Karban and Myers, 1989). Induced defences are only engaged after attacker recognition. Although induced defences allow plants to avoid the costs of establishing defences in the absence of enemies, plants may incur significant harm during the time it takes to develop this defence response in the event of an infestation (Frost et al., 2008). In previous studies, ^{1}H NMR spectroscopy has been extensively applied for monitoring metabolic changes in responses to biotic stress. Different types of small-molecular-weight molecules can be induced by the attack and infection of different organisms. Phenylpropanoids, along with flavonoids, play a biological role in plant signalling and driving plant defence responses. This compound class plays multiple roles, such as a physical or chemical barrier to prevent invasion or a direct toxic weapon against microbial or insect targets (Ramaroson et al., 2022). The levels of gallic acid, caffeic acid, kaempferol and *p*-hydroxybenzoic acid are increased in palm leaves infected with *Ganoderma boninens* (Isha et al., 2019). In other studies, vine infected with Esca disease and *Plasmopara viticola* showed an increase in feruoyl and caffeoyl derivatives, shikimic acid, quercetin glucoside and caffeic acid (Lima et al., 2010; Ali et al., 2012). In a cultivar of chickpea resistant after infection, *F. oxysporum* infection resulted in a rise in the genistein level in the roots, whereas

the susceptible cultivar showed a decrease in the flavonoid luteolin (Kumar et al., 2016). Similarly, *p*-hydroxycinnamic acid and chlorogenic acid concentrations increased in wheat upon inoculation with *Fusarium graminearum* (Liu et al., 2022). Infection of rice with *Magnaporthe grise* increased cinnamic acid levels (Jones et al., 2011), and *Verticillium dahliae* infection in *Arabidopsis thaliana* L. induced the increase in sinigrin and quercetin glucoside levels (Su et al., 2018). Although most studies reported an increase in phenylpropanids, some showed a decrease: sweet orange infected with *Candidatus Liberibacter* spp. showed a decrease in flavones (Pontes et al., 2016). The challenge posed by viruses triggers a similar response to that posed by bacteria, resulting in an elevation in the levels of phenylpropanoids and other phenolic metabolites. In response to viruses, tobacco and tomato synthesised phytoalexins, such as chlorogenic acid and its derivatives (Choi et al., 2006; López-Gresa et al., 2012), whereas tomato specifically produced gentisic acid glycoside in response to *Citrus exocortis viroid* (López-Gresa et al., 2010). Rutin and phenylpropanoid levels were also increased in tomato infected with *Pseudomonas syringae* (López-Gresa et al., 2010). The presence of the nematodes triggered increased levels of chlorogenic acid in coffee (Machado et al., 2012) and caffeic acid in tomato (Afifah et al., 2020). In general, phenolics increased in potato leaves under attack by the aphid *Myzus persicae* (Plischke et al., 2012). Nevertheless, the production of chlorogenic acid, neo-chlorogenic acid and 5-*O*-feruloyl quinic acid was induced in tomato plants infested with the leaf miner *Tuta absoluta* (de Falco et al., 2019). Similarly, the defence mechanisms of grape infested with the insect pest *Daktulosphaira vitifoliae* triggered an increase in caffeic acid, flavonoids and quercetin (Benheim et al., 2014). The production of chlorogenic acids and other phenylpropanoids was induced in *Saccharum officinarum* L. by *Diatraea saccharalis* (Sabino et al., 2019). The Brassicaceae family is characterised by highly specialised secondary metabolites, which can be monitored using ^{1}H NMR spectroscopy. An increase in progoitrin was reported for *Brassica rapa* L. cultivars when exposed to *Leptosphaeria maculans*, *Aspergillus niger* and *F. oxysporum* (Abdel-Farid et al., 2009). Furthermore, an increased level of alkaloids involved in induced plant resistance was reported in *C. roseus* infected with phytoplasmas. The levels of the secoiridoids loganin and secologanin increased in *C. roseus* infected with phytoplasmas (Choi et al., 2004b). Oleuropein in olive trees increased in the presence of the bacterium *Xylella fastidiosa* co-inoculated with xylem-inhabiting fungi (Jlilat et al., 2021). In another study, the response of potato to virus Y was driven by α-chaconine and α-solanine (Plischke et al., 2012). Increases in the saponine 2,4-methylencycloartanol and benzoyl-ingenol-laurate levels and a decrease in *cis*-1,4-polyisoprene in the latex of marsh spurge was observed after attacks by *Fusarium sporotrichioides*, *F. proliferatum* and

Alternaria alternata (Krstić et al., 2016). Interestingly, ^{1}H NMR spectroscopy was capable of detecting changes in ascorbic acid, α-tocopherol and β-cryptoxanthin, involved in induced resistance to *G. boninens* in oil palm and to *Drechslera maydis* in corn (Isha et al., 2019; Vasmatkar et al., 2019). Nevertheless, the induction of complex fatty acids/acyl sugars was detected in tomato plants infested with *T. absoluta* (de Falco et al., 2019).

Another strength of ^{1}H NMR spectroscopy is related to its ability to simultaneously quantify primary and secondary metabolic compounds. Mono-, di- and small oligosaccharides such as sucrose, trehalose, raffinose or galactinol are involved in plant immunity as signalling molecules able to activate plant defence responses and increase plant resistance to pathogens by inducing secondary active metabolites or related pathways (Greco et al., 2012; Morkunas and Ratajczak, 2014; Trouvelot et al., 2014). The reported leaf levels of glucose and sucrose using ^{1}H NMR under fungal pathogen stress were dependent on the pathogen and time post infection, but both of them were mostly simultaneously increasing or decreasing (Lima et al., 2010; Ali et al., 2012; Copley et al., 2017; Su et al., 2018; Isha et al., 2019; Medina-Melchor et al., 2022). Fluctuations were observed in relation with the time post-infection; for example, sucrose increased in *A. thaliana* infected by *V. dahlia* at 12 hours post-infection (h.p.i) but decreased at 6 h.p.i. (Su et al., 2018). Grape infected by *P. viticola* showed an increase in sucrose and glucose levels only at 12 h.p.i (Ali et al., 2012). Changes in fructose were reported in grape in relation to Esca disease (Lima et al., 2010). Other sugars, such as arabinose and xylose, increased in late-stage infection in pail oil trees infected by *G. boninens* (Isha et al., 2019), and galactose decreased in the early-stage infection in onion infected by *Stemphylium vesicarium* (Medina-Melchor et al., 2022). Glucose increased (Choi et al., 2004b; do Prado Apparecido et al., 2017; Jlilat et al., 2021) or decreased (Simoh et al., 2009; López-Gresa et al., 2010) depending on the plant and the type of bacterial infection, whereas the reported changes in sucrose and fructose were minor. Interestingly, the increase in sucrose was related to the type of phytoplasmas (Choi et al., 2004b). The response of glucose varied depending on the plant species and the nematode involved. The levels increased in tomato plants (Afifah et al., 2020) but decreased in coffee (Machado et al., 2012). In general, glucose increased in plants infested by insects (Widarto et al., 2006; Liu et al., 2010; de Falco et al., 2019). Interestingly, trehalose showed a specific increase in *Arabidopsis* infested by *M. persicae* (Hodge et al., 2013). Rice varieties with different levels of resistance post-infection responded with different carbohydrate levels when infested by *Nilaparvata lugens* (Uawisetwathana et al., 2015). The post-infection-susceptible variety responded with an increase in mannitol and a decrease in sucrose, whereas the post-infection-resistant variety

responded with an increase in sucrose in an earlier stage of the infestation (Uawisetwathana et al., 2015).

Overall, the levels of amino acids are generally increased in response to fungal infection. The most commonly reported increases are described for alanine (Ali et al., 2012; Copley et al., 2017; Medina-Melchor et al., 2022) and glutamic acid (Kumar et al., 2016; Copley et al., 2017; Medina-Melchor et al., 2022), whereas proline (Isha et al., 2019), tyrosine (Medina-Melchor et al., 2022) phenylalanine (Medina-Melchor et al., 2022), isoleucine (Medina-Melchor et al., 2022), leucine (Medina-Melchor et al., 2022) and valine (Medina-Melchor et al., 2022) were increased in certain plant species. The response of amino acid levels was highly dependent on the type of bacteria and the stage of the infection. Generally, an increase in amino acids occurred in the early stage, whereas a reduction followed in the late stage of the infection. The variations in amino acids were dependent on the host plant and the viral pathogen. For instance, the level of asparagine increased in vanilla and mung bean after infection with cymbidium mosaic virus and yellow mosaic virus, respectively (Palama et al., 2012; Maravi et al., 2022), whereas it decreased in the early stages of the infection of the vanilla plant steam (Palama et al., 2012). With the exception of tobacco (Choi et al., 2006), alanine increased in the initial stages of infection (López-Gresa et al., 2010, 2012; Palama et al., 2012; Plischke et al., 2012; Maravi et al., 2022). Glutamine also increased, regardless of the plant and pathogen (Choi et al., 2006; Palama et al., 2012). Amino acids generally decreased in coffee as a consequence of herbivory by *Meloidogyne exigua* (Machado et al., 2012).

The levels of organic acids in the tricarboxylic acid cycle tended to be higher after fungal pathogen infections (Choi et al., 2006; López-Gresa et al., 2010; Palama et al., 2012; Plischke et al., 2012; Maravi et al., 2022). Changes in organic acids were reported for *B. rapa* and olive after microbial infection, leading to the accumulation of fumaric (Simoh et al., 2009), succinic (Simoh et al., 2009) and malic acid (Simoh et al., 2009; Jlilat et al., 2021). The levels of organic acids only slightly changed after insect attacks, and an increase was only reported for malic acid (Plischke et al., 2012; de Falco et al., 2019); minor changes were reported for glutamine, glutamate and asparagine (Liu et al., 2010; Uawisetwathana et al., 2015; Sabino et al., 2019).

Chemical constitutive defences

Constitutive defences are initiated and maintained regardless of whether herbi-

vores or pathogens have damaged the plant. They include many preformed physical barriers, such as cell walls, waxy epidermal cuticles and bark, as well as chemical barriers, with a broad range of bioactive small-molecular-weight metabolites. The NMR is relatively lesser exploited when regarding constitutive resistance to fungal pathogens, bacterial pathogens and insects. We did not find any studies related to viral pathogens. Resistant plants mainly show an increased presence of taxonimically restricted secondary metabolites, sugars, amino acids and organic acids. The accumulation of phenylpropanoids and polyketides was associated with resistance to powdery mildew in gerbera and grape (Figueiredo et al., 2008; Mascellani et al., 2022), whereas resistance to blight disease in potato was associated with the accumulation of chlorogenic acid (Tomita et al., 2017). Several phenolic compounds, including flavonoids, coumarins and terpenoids, are high in *Citrus* species resistant to black spot disease (Fernandes et al., 2022). Through focusing on subsets with varying levels of resistance, metabolomics was successfully applied for thrips. The constitutive chemical defences across different species were encoded to secondary metabolites, including phenylpropanoids, pyrrolizidine alkaloids and isoalkyl signals of sugar lipids. The investigation included leaves of carrot (Leiss et al., 2013), chrysanthemum (Leiss et al., 2009b), gladiolus (Wahyuni et al., 2021), senecio (Leiss et al., 2009a) and tomato (Mirnezhad et al., 2010).

Interestingly, resistant traits investigated by ^{1}H NMR spectroscopy are often linked with a higher availability of non-structural soluble sugars, amino acids and organic acids. Sugar beet leaves resistant to *Cercospora* leaf spot disease had high carbohydrate levels than the susceptible genotypes (Sekiyama et al., 2017); this was also observed for kiwi varieties resistant to *P. syringae* (Sciubba et al., 2020). Resistance in wheat to *Fusarium* head blight disease was mainly associated with increased sugar and amino acid metabolism (Browne and Brindle, 2007). Tomato varieties resistant to *Ralstonia solanacearum* showed less organic acids (Murti et al., 2021). An increased concentration of sucrose was linked to thrips resistance in both senecio and gladiolus, with an additional decrease in glucose in the latter (Leiss et al., 2009a; Wahyuni et al., 2021). Additionally, increased amino acid levels were reported in gladiolus (Wahyuni et al., 2021). Higher amounts of glucose and raffinose were reported in watermelon roots resistant to root-knot nematodes (Kantor et al., 2018), with choline and malic acid. Resistance to blight disease in potato was associated with the accumulation of organic acids but lower levels of carbohydrates (Tomita et al., 2017). It is assumed that non-structural soluble sugars, amino acids and organic acids are play an important role in the ability of plants to resist environmental stress. Non-structural soluble sugars increase resistance, buffering the impacts of reductions in carbon balance (McDowell, 2011;

Dietze et al., 2014). Well-established roles of organic acids are as acids modifying pH, as chelators binding metals or as carbon sources for microbes. Additionally, they play a role in the pathogenicity of rot diseases and elicitors of host defences (Panchal et al., 2021) and provide resistance; however, the specific mechanisms are still not clear (Zeier, 2013). Interestingly, that in many plants, resistance was associated with higher free carbohydrate concentrations. As carbohydrates can be a readily available substrate for fungal growth or may increase palatability to herbivores, the opposite would be expected.

NMR-based plant metabolomics pipeline

The proposed pipeline of NMR-based metabolomics comprises several stages, such as setting up the experiment, sampling the plant part of interest, extracting the metabolites, acquiring the NMR spectra and summarising the chemical information following an untargeted or targeted approach (Figure 5). The pipeline for NMR-based metabolomics has been extensively described elsewhere (Verpoorte et al., 2007, 2008, 2022; Kim and Verpoorte, 2010; Kim et al., 2010, 2011; Schripsema, 2010; Rivas-Ubach et al., 2013), and an up-to-date approach consists of well-standardised instrumental conditions with gold-standard pulse sequences (Kim et al., 2010; Mckay, 2011; Le Guennec et al., 2017; Vignoli et al., 2019), in addition to well-established data reduction approaches. However, the aim of this study is to evaluate the necessities for moving plant metabolomics forward. This involves a full factorial design with an adequate number of replicates, the inclusion of a robust validation, the use of standard protocols, the need for semi- or fully-automated pre-processing and annotation algorithms and the application of NMR metabolomics in interdisciplinary and multi-omics studies.

Experimental design: the need for external validation

A plant metabolomics study starts with the development of a solid hypothesis to ensure an appropriate experimental design, adequate sample preparation and suitable statistical methodologies. The experimental design typically includes conditions for plant growth and treatments, sample collection and preparation, as well

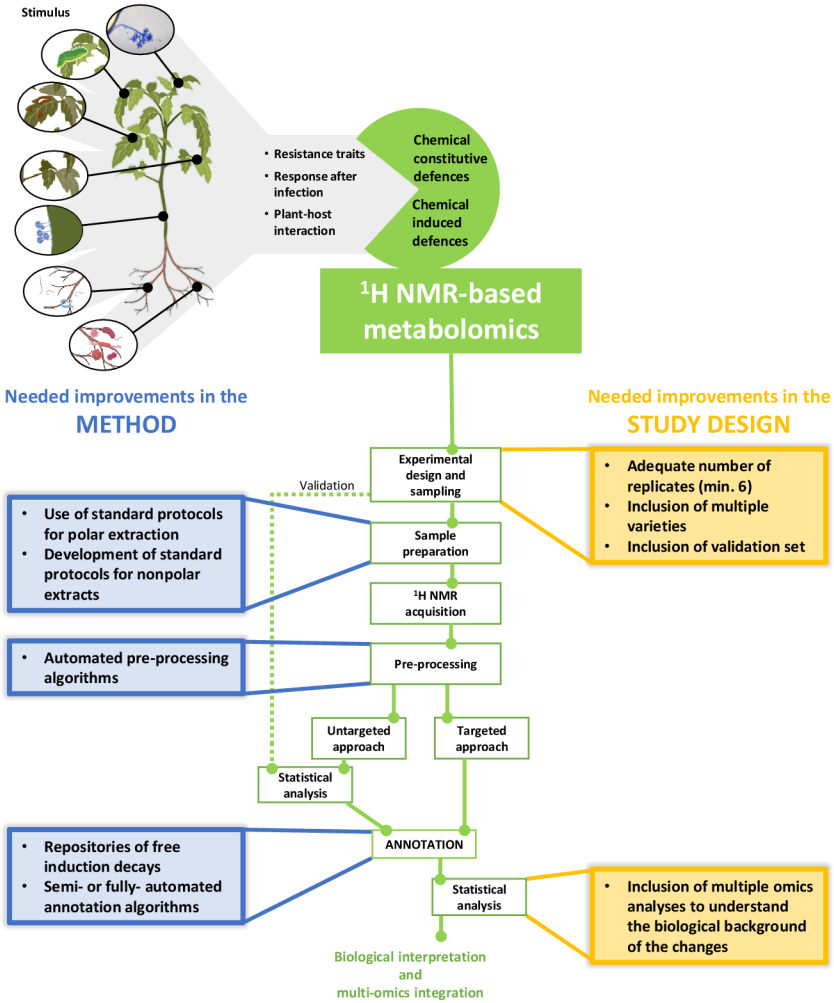

Figure 5 | Workflow overview of ^{1}H NMR-based plant metabolomics approach and the necessities for advancing in the method and in the experimental design. Created with BioRender.com.

as an analytical platform for hypothesis testing (Rodrigues et al., 2019). Ensuring the standardised reporting of metadata when describing the experiments is of similar importance (Sumner et al., 2007; Rodrigues et al., 2019). For a strong statistical analysis and a trustworthy biological interpretation of the data, biological replicates are crucial. As a rule of thumb, six should be the bare minimum number of biological replicates included in a randomised design to ensure biological variability and minimise experimental errors (Rodrigues et al., 2019). Experimental design and randomisation (Rodrigues et al., 2019; Jendoubi, 2021; Uthe et al., 2021) are crucial aspects of the successful completion of a metabolomic study. The inclusion of multiple varieties increases the representation of biological variability and reduces the chance of false positive results. While designing the experiments, the investigator needs to ensure that between 200 and 500 mg of fresh sample (corresponding to 50 to 100 mg dry weight, according to the sample type) will be available during sampling (Kim et al., 2010; Patel et al., 2021). Pooling samples is a typical practice to capture the high biological variety when resources are restricted (Rodrigues et al., 2019). It is strongly advised to incorporate real-world populations and an external validation set if classifier models are employed in data processing. The more often used cross-validation overestimates the classifier performance of supervised models, reducing the guarantee of a good performance across different populations (Westad and Marini, 2015). Independent external validation usually yields more trustable results, especially when employing different varieties and sampling times, but remains rarely applied.

It is crucial to point out that experiments carefully created for other omics technologies (such as transcriptomics and proteomics) may not be suitable for a metabolomics strategy, let alone one that is NMR-based. The most frequent incompatibilities are caused by insufficient repetitions and poor sample storage conditions, affecting the stability of the metabolites (Martins et al., 2018; Jendoubi, 2021).

Importance of standard operating procedures for extraction

The selection of the extraction solvent is essential to ensure the investigation of the biological question since the metabolome contains a wide range of chemicals with different polarity and localisation levels. To ensure intra- and inter-laboratory comparability, several efforts have been made to develop and offer standardised procedures for NMR sample preparation (Verpoorte et al., 2007; Kim and Verpoorte, 2010; Kim et al., 2010; Rivas-Ubach et al., 2013). However, currently, various protocols are used. Extraction may include the direct use of deuterated solvent, which speeds up the process, or non-deuterated solvents, requiring solvent evaporation, but with the potential of concentrating the extract prior to measurement (Schripsema, 2010; Medeiros Selegato et al., 2019). It has to be kept in mind that the use of deuterated solvents may cause the replacement of certain protons with deuterium and obscure the results (Verpoorte et al., 2022).

The extraction method mostly discussed in the field consists of ultrasonication with 1:1 methanol-d_4 and KH_2PO_4 buffer in deuterium oxide at pH 6 (Kim et al., 2010). The advantage lies in the fact that secondary metabolites are extracted, besides primary metabolites such as amino acids and carbohydrates. Alternatives to this extraction method include increasing the methanolic portion to 80%, which could show a clear difference in the quantification of aromatic compounds (Verpoorte et al., 2008). This extraction protocol is eligible to be used as a standard operating procedure (SOP) for spectra repository in shared databases. The present application of NMR-based plant metabolomics requires the use of water for extraction, which limits the extraction of secondary metabolites involved in biological processes.

When non-polar compounds are of interest, chloroform may be used as extracting solvent. To extract both non-polar and polar compounds in the same operation, a two-phase extraction method with chloroform–methanol–water (2:1:1) was developed by Choi et al. (2004b) and Verpoorte et al. (2007) and recently reviewed by Rivas-Ubach et al. (2013). The special case of the extraction of wood samples has recently been reviewed, and ethyl acetate was the most satisfactory solvent for the extraction, whereas and 7:3 chloroform-*d*–methanol-d_4 (v/v) was the most suitable solvent system for NMR analysis (Halabalaki et al., 2014).

Spectrum annotation: seeking for automation

One of the bottlenecks of an NMR approach is that spectrum analysis is a complex and time-consuming process (Patel et al., 2021). Although promising tools were recently developed (Hao et al., 2014; Howarth et al., 2020; Khakimov et al., 2020; Wenk et al., 2023), they still are not as sophisticated and automated as those for HPLC or MS spectra, and they were not targeted for application in plant metabolomics. The metabolites are quantified by a ratio analysis normalised to the number of protons relative to the internal standard (Leiss et al., 2009b), after phase and baseline correction. The primary metabolites are well known, universal and easy to identify and quantify. Their spectra are implemented in many GUI software packages, and their annotation quantification is readily available to medium-experienced NMR users. The real challenge in plant metabolomics is the annotation of the secondary metabolites, which are highly taxonomically restricted and are often found in glycosylated forms. Nowadays, the annotation of secondary metabolites relies on experience and requires an expert, laboratory experience and in-house databases. Much less publications focus on these metabolites (Table 1), although they often account for the largest part of the spectrum signals, leaving the NMR potential completely underused. Multiple approaches can be followed for the elucidation of unknown peaks; statistical spectroscopic tools such as Statistical Total Correlation Spectroscopy (STOCSY), Subset Optimization by Reference Matching (STORM) and Resolution-Enhanced (RED)-STORM are employed to identify other signals in the NMR spectra relating to the same molecule (Dona et al., 2016; Garcia-Perez et al., 2020). This could facilitate data extraction from existing databases; this method is limited in case the signals are not aligned or are in crowded regions overlapping with signals from other molecules. Otherwise, 2D NMR spectroscopy analysis, separation and preconcentration techniques are other alternatives for structure elucidation (Dona et al., 2016; Hall et al., 2018; Garcia-Perez et al., 2020; Mascellani et al., 2022). Search in repositories could lead to suggestions for annotation; despite traditionally known databases in the field (Medeiros Selegato et al., 2019), new databases are emerging, with a different approach for searching and storing the data as spectra (Wishart et al., 2022). However, to date, no databases based on FIDs are available. The incremental spiking of authentic chemical standards remains the only possibility to univocally positively identify the compound (Garcia-Perez et al., 2020).

Integration in interdisciplinary and multi-omics studies

Nowadays, in the post-genomics era, the application of chemometrics is not restricted to a single data source. The aim is to extrapolate information from multiple-omics data sources with data fusion to produce more consistent, accurate and useful information than that provided by any single data source (Olivieri and Farina, 2012; Blanchet and Smolinska, 2016). It is critical to take a holistic approach to understand the biological mechanisms occurring during different environmental stress conditions to consider synergies and antagonisms (Meena et al., 2017; Mosa et al., 2017; Crandall et al., 2020). Nevertheless, the main challenge in multi-omics integration is related to the great metabolic diversity which characterises plants and symbioses with complex interaction networks, although multiple approaches have been proposed (Jamil et al., 2020). The integration of omics approaches in plant ecology consists of including metabolomics, genomics, metagenomics, volatilomics and spectranomics (Crandall et al., 2020).

Outlook, challenges and future prospective

As an integral part of the study of plant responses, metabolomics is an interdisciplinary field that is intimately connected to a number of other fields, including analytical chemistry, bioinformatics, chemometrics and biological sciences. The field of metabolomics research is quickly growing as a result of the advancement of analytical tools, particularly metabolic profiling based on MS and NMR. Although NMR is considered one of the major analytical techniques applied in metabolomics studies, it is still limited in plant research, in particular for the assessment of biological alterations related to biotic stress. This review provides the state-of-the art in applying the ^{1}H NMR-based metabolomics approach for plant resistance to biotic stress, post-infection stress responses and plant-host interactions.

The main challenge in the application of this method consists of the availability of the NMR spectrometers dedicated to metabolomics, including the implementation of trainings and summer schools for the young community. Nevertheless, we acknowledge that there are still several gaps in the approach that need to be addressed, such as databases, attempts to make databases, improved deconvolution and spectral processing. Vigorous research activities are being conducted applying ^{1}H NMR; however, the full potential of this method remains largely untapped due to the focus on primary metabolism and a lack of comprehensive annotation and shared databases for secondary metabolites. Even though the instrument records secondary metabolites, the limited attention it receives significantly diminishes the capabilities of the method. The high reproducibility is a great advantage to exchange spectral collections across laboratories, leading to broad collaboration opportunities and large sets of data. Vendors may facilitate the standardisation of used buffers by offering ready-to-use buffers, granting high reproducibility. In addition, computer-assisted intelligent metabolite data annotation is also important for advancing the method elucidating the diversity of plant-specific metabolites. Hence, we believe that ^{1}H NMR can soon be widely applied in suitable studies where the limitations of the technique do not hide the investigated biological responses expanding the catchment area. The field of ^{1}H NMR spectroscopy in plant science needs higher visibility and the promotion of the method advancements. Researchers must have the possibility to decide whether to use NMR or MS coupled with a separation method when conducting metabolomics studies. Given that ^{1}H NMR-based metabolomics can be largely applied in plant biology, it is my hope that this review will be useful not only for researchers active in this field but also for students and researchers with a more general interest in applying metabolomics in their studies to enable fully factorial multi-omics studies.

Acknowledgements

This work was supported by SGS CZU FAPPZ (grant number SV21-12-21310).

CHAPTER 4

Polyketide derivatives in the resistance of *Gerbera hybrida* to powdery mildew

Based on:
Mascellani, A., Leiss, K., Bac-Molenaar, J., Malanik, M., Marsik, P., Hernandez Olesinski, E., Tauchen, J., Kloucek, P., Smejkal, K., and Havlik, J. (2022). Polyketide derivatives in the resistance of *Gerbera hybrida* to powdery mildew. *Front. Plant Sci.* 12, 790907. doi: 10.3389/fpls.2021.790907.

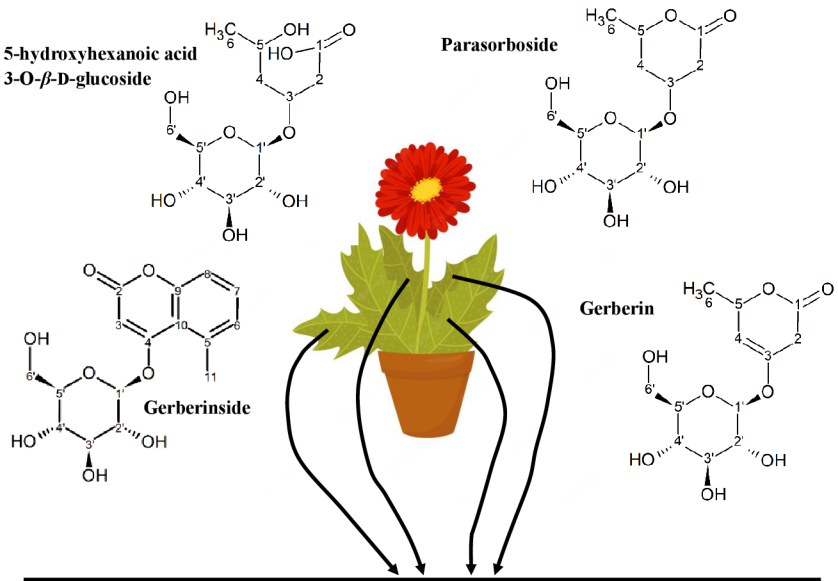

Bars show proportions of plants described in the training subset as resistant (light color) and susceptible (dark color). Concentrations are expressed as mg/g of dry leaves.

Abstract

Powdery mildew is a common disease affecting the commercial production of gerbera flowers (*Gerbera hybrida*, Asteraceae). Some varieties show a certain degree of resistance to it. Our objective was to identify biomarkers of resistance to powdery mildew using an ^{1}H nuclear magnetic resonance spectroscopy and chemometrics approach in a complex, fully factorial experiment to suggest a target for selection and breeding. Resistant varieties were found to differ from those that were susceptible in the metabolites of the polyketide pathway, such as gerberin, parasorboside, and gerberinside. A new compound probably involved in resistance, 5-hydroxyhexanoic acid 3-*O*-*β*-D-glucoside, was described for the first time. A decision tree model was built to distinguish resistant varieties, with an accuracy of 57.7%, sensitivity of 72%, and specificity of 44.44% in an independent test. Our results suggest the mechanism of resistance to powdery mildew in gerbera and provide a potential tool for resistance screening in breeding programs.

Keywords: ^{1}H NMR; *Gerbera hybrida*; decision tree; polyketides; powdery mildew resistance.

Author contribution: I contributed to the current study by carrying on the NMR metabolomics analysis including extraction, data acquisition and processing. I contributed to NMR structural elucidation and compound isolation. I carried out the statistical analysis and created the artwork. I drafted the original manuscript and curated the article until acceptance.

Introduction

Plants as sessile organisms cannot escape from unfavourable conditions in their surroundings. For this reason they have acquired the ability to produce a remarkable diversity of low-molecular-weight compounds to protect themselves. They produce a vast range of so-called secondary metabolites, specifically adapted to combat exposure to pathogens or herbivores both above and below the ground (Pichersky and Gang, 2000; Sirikantaramas et al., 2008). Those defensive compounds are subjected to changes as the plant continues to evolve and adapt. Differences in the content of such chemicals between plants are a key factor in the study of plant resistance, an important part of the integrated management of disease (Leiss et al., 2009b). More than one compound is usually involved in such biological processes, providing additional if not synergistic effects and reducing the chance that pathogens and herbivores might develop resistance.

Metabolomics is a suitable tool for the chemical characterization of compounds involved in plant resistance. It allows the simultaneous detection of a wide range of compounds (Kim et al., 2010). NMR spectroscopy can identify and quantify compounds quickly and reproducibly with little sample preparation (Allwood et al., 2008; Verpoorte et al., 2008; Kim et al., 2010). Chemometric tools for data mining encourage the exploratory use of NMR for metabolic fingerprinting (Winning et al., 2008). NMR has been successfully applied to study metabolites associated with pathogen (Kashif et al., 2009) and herbivore (Leiss et al., 2009b, 2011, 2013) resistance. In comparison with the most common analytical metabolomics techniques, NMR is characterized by its high reproducibility. Throughout the years, chromatographic methods and mass spectrometry have shown to be affected by intra- and inter-day variability and inconsistency in reproducing the same results in another lab. Unlike chromatographic methods, NMR does not require continual calibration curves for each compound to be quantified, but instead can rely on in-house databases (Verpoorte et al., 2007). NMR is very well-suited for high-throughput methodology, including the possibility of robotization. A 3-minute analysis can provide quantitative data. Despite the limited number of compounds detected in an extract and that certain minor compounds might not be observed, the major trends are clear (Verpoorte et al., 2007); NMR can be well-integrated with other spectroscopic or spectrometric techniques to identify metabolites and elucidate their structures (Wolfender et al., 2003; Kim et al., 2010).

Gerbera is one of the ten most economically important flower crops in Europe (Teeri et al., 2006) and the United States (USDA, 2019). It is a popular orna-

mental plant used as a cut flower, potted plant, or landscape bedding plant to decorate gardens, terraces, and patios. Cultivated gerberas are derived from crosses between the wild species *Gerbera jamesonii* Bolus ex. Hook f. and *G. viridifolia* (DC.) Sch.Bip. and have been given the provisional name *G. hybrida*. An important objective for gerbera breeders is to improve the resistance of the varieties to major fungal diseases, particularly powdery mildew (Kloos et al., 2005b; Deng and Harbaugh, 2010). Powdery mildew, a key economically important fungal disease of gerbera, is caused by *Podosphaera xanthii* (Castagne) U. Braun and N. Shishkoff (syn. *Sphaerotheca fuliginea*, formerly *S. fusca* Blumer). This disease is considered to be the most common and destructive disease of gerbera in commercial production and landscape use, affecting all parts of the plant, leading to substantially reduced growth and loss of quality (Kloos et al., 2005b; Song and Deng, 2013; Ghani and Sharma, 2019). Symptoms of powdery mildew consist of white spots on the upper surfaces of the leaf, which gradually enlarge to form a white powder-like mat that can spread to the flowers and the stems. The genetic basis of resistance to powdery mildew in gerbera is poorly understood; putative sequences and markers have been studied (Song et al., 2012; Song and Deng, 2013). The dominant allele determining powdery mildew resistance, *Pmr1*, has been identified in a wild type of gerbera (Kloos et al., 2005b). Recently, resistance and susceptibility genes in gerbera associated with powdery mildew were revealed (Bhattarai et al., 2020). However, this study is only based on two breeding lines, a resistant and a susceptible one, respectively. Gerbera is considered a model plant for plant reproduction exhibiting secondary metabolism of anthocyanins and polyketides (Eckermann et al., 1998; Koskela et al., 2001; Kloos et al., 2005a; Teeri et al., 2006; Broholm et al., 2010; Ruokolainen et al., 2010; Bashandy et al., 2015; Pietiäinen et al., 2016).

Information about resistance to powdery mildew in gerbera is scarce and little is known about the underlying mechanisms. Thus, in this study, we looked at differences in the composition of metabolites, both identities and concentrations, between resistant and susceptible varieties and aimed at providing a tool for the prediction of the resistance to powdery mildew based on the metabolome. An untargeted NMR-based metabolomics approach was applied to a set of 120 samples, including eight different varieties, four classified as resistant and four as susceptible. Standard and mini gerbera and five replicates of young and old leaves were included. Compounds for which the peaks in the NMR spectrum differed between the groups were further isolated and their structures elucidated by means of semi-preparative HPLC, LC-MS, and NMR, and quantified by ^{1}H NMR to build a decision tree enabling rapid screening for the selection of varieties and systematic plant breeding.

Materials and methods

Plant material

Eight varieties of *G. hybrida* grown by three Dutch breeders were used for this study (Figure 6). The plants were described as either resistant or susceptible to powdery mildew based on the empirical experience of the breeders. Half of the samples were gerbera mini varieties, of which two (varieties Evra and Jumbo) were resistant to powdery mildew and two were susceptible (Franky and Mokka). The other four were standard varieties of gerbera, of which two (varieties Snowking, and Passoa) were resistant to powdery mildew and two were susceptible (Madeira and Fahrenheit). The samples were collected in spring and autumn (Figure 6). For each variety, young and old leaves were collected separately in five biological replicates, each consisting of 3 old or 5 young, pooled leaves. From each individual plant, the third (young) leaf from above and each third (old) leaf from below was sampled for the analysis. This resulted in a total of 120 samples. A second sample set was collected for the external validation of the model (Figure 6). A pooled sample of 5 leaves from different plants was collected from 27 mildew-susceptible and 25 mildew-resistant varieties (Supplementary Table S2), based on the empirical experience of the breeders. It included the varieties used

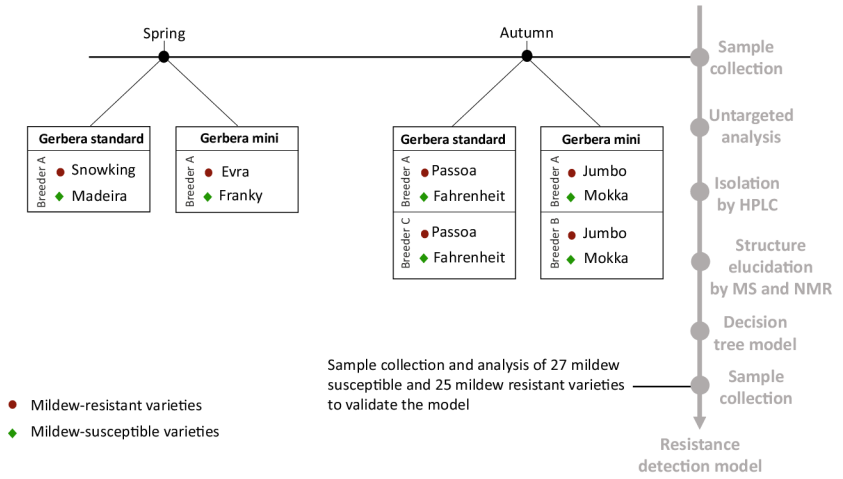

Figure 6 | Timeline diagram of the study design.

to build the models and other varieties not previously included, the same varieties from different breeders were included. The plant material was immediately frozen in liquid nitrogen upon harvesting and freeze dried. After freeze drying, samples were ground using a laboratory grinder IKA A 11 basic Analytical Grinder Mill and stored at −80°C until extraction.

Chemicals

All chemicals and reagents used were of analytical grade. Potassium dihydrogen phosphate (99%, KH_2PO_4), deuterium oxide (99.9%, D_2O), methanol-d_4 (>99.8%, MeOD), and methanol were purchased from VWR (Radnor, PA, USA). Sodium deuteroxide 40% w/v solution in D_2O (99.5%, NaOD) was obtained from Alfa Aesar (Kandel, Germany). 3-(trimethylsilyl) propionic-2,2,3,3-d_4 acid sodium salt (99%, TMSP) was obtained from Sigma-Aldrich (St. Louis, MO, USA). A Millipore Direct-Q® 3 UV Water Purification System (Millipore Corp., Bedford, MA, USA) or (Merck KGaA, Darmstadt, Germany) for ultrapure water was used throughout the study.

Extraction of plant material and acquisition of NMR data

Each 50 mg of the finely ground leaves, were extracted in MeOD-D_2O (1:1, v/v) as previously described (Kim et al., 2010; Mascellani et al., 2021). All spectra were recorded on a Bruker Avance III spectrometer equipped with a broad band fluorine observation (BBFO) SmartProbe™ with z-axis gradients (Bruker BioSpin GmbH, Rheinstetten, Germany), operating at the ^{1}H NMR frequency of 500.23 MHz. All ^{1}H NMR spectra were acquired and processed under the same conditions (Mascellani et al., 2021). All samples were calibrated to the internal standard TMSP at 0.0 ppm, subject to exponential apodization of 0.3 Hz, and phase- and baseline corrections were made using Mnova software, version 14.1.0 (Mestrelab Research, S.L., Santiago de Compostela, Spain).

Data analysis

Spectral intensities of the ^{1}H-NMR spectra were scaled to the intensity of the

internal standard (TMSP, 0.01% [w/v]) and reduced to spectral bins of 0.04-ppm by the sum of data points corresponding to the region of δ_H 0.02 to δ_H 10.0. The regions corresponding to water (δ_H 4.70−5.00 ppm) and methanol (δ_H 3.28–3.40 ppm) were excluded from the analysis. A script built in-house was used for data reduction. PCA and OPLS-DA were performed using the package MetaboAnalystR (Pang et al., 2020) version 3.0.2 in R 4.0.0(R Core Team, 2020). PQN, log transformation, and auto-scaling were applied for PCA and OPLS-DA. The OPLS-DA model was validated by R^2Y and Q^2 metrics using the permutation method through 100 applications, to describe the percentage of variation explained by the model and its predictive ability, respectively. Graphs were constructed using the package ggplot2 (Wickham, 2016) version 3.3.3 in R 4.0.0 (R Core Team, 2020). A two-tailed unpaired *t*-test comparison (no correction for multiple comparison) was performed for each 0.04 ppm bin. Color-coded graphs were generated from an in-house script in MATLAB® R2020a (The Mathworks). The signals from the most significant ($p(corr) > |0.5|$ and/or $p < 0.05$) bins results were identified and quantified.

Extraction and isolation to identify the compounds

The discriminating NMR signals between the two varieties were isolated by NMR-guided semi-preparative HPLC. To identify the metabolites, pooled samples of resistant leaves were extracted by decoction for 15 min and filtered. The resulting extract with an approx. concentration of 5 mg/mL of dry weight was used for fractionation collection using an HPLC (UltiMate™ 3000 system, Thermo Fisher Scientific, Waltham, MA, USA) equipped with a Dionex Ultimate 3000 UV detector and fraction collector (Thermo Fisher Scientific, Waltham, MA, USA). The chromatographic separation was carried out on a Triart C18 column (5 µm, 250 × 4.6 mm) (YMC CO., LTD., Kyoto, Japan) coupled with Polar C-18 Security-Guard Cartridges (Phenomenex, Torrance, CA, USA) at 35°C, with a flow rate of 0.8 mL/min and an injection volume of 100 µL. The mobile phase consisted of (A) Milli-Q water and (B) methanol. The gradient was as follows: 0% B isocratically for 5 min followed by increase to 100% B over 10 min, a hold for 5 min, and a subsequent return to the initial conditions. Fractions were collected every 24 sec, resulting in a total of 48 fractions. Multiple injections were pooled. The fractions collected were freeze dried and each residue was resuspended in MeOD and D_2O (1:1, v/v) for NMR fast screening. Selected fractions were pooled and purified by a second HPLC fractionation with the same conditions as described above.

Identification of the isolated compounds

The acquired 2D NMR spectra consisted of DQF-COSY, HMBC, and HSQC with common standard settings (Supplementary Table S3). NMR spectra were recorded on the spectrometer previously described. The spectra were processed with Mnova software version 14.1.0 (Mestrelab Research). The MS/MS spectra were acquired using a qualitative tandem liquid chromatography quadrupole time of flight mass spectrometry (LC-QTOF-MS/MS) system consisting of Dionex Ultimate 3000 ultra-high performance liquid chromatography chromatograph (Thermo Fisher Scientific, Waltham, MA, USA) coupled with an Impact II quadrupole time-of-flight mass spectrometer with high resolution accurate mass (Bruker Daltonics, Bremen, Germany), equipped with an electrospray ionization source in both positive and negative ionization modes. Liquid chromatography separations and the ionization parameters for mass spectrometry were performed using the conditions described in Supplementary Table S4. The chromatography was controlled by Chromeleon Xpress link (Thermo Fisher Scientific, Waltham, MA, USA). The MS/MS fragmentation spectra were acquired by O-Tof Control 4.0 and HyStar 3.2 software (Bruker Daltonik, Bremen, Germany). The spectra were processed using Compass DataAnalysis 4.3 (Bruker Daltonik, Bremen, Germany). The fragments were analysed using Mass Frontier 7.0.5.9 SR3 (High Chem Ltd., Bratislava, Slovakia) and Thermo Excalibur 3.0.63 (Thermo Fisher Scientific, Waltham, MA, USA) software. The exact masses obtained were searched using Bruker Compound Crawler 3.0 databases (Bruker Daltonik, Bremen, Germany) and their fragmentation spectra were compared with MetFrag free on-line software results.

Quantification of metabolites

The peak areas of selected ^{1}H NMR signals belonging to the target compounds, and the peak area of TMSP, were integrated manually for all of the samples and the metabolites were quantified by a ratio analysis normalised to the number of protons (Leiss et al., 2009b). These quantitative data were used to test differences in the concentration between varieties and between leaf ages by a two-tailed unpaired *t*-test and also to build a decision tree model. The criterion for statistical significance was a probability value of $p \leq 0.05$.

Statistical modelling

The concentrations of the targeted compounds used to build a conditional interference tree were chosen using the package party (Hothorn et al., 2006) v. 1.3-5in R version 4.0.0. Of the samples, 70% were used for training, and the remaining 30% as testing subsets. Accuracy, sensitivity, and specificity were used to evaluate the performance of the decision trees based on the confusion matrix. Accuracy is the probability that a sample is correctly predicted. Sensitivity constitutes the probability that a resistant sample is correctly predicted to be resistant, specificity expresses the probability that a susceptible sample has been correctly identified as susceptible. The model was successively validated with the second dataset collected to evaluate its performance for the applications in breeding.

Results

Data reduction

Application of the PCA model resulted in eight principal components explaining 50.3% of the total variance. Intergroup separation between the resistant and susceptible varieties occurred across the principal component 5, representing 4.1% of the variation (Figure 7A). Relatively dispersed mildew- resistant and -susceptible samples were observed, reflecting the varied character of the samples. Difference in the ages of the leaves between samples seemed to be relatively unimportant. To explore the segregation between the two classes concerned, a supervised OPLS-DA model was compiled (Figure 7B) to distinguish resistant varieties from these which susceptible. It showed a clear separation between mildew-resistant and -susceptible varieties, with an R^2Y value of 0.88 and a Q^2 value of 0.66, suggesting a strong prediction. An additional set of *t*-tests comparing samples (no correction for multiple comparisons was made) from resistant and susceptible varieties was performed ($p < 0.05$). Graphical projection of p(corr) using the OPLS-DA and p-value values from the *t*-test (Figure 7C–D) indicated the signals contributing most to the class discrimination. Combining multivariate and univariate statistical analyses showed that the characteristic metabolites of resistant varieties had stronger proton resonance signals for bins centred at δ_H 7.50 ppm ($p \leq 0.01$, p(corr) = -0.55), δ_H 7.46 ppm ($p \leq 0.01$, p(corr) = -0.50), δ_H 7.18 ppm

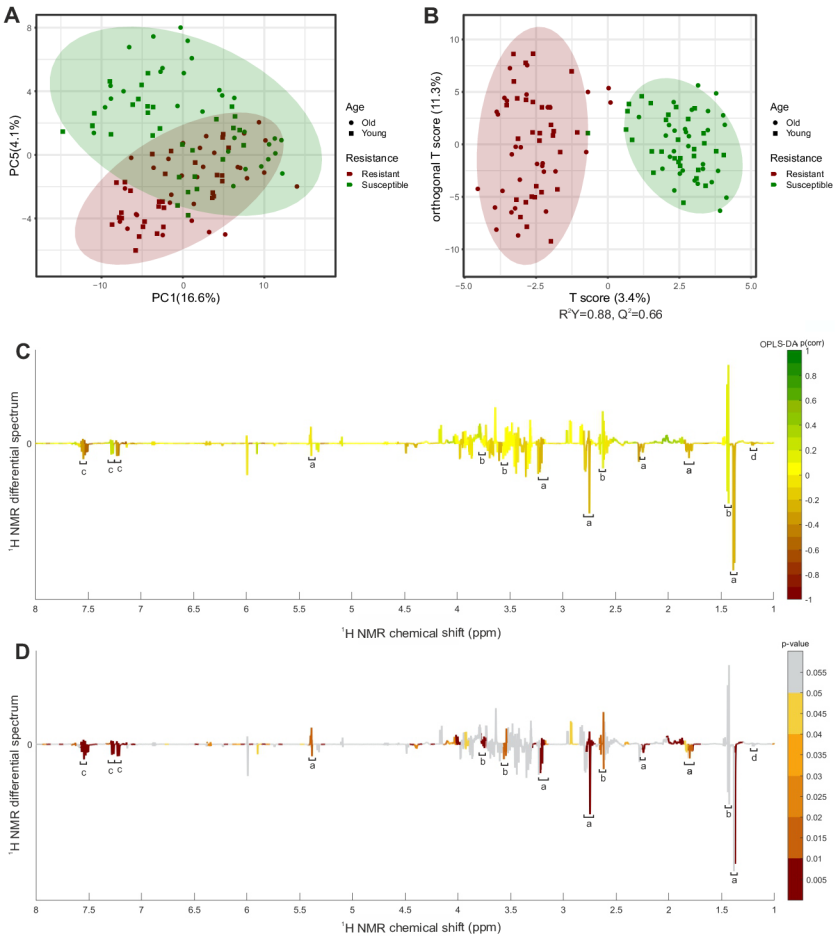

Figure 7 | Univariate and multivariate statistical analysis of leaves extracted in MeOD-D_2O (1:1, v/v). (**A**) PCA scores plot. (**B**) OPLS-DA scores plot. (**C**) based on the ^{1}H NMR differential spectrum (mean susceptible spectrum, N=60, minus mean resistant spectrum, N=60). (**D**) *t*-test coefficient plot based on the ^{1}H NMR differential spectrum (mean susceptible spectrum, N=60, minus mean resistant spectrum, N=60). Parasorboside (a), gerberin (b), gerberinside (c), 5-hydroxyhexanoic acid 3-*O*-*β*-D-glucoside (d) are shown. Peaks in the positive direction indicate metabolites more abundant in varieties susceptible to mildew. Metabolites more abundant in leaves of varieties resistant to mildew are shown as peaks in the negative direction. The color bar indicates the correlation of the bins with the predicting variation (**C**) and *p*-value (**D**). The filled red circle represents the 95% confidence region of varieties resistant to mildew and the filled green circle the 95% confidence region of varieties susceptible to mildew. Filled squares represent the young leaves and filled dots the old leaves of varieties resistant (red) or susceptible (green) to mildew.

($p \leq 0.01$, p(corr) = -0.48), δ_H 7.14 ppm ($p \leq 0.01$, p(corr) = -0.56), δ_H 5.94 ppm ($p \leq 0.01$, p(corr) = -0.55), δ_H 5.38 ppm ($p \leq 0.01$), and δ_H 1.34 ppm ($p \leq 0.01$, p(corr) = -0.21). These signals were selected as candidates for further investigating and quantification. Additionally, we included signals at δ_H 1.44 ppm, and 1.20 ppm in the comparisons because they were structurally similar to the candidate signal at δ_H 1.34 ppm in the centred bin.

Identification of metabolites

The candidate signals chosen as markers of resistance to mildew were isolated and assigned to the four compounds gerberin, parasorboside, gerberinside and 5-hydroxyhexanoic acid 3-*O*-*β*-D-glucoside, using MS/MS and NMR (Table 3, Supplementary Figure S1–S16). The resonance signals observed for these compounds corresponded to the signals in the bins described above, as illustrated in Figure 8. To the best of our knowledge, the spectral data for 5-hydroxyhexanoic acid 3-*O*-*β*-D-glucoside do not correspond to data of any compound previously published, but they agree partially with the data for methyl and ethyl esters previously described (Tschesche et al., 1971; Numata et al., 1990), who considered them to be artefacts. The 5-hydroxyhexanoic acid 3-*O*-*β*-D-glucoside (purity 95%) was isolated as a colourless amorphous substance. Gerberin and parasorboside were isolated and identified as an inseparable mixture (Yrjönen et al., 2002). The NMR data obtained were in good agreement with those published (Nagumo et al., 1989), as well for gerberinside (Nagumo et al., 1989; He et al., 2014) although different solvents were used and H-3‘ and H-5‘ of the structure were probably erroneously assigned (He et al., 2014).

Quantitative ^{1}H NMR of the isolated compounds

The concentrations of 5-hydroxyhexanoic acid 3-*O*-*β*-D-glucoside, gerberin, parasorboside, and gerberinside differed for young and old leaves in resistant and susceptible varieties of *Gerbera* (Supplementary Figure S17, Supplementary Table S5). Independent of leaf age, leaves of resistant varieties generally accumulated more parasorboside ($p \leq 0.001$) and gerberinside ($p \leq 0.001$), with younger leaves containing higher concentrations of parasorboside ($p = 0.01$) and gerberinside ($p = 0.002$) than older leaves. This was also the case for susceptible varieties with younger leaves containing more parasorboside ($p \leq 0.001$) and gerberinside ($p \leq$

Table 3 | ^{1}H and ^{13}C NMR spectroscopic assignments in ppm [at 500 and 125 MHz, MeOD-D_2O (1:1, v/v)] and LC-QTOF-MS/MS assignments of compounds from fractionation of *Gerbera hybrida* aqueous extract.

Compound name & structure.	LC-QTOF-MS/MS				^{1}H and ^{13}C NMR		
	Retention time (conditions)	m/z $[M+H]^+$ (formula, calculated mass) [a]	m/z $[M-H]^-$ (formula, calculated mass)	Formula	Pos.	δ_H (mult; J in Hz) ppm	δ_C
5-hydroxyhexanoic acid 3-*O*-*β*-D-glucoside 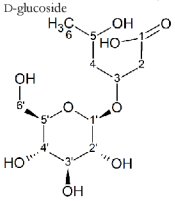	3.6 min (0.2% formic acid and methanol)	311.1336 ($C_{12}H_{23}O_9$, calcd 311.1342)	309.1197 ($C_{12}H_{21}O_9$, calcd 309.1186)	$C_{12}H_{22}O_9$	1	-	*176.7* [c]
					2	*2.46 (qd, 14.4, 14.4, 14.4, 6.3)*	*43.7*
					3	*4.23 (m)*	*77.1*
					4	*1.65 (dt, 14.2, 5.4)*	*44.1*
						1.87 (m)	
					5	*4.00 (m)*	*66.8*
					6	*1.21 (d, 6.2)*	*22.6*
					1'	*4.52 (d, 7.9)*	*70.1*
					2'	*3.21 (dd, 7.9, 9.2)*	*74.2*
					3'	*3.46 (dd, 9.2, 8.6)*	*76.8*
					4'	*3.35 (dd, 8.6, 9.8)*	*70.0*
					5'	*3.40 (ddd, 9.8, 5.5, 2.1)*	*76.8*
					6'	*3.89 (dd, 12.1, 2.1)*	*61.6*
						3.71 (dd, 12.1, 5.5)	
Gerberin 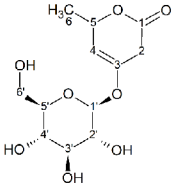	3.9 min (0.2% formic acid and methanol)	291.1071 ($C_{12}H_{19}O_8$, calcd 291.1079)	289.0932 ($C_{12}H_{17}O_8$, calcd 289.0923)	$C_{12}H_{18}O_8$	1	-	*180.3* [c]
					2	*5.40 (d, 1.3)*	*92.8*
					3	-	*171.6* [c]
					4	*2.60 (dd, 1.3 17.5)*	*32.1*
						2.64 (dd, 4.7, 17.5)	
					5	*4.59* [c]	*72.8*
					6	*1.45 (d, 6.3)*	*18.2*
					1'	*5.11(d, 7.7)*	*97.5*
					2'	*3.50 (dd, 7.7, 9.3)*	*71.5*
					3'	*3.56 (m)*	*75.2*
					4'	*3.45 (m)*	*68.2*
					5'	*3.56 (m)*	*75.2*
					6'	*3.73 (dd, 5.4, 12.4)*	*59.6*
						3.90 (dd, 2.2, 12.4)	
Parasorboside 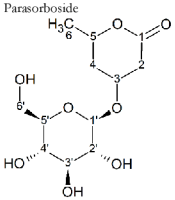	4.0 min (0.2% formic acid and methanol)	293.1225 ($C_{12}H_{21}O_8$, calcd 293.1236)	291.1086 ($C_{12}H_{19}O_8$, calcd 291.1080)	$C_{12}H_{20}O_8$	1	-	[b]
					2	*2.80 (m)*	*33.8*
					3	*4.41 (m)*	*69.7*
					4	*2.26 (m)*	*33.8*
						1.81 (ddd, 2.9, 11.3, 14.4)	
					5	*4.91* [c]	*73.5*
					6	*1.39 (d, 6.4)*	*18.8*
					1'	*4.50 (d, 7.8)*	*100.5*
					2'	*3.22 (dd, 7.8, 9.3)*	*72.2*
					3'	*3.45 (m)*	*75.8*
					4'	*3.34 (dd, 8.8, 9.8)*	*68.7*
					5'	*3.40 (ddd, 2.2, 5.8, 9.8)*	*75.1*
					6'	*3.88 (dd, 2.2, 12.3)*	*59.6*
						3.68 (dd, 5.8, 12.3)	
Gerberinside 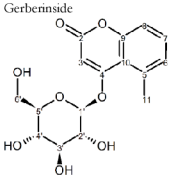	8.0 min (5 mM ammonium formate)	339.1070 ($C_{16}H_{19}O_8$, calcd 339.1079)	337.0927 ($C_{16}H_{17}O_8$, calcd 337.0923)	$C_{16}H_{18}O_8$	2	-	[b]
					3	6.03 (s)	93.3
					4	-	169.2 [c]
					5	-	138.7 [c]
					6	7.24 (d, 7.6)	129.4
					7	7.65 (t, 7.8)	133.7
					8	7.30 (d, 8.1)	116.1
					9	-	155.7 [c]
					10	-	114.7 [c]
					11	2.77 (s)	23.7
					1'	5.34 (d, 7.8)	100.3
					2'	3.73 (dd, 9.2, 7.8)	73.9
					3'	3.62 (t, 9.2)	77.1
					4'	3.52 (m)	70.1
					5'	3.68 (ddd, 10, 5.6, 2.3)	77.9
					6'	3.78 (dd, 12.4, 5.6)	61.5
						3.94 (dd, 12.4, 2.3)	

Coupling constants (J in Hz) in parentheses.
s = singlet, d = doublet, t = triplet, m = multiplet, dd = doublet of doublets, dt = doublet of triplets.
a = fragment ions are reported in Supplementary Figure S5, S10, S11, S16.
b = not observed, c = observed in HMBC.

0.001) than older leaves. Greater amounts of gerberin occurred only in the leaves of resistant standard gerbera ($p \leq 0.001$), but not in the resistant mini varieties.

Resistance detection model

Based on the selected candidate markers for resistance, a decision tree predictive model was constructed to predict the detection of resistance for breeding purposes. Decision trees are one of the most popular classification algorithms in current use in data mining and machine learning. The algorithms can easily handle multi-class discrimination and its constructed decision tree has a structure that is easy to understand as a flowchart. The algorithms are based on a recursive procedure which logically combines a sequence of simple tests (Kotsiantis, 2013). Each sample was characterized only by the concentrations of the candidate markers. To reduce the risk of over-fitting, 30% of the dataset was not used to construct the model but rather to evaluate the model. The resulting predictive model achieved 92.5% accuracy, 90% sensitivity, and 95% specificity. It is depicted in Figure 9. Gerberinside was the key compound for class discrimination, with varieties rich in gerberinside being mildew resistant. When the concentration of gerberinside is lower, greater concentrations of gerberin and parasorboside lead to resistance to powdery mildew. If a smaller amount of parasorboside was present, then the resistance dependent on the concentration of 5- hydroxyhexanoic acid 3-*O*-*β*-D-glucoside. A total of 52 samples were used as an external validation dataset to test the applicability of the model for breeding purposes. The model showed an accuracy of 57.7%, sensitivity of 72%, and specificity of 44.44% (Table 4). Four varieties already used in the first test set were included in the validation set. They

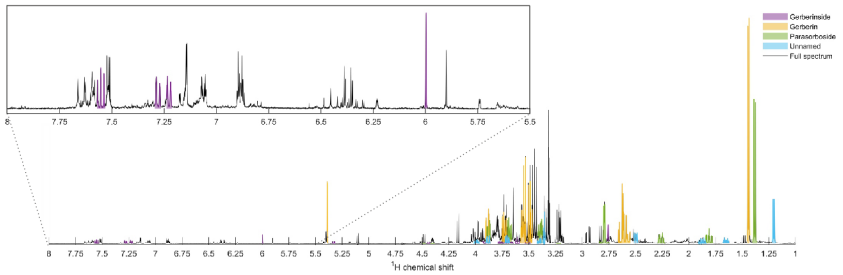

Figure 8 | Representative annotated ^{1}H NMR spectrum of young leaves of the powdery-mildew-resistant variety Snowking extracted in MeOD-D_2O (1:1, v/v).

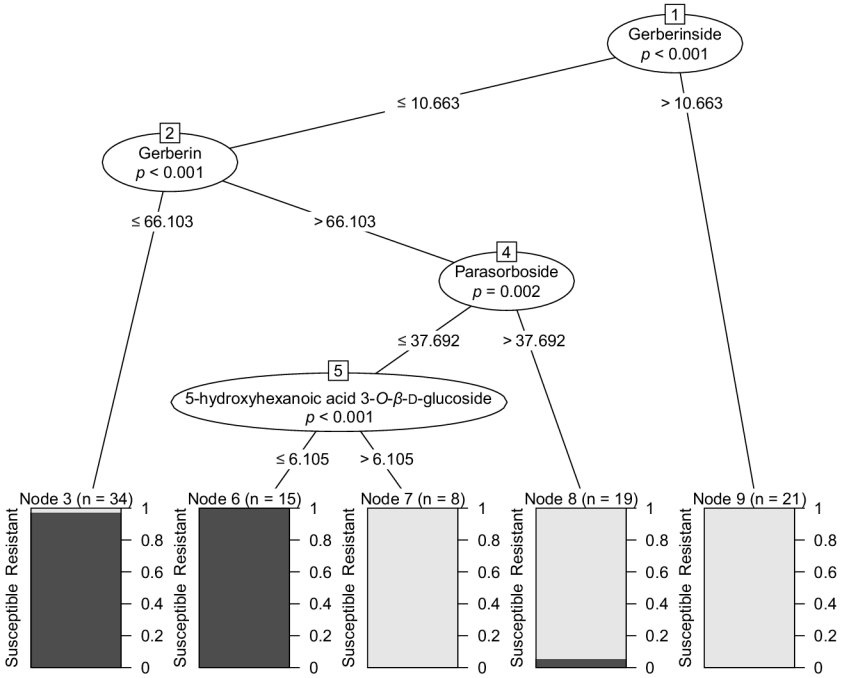

Figure 9 | Decision tree showing the concentrations (mg/g of dry leaves) of the selected metabolites responsible for resistance to powdery mildew based on the ^{1}H NMR spectra of gerbera leaves extracted in MeOD-D_2O (1:1, v/v). Concentrations are expressed as mg/g of dry leaves. Nodes are either numbered in squares or as Node #. Bars show proportions of plants described in the training subset as resistant (light color) and susceptible (dark color).

Table 4 | Decision tree confusion matrix classification of gerbera leaves resistant and susceptible to mildew in the validation sample set extracted in MeOD-D_2O (1:1, v/v). Misclassification error: 44%, sensitivity: 72%, specificity: 44%.

		Predicted class	
		Resistant	**Susceptible**
Real class	**Resistant**	18	7
	Susceptible	15	12

were predicted within the same class. The same varieties but derived from different breeders have also been predicted within the same class.

Discussion

Discriminating analysis of resistant and susceptible gerbera plants showed that gerberin, parasorboside, gerberinside, and 5-hydroxyhexanoic acid 3-*O*-*β*-D-glucoside can be used as biomarkers for resistance to powdery mildew. Independent of leaf age, these compounds showed greater concentrations in the resistant compared to the susceptible varieties. These polyketide-derived glycosylated molecules are compounds well-known present in gerbera (Bohlmann et al., 1973; Teeri et al., 2006), where the aglycones are considered to play a role in defending the plant against pathogens (Koskela et al., 2001, 2011; Pietiäinen et al., 2016). Gerberin and parasorboside are produced in large amounts in all gerbera tissues and are described as bitter tasting glycosidic lactones (Yrjönen et al., 2002; Pietiäinen et al., 2016). Gerberin aglycone is known as 5,6-dihydro-4-hydroxy-6-methyl-2*H*-pyran-2-one. Gerbera and its close relatives produce rare coumarin-like compounds. 4-hydroxy-5-methylcoumarin, which is the aglycone component of gerberinside. This compound is somewhat taxonomically restricted to *Gerbera* spp. (Inoue et al., 1989; Nagumo et al., 1989; Pietiäinen et al., 2016), however, its derivatives occur in other taxa within the Asteraceae family, such as in *Mutisia* spp. (Zdero et al., 1988). Moreover, an occurrence in taxonomically unrelated *Diospiros* spp. has been reported (Paknikar et al., 1996). It is important to mention, that this compound is formed by a polyketide synthase in the acetate-mevalonate pathway and not the shikimate (phenylpropanoid) pathway, the source of relatively common coumarins found particularly in plants of the Apiaceae and Rutaceae families (Bourgaud et al., 2006; Pietiäinen et al., 2016).

Gerbera expresses three genes encoding for 2-pyrone synthases (*G2PS1*, *G2PS2*, and *G2PS3*) which are chalcone synthase-like polyketide synthases with altered starter substrate specificity (Helariutta et al., 1996). *G2PS1* is present in the whole plant and is responsible for the synthesis of 4-hydroxy-6-methyl-2-pyrone (triacetolactone), a putative precursor of gerberin and parasorboside (Eckermann et al., 1998). *G2PS2*, expressed in the leaf blades and inflorescences, and *G2PS3*, expressed in the roots, are necessary for the biosynthesis of 4-hydroxy-5-methylcoumarin. *G2PS2* and *G2PS3* lead to the formation of 4,7-dihydroxy-5-methylcou-

marin. The further pathway is unknown, but a reductase enzyme is likely required to complete the pathway for the biosynthesis of 4-hydroxy-5-methylcoumarin (Pietiäinen et al., 2016).

Chemometrics gives us a tool to study the relationships among multiple metabolites at the same time. The decision tree explains more complex relationships between compounds, which are not elucidated by a univariate statistical approach. The main node of the decision tree is gerberinside, which suggests that this compound plays the most important role in defining resistance. A comparable result was obtained from the OPLS-DA. Signals from the compound were assigned the highest values of absolute *p*(corr) and significance by the *t*-test. The antifungal activity of plant coumarins has been investigated and confirmed (Sardari et al., 2000). In particular, gerberinside aglycone (4-hydroxy-5-methylcoumarin) was observed to be more effective than gerberin aglycone, triacetolactone, and sorbic acid for inhibiting the growth of *B. cinerea*, *Heterobasidium annosum*, and *Rhizoctonia solani* in *in-vitro* tests using artificial media (Koskela et al., 2011). According to the decision tree, resistant varieties with low concentrations of gerberinside were characterized by greater concentrations of gerberin and parasorboside. Parasorboside is regarded as a precursor of parasorbic acid, the plant form of the widely used food preservative sorbic acid (Tschesche et al., 1971; Koskela et al., 2011). In agreement with our results, the concentrations of gerberin and parasorboside varied greatly between different gerbera varieties, with varieties resistant to B. cinerea containing greater concentrations than these more susceptible (Koskela et al., 2001). In most varieties, gerberin was most abundant in the flowers, whereas the highest level of parasorboside was observed in both the leaf and the scape (Koskela et al., 2001). Plants in which the pathway was inhibited with antisense *G2PS1* blocking the synthesis of gerberin and parasorboside showed increased susceptibility to *Botrytis cinerea* (Koskela et al., 2011). Geberin aglycone inhibited the growth of *B. cinerea*, *Heterobasidium annosum*, and *Rhizoctonia solani* (Koskela et al., 2011). In addition, parasorboside has been demonstrated to be an antifeedant agent for the larvae of the yellow butterfly *Eurema hecabe mandarina* (Numata et al., 1990). The decision tree suggested that 5-hydroxyhexanoic acid 3-*O*-*β*-D-glucoside may also play a role in resistance to mildew. Strong structural similarities to parasorboside suggest that this compound may be part of the gerberin pathway. Further investigation is needed to clarify the role of this compound in gerbera.

The segregated class of isolated compounds was glycosylated. As the first chemical barriers to attacking organisms, preformed inhibitory compounds play a key role in the early stages of plant defence. However, these compounds may also be toxic for plant itself. One of the strategies implemented by the plants,

and shaped by continuous evolutionary forces regulated by the adaptation of the host-plant, is therefore conjugation of the toxic defense compound with various organic molecules, including sugars. The detoxification of a harmful compound by glycosylation can generate a non-toxic agent and often leads to sequestration in a storage compartment such as the cell vacuole (Jones and Vogt, 2001; Gachon et al., 2005). When a pathogen attacks, the detoxified compound is activated by glycosyl hydrolases released by the host plant or the invading organism (Osbourn, 1996; Minic, 2008; Murphy et al., 2011). Glycosylation increases the water solubility and also stability of hydrophobic metabolites, improving their bio-distribution and metabolism (Jones and Vogt, 2001; Gachon et al., 2005).

Conclusion

NMR-based metabolomics coupled with chemometrics can detect plant metabolites involved in resistance to powdery mildew in plants. Based on the contents of gerberin, parasorboside, gerberinside and 5-hydroxyhexanoic acid 3-*O*-*β*-D-glucoside, model for the prediction of resistance to a powdery mildew was developed. Collecting more data on more varieties and on more time points during crop growth will improve the model even further. Such a model enables screening of existing varieties and also breeding population intended for the development of new varieties. As such, the metabolites can function as biomarkers for resistance to mildew and represent a crucial tool for resistance breeding programs. Especially so since powdery mildew is an obligate biotroph pathogen, which until now only could be tested by using relatively small scale, labor- and capital-intensive plant bio-assays; validation of the single compounds by *in-vitro* bioassays is hampered. Single compounds would need to be separated, whereby the separation of gerberin and parasorborside would form a major challenge (Yrjönen et al., 2002). Even if compounds would be applied as a mixture, powdery mildew as an obligate fungus does not grow on artificial substrates to which the compounds in question could be added. Here we have an alternative metabolomics-based approach to create decision trees that enabled us to detect the compounds responsible for plant resistance, and to determinate their synergies and relative contributions to the overall effect. This approach seems to be particularly important for obligate biotrophic plant pathogens such as powdery mildew, for which bioassays are not easy to carry out.

Acknowledgements

We thank Marianne Noordam for her technical assistance in regard to collection and preparation of samples. This work was supported by the Dutch Top Sector project 'Natural resistance to powdery mildew' (TU 18007). We thank the Dutch Greenhouse Horticulture (Glastuinbouw Nederland), the Foundation Kijk, the Dutch gerbera and rose growers' association, and the cooperation Royal FloraHolland for their financial assistance. This study was also supported by the European Regional Development Fund-Project No. CZ.02.1.01/0.0/0.0/16_019/0000845 and by a METROFOOD-CZ research infrastructure project (MEYS Grant No: LM2018100) including access to its facilities.

4

CHAPTER 5

Biochemical and physiological changes in *Zea mays* L. after exposure to the environmental pharmaceutical pollutant carbamazepine

Based on:
Mascellani, A., Mercl, F., Kurhan, S., Pierdoná, L., Kudrna, J., Zemanová, V., Hnilička, F., Kloucek, P., Tlustos, P., and Havlik, J. (2023). Biochemical and physiological changes in *Zea mays* L. after exposure to the environmental pharmaceutical pollutant carbamazepine. *Chemosphere* 329, 138689. doi:10.1016/j.chemosphere.2023.138689.

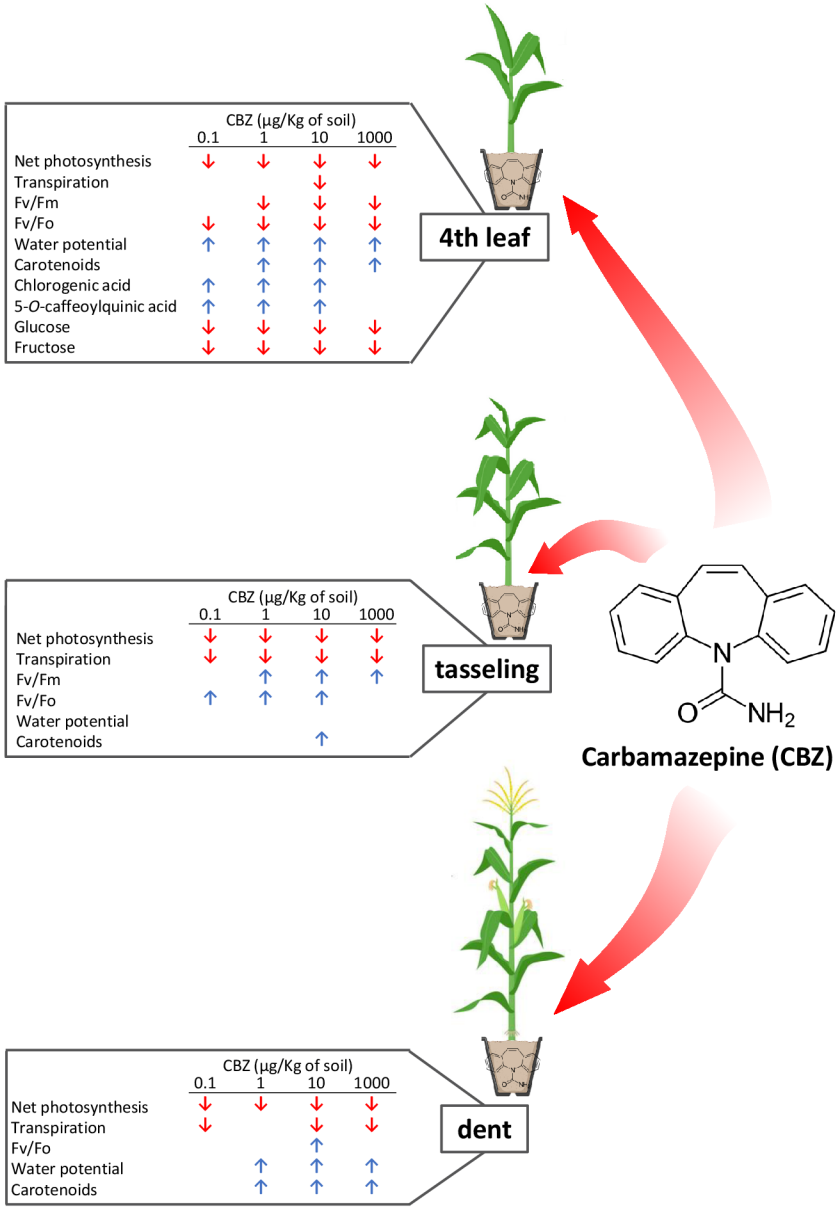

Abstract

The presence of pharmaceuticals in the environment is a matter of great concern. They are consistently found in the environment, raising concerns regarding human exposure through dietary intake. In this study, we observed the effect of the application of carbamazepine at 0.1, 1, 10, and 1000 µg per kg of soil contamination levels to assess stress metabolism in *Zea mays* L. cv. Ronaldinio at the 4th leaf, tasselling, and dent phenological stages. The transfer of carbamazepine to the aboveground and root biomass was assessed, and uptake increased dose-dependently. No direct effect on biomass production was observed, but multiple physiological and chemical changes were observed. Major effects were consistently observed at the 4th leaf phenological stage for all contamination levels, including reduced photosynthetic rate, reduced maximal and potential activity of photosystem II, decreased water potential, decreased carbohydrates (glucose and fructose) and γ-aminobutyric acid in roots, and increased maleic acid and phenylpropanoids (chlorogenic acid and its isomer, 5-*O*-caffeoylquinic acid) in aboveground biomass. A reduction in net photosynthesis was observed for the older phenological stages, whereas no other relevant and consistent physiological and metabolic changes related to contamination exposure were detected. Our results indicate that *Z. mays* can overcome the environmental stress caused by the accumulation of carbamazepine with notable metabolic changes at the early phenological stage; however, older plants adapted and only exhibited minor effects in the presence of the contaminant. The potential implications for agricultural practice could be associated with the plant's response to simultaneous stresses due to metabolite changes associated with oxidative stress.

Keywords: carbohydrate; carotenoid; GABA, chlorogenic acid; photosynthesis; soil contaminant.

Author contribution: I contributed to the current study by carrying on the NMR metabolomics analysis including extraction, data acquisition and processing. I contributed to NMR structural elucidation and compound isolation. I carried out the statistical analysis and created the artwork. I drafted the original manuscript and curated the article until acceptance.

Introduction

Pharmaceutical residues in aquatic and soil environments and their potential ecotoxicity are environmental concerns. Recent scientific evidence has revealed an alarming number of pharmaceutical residues in the effluents of wastewater treatment plants, surface and ground waters, and drinking water (Miège et al., 2009). Irrigation with treated wastewater and the application of biosolids and manure to arable land exposes the agro-environment to pharmaceuticals and personal care products which can be taken up by crops. The current study focused on the widely used antiepileptic drug carbamazepine (CBZ), a ubiquitous pharmaceutical that is frequently detected in wastewater, natural water bodies, and arable soils at concentrations ranging from ng/L to µg/L in water and ng/kg to mg/kg in biosolids and arable land (Calderón-Preciado et al., 2011; Dordio et al., 2011; Dalkmann et al., 2012; Aznar et al., 2014; Shao et al., 2018; Mejías et al., 2021). CBZ is one of the most recalcitrant pharmaceutical compounds in wastewater and aquatic environments (Dordio et al., 2011; Li et al., 2013; Shao et al., 2018) with high bioaccumulation factors in plants (Hurtado et al., 2017). The fate of CBZ and its metabolites in the agro-ecosystem, including sorption, leaching, and plant uptake, has been previously studied (Fenet et al., 2012; Paz et al., 2016). CBZ accumulates in the top soil layer because of its sorption onto soil organic matter, and its availability for plant uptake is caused by desorption (Williams et al., 2006; Arye et al., 2011; Paz et al., 2016). CBZ in soil can be further degraded into different biologically active products, including 10,11-dihydro-10-hydroxycarbamazepine, carbamazepine-10,11-epoxide, acridone-*N*-carbaldehyde, 4-aldehyde-9-acridone, and acridine (Li et al., 2013). The most commonly present metabolites in wastewater, carbamazepine-10,11-epoxide and 10,11-dihydro-10,11-dihydroxycarbamazepine, have lower sorption affinities and higher mobilities in soils than the parental drug (Fenet et al., 2012; Paz et al., 2016); therefore, they can be easily transported from the soil surface to the aquifer. CBZ is taken up from the soil by a range of agriculturally important vegetables; the plant uptake of CBZ differs among different plant species and cultivation conditions. CBZ accumulation was reported for radish, arugula, lamb's lettuce (Kodešová et al., 2019), lettuce (Wu et al., 2013; Hurtado et al., 2017; Kodešová et al., 2019; Leitão et al., 2021), spinach (Wu et al., 2013; Kodešová et al., 2019), cucumber (Shenker et al., 2011; Wu et al., 2013), celery, carrot, pak-choi (Li et al., 2018a), maize (Marsoni et al., 2014; Ryšlavá et al., 2015; Beltrán et al., 2020; Pérez et al., 2022), tomato (Goldstein et al., 2014; Riemenschneider et al., 2017), zucchini (Goldstein et al., 2014; Carter et al., 2015; Knight et al., 2018), pepper

(Wu et al., 2013), and rocket (Marsoni et al., 2014). Although pharmaceuticals are consistently found in the environment and absorbed by plants, little is known about their effects on plant biochemistry, health, or crop yield parameters, which may affect the resilience of production systems. *Zea mays* L. is one of the most economically important food crops worldwide and its cultivation cycle requires significant amounts of water during plant growth and flowering (Marsoni et al., 2014). Reclaimed water could be important for maize irrigation (Pérez et al., 2022) and CBZ residues in treated wastewater can lead to soil contamination and affect growth, biomass yield, and yield quality. Maize is an important crop and a potential gateway for pharmaceuticals to enter the food chain. This study aimed to mimic the presence of CBZ in soil as consequence of application of biosolid amendments or treated wastewater containing pharmaceuticals and uncover the physiological and metabolic effects of CBZ exposure on maize (*Zea mays* L. cv. Ronaldinio) to point out the agronomic possible impact of CBZ presence in soil. On the basis of confirmed soil pollution, four contamination levels were selected: 0.1 µg CBZ/kg mimics contamination from short-term irrigation using surface waters (Calderón-Preciado et al., 2011), 1 µg CBZ/kg simulates the use of surface waters for irrigation on a regular basis (Aznar et al., 2014), 10 µg CBZ/kg represent the soil concentration produced by the application of sewage sludge (Mejías et al., 2021) and 1000 µg CBZ/kg was chosen as positive control. Therefore, changes in CBZ accumulation, yield, selected physiological parameters, photosynthetic pigments, and plant metabolites at the three different phenological stages corresponding to the 4th leaf, tasselling, and dent were examined. This study highlights the impact of CBZ on the metabolic profiles of major phytochemical constituents at various developmental stages and explores the effect of low contaminant concentrations, similar to environmentally detected doses found in contaminated soils, on maize. To date, there have been no metabolomics studies on major cereal crops reflecting the CBZ contamination levels normally achieved with common agricultural practices.

Materials and methods

Plant material, experimental design, growth conditions, and sampling

The pot experiment was performed in a 3 × 5 full factorial design (three sampling times, five pollution/control treatments), where each treatment was replicated three times, resulting in a total of 45 pots. Each pot contained 5 kg (dry weight, d.w.) of soil or soil-carbamazepine mixture. Four experimental concentrations of CBZ were used, 0.1, 1, 10, and 1000 µg CBZ per kg (d.w.) of soil, and were reported in this study as CBZ0.1, CBZ1, CBZ10, and CBZ1000, respectively. The CBZ standard solution was thoroughly mixed with the unpolluted soil prior to sowing. The soil used was Chernozem (Mollisol) collected from a long-term field trial (plough depth 30 cm) at the Czech University of Life Sciences in Prague, where no fertilisers have been applied since 1996. The soil was neutral sandy loam (pH_{CaCl2} = 7.1) with 1.6% C_{ox}f, 0.14% N_{tot} and 118 mg/kg available $P_{Mehlich III}$. More details about the field trial and site (Suchdol, Prague) are reported by Kulhánek et al. (2016). Eight *Z. mays* L. cv. Ronaldinio seeds (KWS saat SE & Co. KGaA, Einbeck, Germany) were sown on June 5th, 2020, and the germinated plants were reduced to three plants per pot at the emergence of the 3rd leaf. The experiment was conducted in an outdoor precipitation-controlled vegetation hall under natural lighting and temperature conditions. The positions of the pots were fully randomised on a weekly basis. The plants were irrigated with tap water, demineralised by reverse osmosis, till 50% of the soil water-holding capacity was reached (controlled gravimetrically every third day). Three biological replicates (three pots, three plants each) were collected for each experimental condition at 46, 75, and 117 days after sowing, which corresponded to the 4th leaf, tasselling, and dent phenological stages, respectively. Harvested plants were separated into roots and shoots. The collected samples were weighed, washed in demineralised water, immediately frozen in liquid nitrogen, ground to a fine powder using a mortar and pestle, freeze-dried, and stored at −80 °C till further analyses.

Reagents and materials

All the chemicals and reagents used were of analytical grade. Potassium dihydrogen phosphate (99%, KH_2PO_4), deuterium oxide (99.9%, D_2O), methanol-d_4 (99.8%, MeOD), and methanol (MeOH) were purchased from VWR Interna-

tional (Radnor, Upper Marion, PA, USA). Sodium deuteroxide in D_2O (99.5%, NaOD; 40% w/v) solution was purchased from Alfa Aesar (Kandel, Germany). The 3-(trimethylsilyl) propionic-2,2,3,3-d_4 acid sodium salt (99%, TSP) and carbamazepine (>99% purity) were purchased from Sigma-Aldrich (St. Louis, MO, USA). Carbamazepine-$^{13}C_6$ (CBZ-$^{13}C_6$) in MeOH was purchased from Cerilliant (Round Rock, TX, USA). Chemicals used for CBZ quantification by liquid chromatography coupled with mass spectrometry (LC-MS), namely MeOH, acetonitrile (MeCN), and formic acid (HCOOH), were of LC-MS grade and purchased from Honeywell (Charlotte, NC, USA). Dimethylformamide (99%) for determining pigment content in the leaves was purchased from VWR International (USA).

Pigment and physiological analysis

Chlorophyll A (Chl A), chlorophyll B (Chl B), total chlorophyll (ΣChl), and carotenoid (Crt) pigment levels in the leaves were measured using an Evolution 2000 UV-Vis spectrophotometer (Thermo Fisher Scientific Inc., Waltham, MA, USA), following the method described by Zemanová et al. (2020). The mean value of five replicates was calculated for each biological replicate. Additionally, chlorophyll fluorescence, expressed as maximal photosystem II (PSII) photochemical efficiency (Fv/Fm), and potential activity of PSII (Fv/Fo) were measured using a modulated chlorophyll fluorometer OS1-FL (OptiSciences, ADC BioScientific, Ltd., Hoddesdon, UK) as previously described (Zemanová et al., 2020). The mean value of five technical replicates is presented for each biological replicate. The leaf net photosynthetic rate (*A*), transpiration rate (*E*), and stomatal conductance (g_s) were determined using the portable gas-exchange system LCpro+ (ADC BioScientific Ltd., Hoddesdon, UK), as previously described (Zemanová et al., 2020). The mean value of ten replicates was used for each biological replicate. All measurements were conducted between 8:00 a.m. and 11:30 a.m., just before harvesting. Plant water status (water potential) was measured as the leaf water potential (WP) using a dew point PotentiaMeter (Decagon Devices, Inc., Pullman, WA, USA), as previously described (Zemanová et al., 2020). The mean value of three replicates was used for each biological replicate.

Quantification of carbamazepine in plant tissues

Root and aboveground biomass samples from the CBZ10 and CBZ1000 treatments were extracted using a protocol previously described by Mercl et al. (2021). Briefly, 0.1 g of freeze-dried biomass in a 15 mL polypropylene test tube was spiked with CBZ-$^{13}C_6$ and extracted twice with 5 mL of MeOH:H_2O (50:50, v:v). The aqueous solution (pH = 2.5) consisted of 0.5% HCOOH and 0.1% Na_2EDTA. Extraction was performed by sonication for 15 min. Supernatants obtained by centrifugation at 6000 × g for 5 min were mixed. Proteins were then precipitated from a 2-mL aliquot by adding 200 µL of 5-sulfosalicylic acid (450 mg/mL, water solution). Finally, the protein-free supernatant was filtered through a syringe filter (regenerated cellulose, 0.22-µm pore size) and analysed by liquid chromatography with tandem mass spectrometry (LC-MS/MS). Matrix-matched calibrations were prepared from aboveground and root control treatment biomass. The CBZ concentrations in samples CBZ0.1 and CBZ1 were below or close to the limit of quantification of the method described above. Therefore, these samples (1 g) were spiked as described above and extracted twice by sonication for 15 min in 5 mL of MeOH. The supernatant obtained by centrifugation (6000 × g, 5 min) was passed through a solid-phase extraction cartridge (Chromabond HLB, 60 µm, 6 mL/150 mg; Macherey-Nagel GmbH & Co. KG, Dueren, Germany), previously washed with MeOH, and conditioned with MilliQ water. After passing the sample through the cartridge, the cartridge was flushed with MeOH. The filtrate collected was evaporated under a gentle stream of nitrogen until dry and re-dissolved in 2 mL of H_2O:MeCN (75:25 v:v) for LC-MS/MS analysis. Matrix-matched calibrations were prepared for aboveground and root biomass separately. Chromatographic separation of CBZ was performed using an ultra-high performance liquid-chromatography system (Agilent 1290 Infinity II, Agilent Technologies, Santa Clara, CA, USA) with 0.005% HCOOH and MeOH as mobile phases A and B, respectively. A triple quadrupole mass spectrometer (MS) (6495B, Agilent Technologies, Santa Clara, CA, USA) equipped with electrospray ionisation (ESI) was used in multiple reaction monitoring mode. The detailed parameters of chromatographic separation, ESI, and MS were identical to those described by Mercl et al. (2021). Overall details of the method performance can be found in Supplementary Table S6 including the method limits of quantification, and absolute recoveries.

Metabolic profile analysis

Nuclear magnetic resonance (NMR) was the analytical method of choice for quantitatively determining the 24 abundant primary and secondary metabolites in this study. Fifty milligrams of the homogenised, freeze-dried finely ground plant part was extracted in MeOD-D_2O (1:1, v/v), as previously described (Kim et al., 2010; Mascellani et al., 2021). All spectra were recorded at 298 K at a ^1H NMR frequency of 500.23 MHz using a Bruker Avance III spectrometer equipped with a broadband fluorine observation SmartProbe™ with z-axis gradients (Bruker BioSpin GmbH, Rheinstetten, Germany). After acquisition, spectra were processed as previously described (Mascellani et al., 2021). All samples were subjected to exponential apodization (0.3 Hz), and phase correction was performed using Topspin 3.6.1 (Germany). The spectral intensities of the ^1H NMR spectra were scaled to the intensity of the internal standard (TSP, 0.01% [w/v]) and preprocessed using an in-house script and MATLAB® R2020a (MathWorks, Natick, MA, USA) consisting of multipoint baseline correction in user-defined segments, ensuring the same pre-processing for all spectra. Spectra were reduced to predefined spectral bins containing annotated peaks by the sum of data points included in the region between δ_H 0.05–9, considering the peak shape for segment definition with bin borders set in baseline regions. The regions corresponding to water (δ_H 4.70–5.00 ppm) and methanol (δ_H 3.28–3.40 ppm) were excluded from the analysis. Annotation was based on previous publications and operator knowledge (Leiss et al., 2009b; Vinci et al., 2018).

Statistical analyses

Three independent biological replicates were used for each experiment. The data analysis was conducted using MATLAB® R2020a (USA). Comparisons were performed between control and CBZ-exposed plants with each plant part and phenological stage being considered as an independent experiment; therefore, a one-way analysis of variance followed by Dunnett's post-hoc test was used with CBZ concentration as a factor (Pokala, 2012). Fold change (FC) was calculated as the ratio of the average changes between treatments and the control. The principal component analysis (PCA) algorithm used was implemented in PLS_Toolbox 8.9 (Eigenvector Research, Manson, WA, USA).

Results

Biomass production and CBZ accumulation

The level of CBZ contamination did not affect the production of root or aboveground biomass (Table 5) at any phenological stage. The plants accumulated CBZ in both aboveground and root biomass, which increased with increasing concentrations of CBZ in the soil (Table 6).

Table 5 | Dry yield of *Z. mays* biomass grown in CBZ-contaminated soil. Values are means ± standard deviation of three biological replicates expressed as g of dry matter/pot.

Phenological stage	Plant part	Yield				
		control	CBZ0.1	CBZ1	CBZ10	CBZ1000
4th leaf	aboveground biomass	5.32±0.48	4.50±0.21 $^{n.s.}$	4.05±0.52 $^{n.s.}$	5.04±0.99 $^{n.s.}$	4.82±0.40 $^{n.s.}$
tasseling	aboveground biomass	14.47±0.63	16.37±1.77 $^{n.s.}$	14.19±0.53 $^{n.s.}$	14.65±0.99 $^{n.s.}$	14.68±1.53 $^{n.s.}$
dent	aboveground biomass	18.09±2.03	20.15±3.69 $^{n.s.}$	20.35±0.51 $^{n.s.}$	20.92±1.49 $^{n.s.}$	20.27±1.75 $^{n.s.}$
4th leaf	root biomass	3.42±0.14	2.87±0.43 $^{n.s.}$	2.66±0.25 $^{n.s.}$	3.14±0.46 $^{n.s.}$	2.79±0.52 $^{n.s.}$
tasseling	root biomass	5.82±0.62	6.39±1.19 $^{n.s.}$	5.05±1.35 $^{n.s.}$	5.84±0.87 $^{n.s.}$	7.09±0.09 $^{n.s.}$
dent	root biomass	6.30±1.98	6.92±1.06 $^{n.s.}$	7.42±0.90 $^{n.s.}$	8.08±1.45 $^{n.s.}$	7.89±0.41 $^{n.s.}$

Table 6 | CBZ content in dry *Z. mays* biomass. Values are means ± standard deviation of three biological replicates expressed as ng/g d.w.

Phenological stage	Plant part	Soil contamination				
		control	CBZ0.1	CBZ1	CBZ10	CBZ1000
4th leaf	aboveground biomass	n.d.	0.07 ± 0.03	0.21 ± 0.01	4.19 ± 0.14	717.09 ± 44.48
tasseling	aboveground biomass	n.d.	0.04 ± 0.01	0.50 ± 0.05	6.41 ± 1.28	1,669.35 ± 148.22
dent	aboveground biomass	n.d.	0.07 ± 0.04	0.47 ± 0.11	5.70 ± 1.93	1,739.59 ± 116.72
4th leaf	root biomass	n.d.	0.10 ± 0.00	1.12 ± 0.13	12.29 ± 0.94	2,223.62 ± 252.74
tasseling	root biomass	n.d.	0.11 ± 0.00	0.92 ± 0.05	11.30 ± 0.86	1,698.63 ± 161.01
dent	root biomass	n.d.	0.11 ± 0.00	0.76 ± 0.14	10.49 ± 0.67	1,630.83 ± 132.72

Physiological and pigment changes

The 4th leaf phenological stage of *Z. mays* in the CBZ-contaminated soil result in a decrease in A (Figure 10A) at all CBZ concentrations. Fv/Fm, as an indicator of plant photosynthetic activity, and Fv/Fo, as an indicator of the number and size of active photosynthetic reaction centres, statistically decreased for CBZ1, CBZ10, and CBZ1000, with the exception of CBZ0.1, where only Fv/Fm decreased (Figure 10B, C). WP increased in the presence of pollutants in the soil (Figure 10D). Regardless of the presence of CBZ in the soil, g_s and *E* were not statistically different from those of the control, except for CBZ10, where a decrease was observed (Figure 10E, F). Concerning the pigments, the amount of Crt increased with the presence of CBZ in the soil at contamination levels above and equal to 1 µg CBZ per kg (d.w.) of soil (Figure 11A). The ΣChl and Chl A were not affected by the treatments (Figure 11B, C), whereas Chl B only decreased with the highest CBZ exposure (Figure 11D).

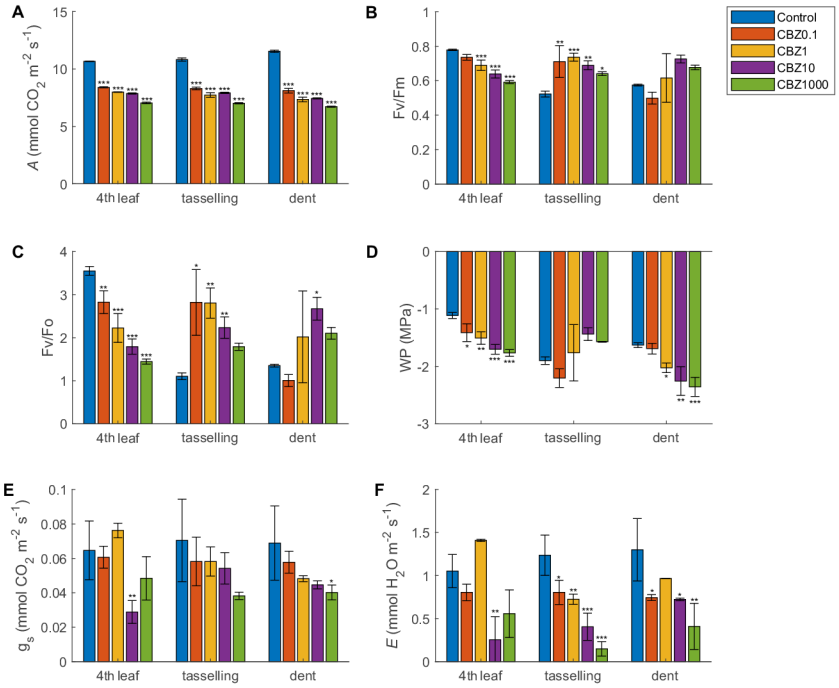

Figure 10 | Physiological parameters of control and CBZ-exposed *Zea mays* cv. Ronaldinio plants. Treatments include 0.1 (CBZ0.1), 1 (CBZ1), 10 (CBZ10), and 1000 µg (CBZ1000) CBZ per kg (d.w.) of soil at the 4th leaf, tasselling, and dent phenological stages. (**A**) Leaf net photosynthetic rate; (**B**) maximal photosystem II photochemical efficiency; (**C**) potential PSII activity; (**D**) leaf water potential. Values are means ± standard deviation; (**E**) stomatal conductance; (**F**) leaf transpiration rate. Asterisks indicate significant differences in comparison with the control (*$p \leq 0.05$, ** $p \leq 0.01$, *** $p \leq 0.001$). CBZ, carbamazepine.

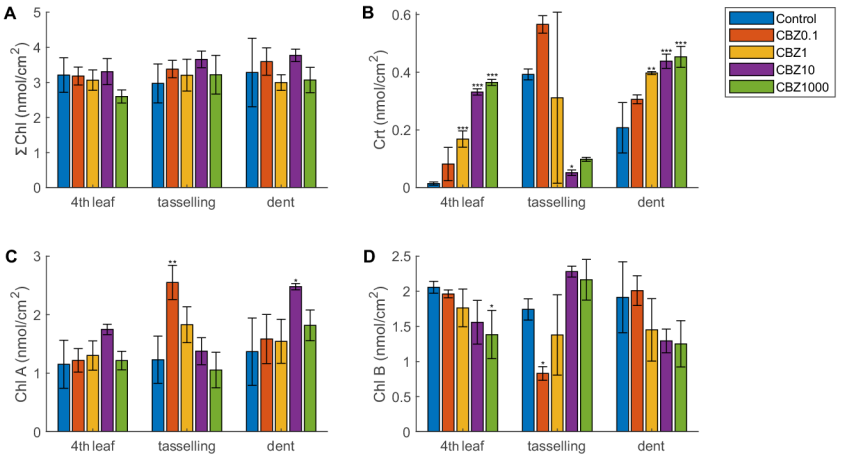

Figure 11 | Pigment content in control and CBZ-exposed *Zea mays* cv. Ronaldinio plants. Treatments included 0.1 (CBZ0.1), 1 (CBZ1), 10 (CBZ10), and 1000 µg (CBZ1000) CBZ per kg (d.w.) of soil at the 4th leaf, tasselling, and dent phenological stages. (**A**) carotenoids; (**B**) total chlorophyll; (**C**) chlorophyll A; (**D**) chlorophyll B. Values are means ± standard deviation. Asterisks indicate significant differences in comparison with the control (*$p \leq 0.05$, ** $p \leq 0.01$, *** $p \leq 0.001$). CBZ, carbamazepine.

At tasselling, *A* reduced for all treatments (Figure 10A), similarly to the other phenological stages. Fv/Fm and Fv/Fo increased significantly for CBZ0.1, CBZ1, and CBZ10, and only Fv/Fm increased significantly for CBZ1000 (Figure 10B, C). *E* decreased with increasing concentrations of pollutants in the soil (Figure 10F). Irrespective of the presence of CBZ in the soil, g_s and WP were not statistically different from the control (Figure 10D, E). Crt only significantly decreased for CBZ10 (Figure 11A), whereas ΣChl, Chl A, and Chl B were not affected by the treatments, except for Chl A and Chl B which were affected by the lower CBZ concentration (Figure 11B–D).

Growth of *Z. mays* in CBZ-contaminated soil resulted in a decrease in *A* (Figure 10A) at the dent phenological stage as reported for the previous phenological stages; however, Fv/Fm was not different compared with the control and Fv/Fo was significantly increased for CBZ10 (Figure 10B, C). *E* decreased in CBZ0.1,

CBZ10, and CBZ1000 (Figure 10F). Significant decreases were observed in g_s for CBZ1000 (Figure 10E) and WP for CBZ1, CBZ10, and CBZ1000 (Figure 10D). Crt was significantly increased for higher contaminations, namely CBZ1, CBZ10, and CBZ1000 (Figure 11A), whereas the chlorophyll contents (Chl A, Chl B, and ΣChl) remained unchanged (Figure 11B–D), except for Chl A for CBZ10.

Metabolic changes

Metabolic changes were reflected in the primary metabolism of the root biomass and amino acids and the secondary metabolism of aboveground biomass (Figure 12) at the 4th leaf phenological stage. Decreased levels of root carbohydrates (glucose and fructose) and γ-aminobutyric acid (GABA) were observed in the pollutant treatments (Figure 12 and 13A–C). A decrease in the amino acid leucine was detected for CBZ0.1 and CBZ1 when compared with the control (Figure 12 and 13D). Metabolic changes in the aboveground biomass included a decrease in isoleucine and valine levels with CBZ0.1 and CBZ1 exposure (Figure 12 and 13E–F). A decreased concentration of threonine was only observed for the lowest CBZ concentration (Figure 12 and 13G). Maleic acid increased significantly in the aboveground biomass for the CBZ0.1 (FC 6.7), CBZ1 (FC 7.0), and CBZ10 (FC 13.4) concentrations (Figure 12 and 13H). The secondary metabolite organic acids, 3-*O*-caffeoyl and 5-*O*-caffeoylquinic acids, were highly correlated with an increase in CBZ concentration, except for the highest concentration (Figure 12 and 13I–J). Multivariate analysis of the metabolome suggested similar differences in the metabolites as described by the univariate method (Figure 14). The variance representing the differences in the aboveground biomass between the treatments was explained by PC1 and PC3, with a total variance of 53.3% (Figure 14A). The CBZ0.1, CBZ1 and CBZ10 treatments displayed increased concentrations of aspartic acid, maleic acid, malic acid, 3-*O*-caffeoylquinic acid (chlorogenic acid), 5-*O*-caffeoylqyinic acid, sucrose, and *trans* aconitic acid compared with the control (Figure 14B). Treatment with CBZ1000 was characterised by increased levels of quinic acid, shikimic acid, aspartic acid, glutamine, and choline compared with the control.

All treatments showed decreased concentrations of ethanolamine, glycine betaine, and amino acids (alanine, leucine, isoleucine, and threonine). The variance of the differences between the treatments in root biomass was explained by PC1 and PC3, with a total variance of 62.8% (Figure 14C). The variance expressed by

PC2 is not related to our hypotheses. The control differed from the treatments predominantly because of increased concentrations of fructose, glucose, leucine, glycine betaine, GABA, and 3-*O*-caffeoylquinic acid (Figure 14D).

At the tasselling phenological stage, no significant metabolic changes were identified by the NMR-based metabolomic approach (Figure 12). In the aboveground biomass, aspartic acid significantly decreased in the CBZ1 and CBZ10 treatments, and malic acid significantly decreased in CBZ1000 (Figure 12). No significant metabolic changes were observed at the dental phenological stage (Figure 12), similar to the tasselling phenological stage. In the aboveground biomass, maleic acid content increased for CBZ1 (Figure 13H).

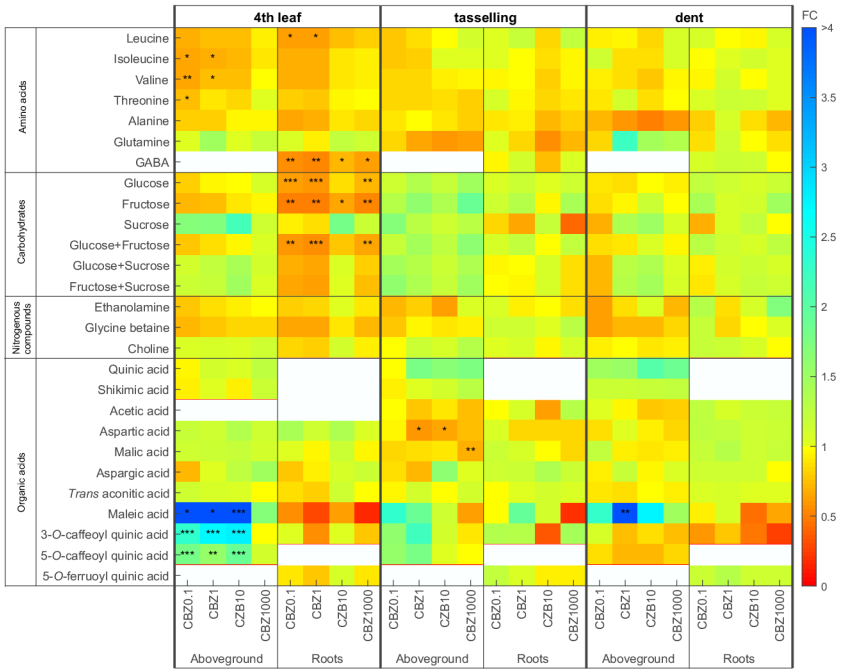

Figure 12 | Metabolites quantified in root and aboveground biomass of *Zea mays* cv. Ronaldinio. Values are fold change (FC) of means of three replicates compared to the control. Treatments included 0.1 (CBZ0.1), 1 (CBZ1), 10 (CBZ10), and 1000 µg (CBZ1000) carbamazepine per kg (d.w.) of soil at the 4th leaf, tasselling, and dent phenological stages. Asterisks indicate significant differences in comparison with the control (* $p \leq 0.05$, ** $p \leq 0.01$, *** $p \leq 0.001$). FC, fold change.

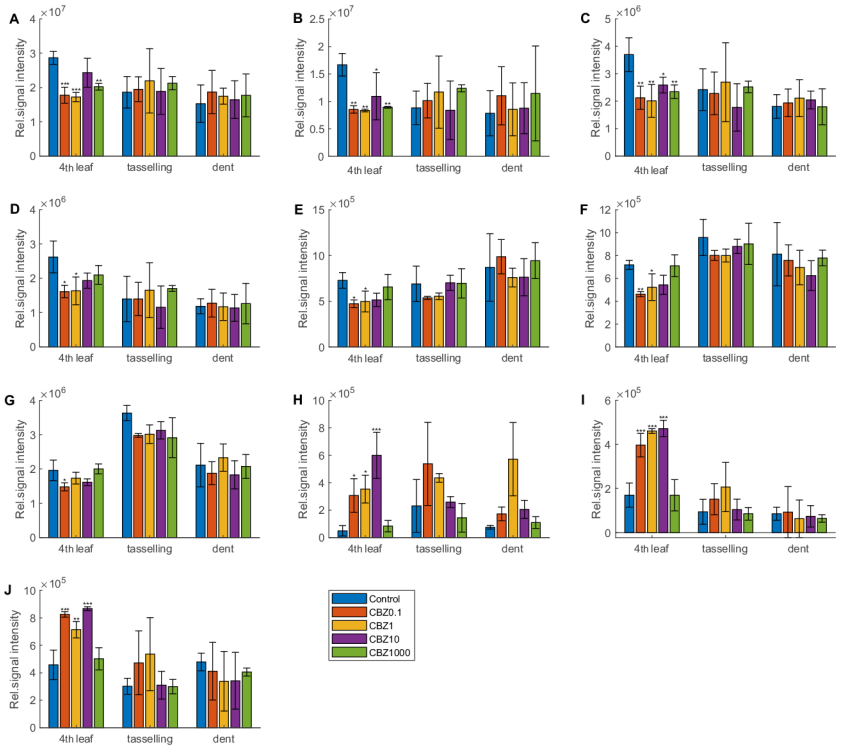

Figure 13 | Metabolite changes at the 4th leaf phenological stage in root or aboveground biomass of *Zea mays* cv. Ronaldinio. Treatments included 0.1 (CBZ0.1), 1 (CBZ1), 10 (CBZ10), and 1000 µg (CBZ1000) carbamazepine per kg (d.w.) of soil at the 4th leaf, tasselling, and dent phenological stages. (**A**) glucose in root biomass; (**B**) fructose in root biomass; (**C**) GABA in root biomass; (**D**) leucine in root biomass; (**E**) isoleucine in aboveground biomass; (**F**) valine in aboveground biomass; (**G**) threonine in aboveground biomass; (**H**) maleic acid in aboveground biomass; (**I**) 3-*O*-caffeoylquinic acid in aboveground biomass; (**J**) 5-*O*-caffeoylquinic acid in aboveground biomass. Values are means ± standard deviation. Asterisks indicate significant differences in comparison with the control (*$p \leq 0.05$, ** $p \leq 0.01$, *** $p \leq 0.001$).

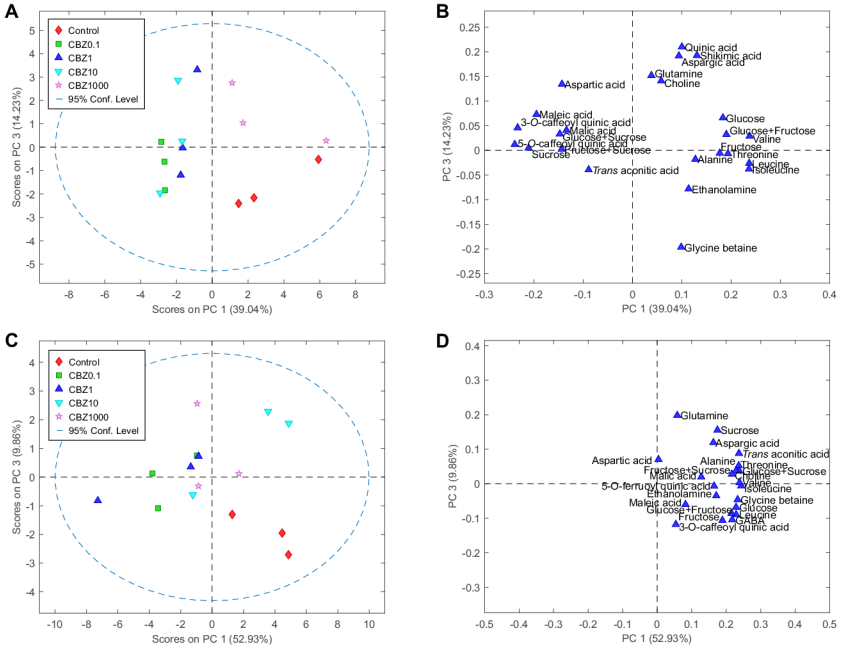

Figure 14 | Principal component analysis score and loading plots of metabolites present in aboveground and root biomass at the 4th leaf phenological stage of *Zea mays* cv. Ronaldinio. Treatments included 0.1 (CBZ0.1), 1 (CBZ1), 10 (CBZ10), and 1000 µg (CBZ1000) CBZ per kg (d.w.) of soil. (**A**) Score plot aboveground biomass; (**B**) Loading plot aboveground biomass; (**C**) Score plot root biomass; (**D**) Loading plot root biomass.

Discussion

The presence of pharmaceuticals in the environment is of major concern. CBZ is present in arable soil and water and is one of the most recalcitrant pharmaceutical compounds (Dordio et al., 2011; Li et al., 2013; Shao et al., 2018) which is taken up and accumulated in *Z. mays* (Marsoni et al., 2014; Ryšlavá et al., 2015; Beltrán et al., 2020; Pérez et al., 2022). Our results showed that *Z. mays* accumulated CBZ in the aboveground and root biomass (Table 5) when grown in Chernozem soil spiked with 0.1, 1, 10, and 1000 µg CBZ per kg (d.w.) of soil. This confirmed the plant uptake and translocation of CBZ previously reported in *Z. mays* (Mar-

soni et al., 2014; Beltrán et al., 2020; Pérez et al., 2022). The increased uptake of CBZ with increasing concentration (Table 5) in the soil suggests the potential for greater CBZ uptake by *Z. mays* at higher soil concentrations. Several plant species are capable of absorbing and detoxifying xenobiotics. However, stress typically induced by chemical pollutants leads to the activation of several biochemical and physiological pathways which may cause a significant decrease in growth, development, and productivity. The exposure of plants to active pharmaceutical ingredients is likely to impact plant development with unknown implications (Carter et al., 2015). In the present study, we did not observe any changes in biomass production, whereas multiple physiological and chemical changes were recorded, with notable effects observed in the early phenological stage. The young plants (4th leaf) were highly affected by the metabolic disruption, resulting in a decrease in the majority of physiological parameters, such as *A*, Fv/Fm, and Fv/Fo, possibly showing reduced transport of assimilates, owing to the lower WP. At later phenological stages, *Z. mays* plants were less affected by the stress, with an overall reduced effect on physiology and negligible effect on metabolite levels. The reduction in photosynthetic activity which was previously described in different crops exposed to different pharmaceuticals (Sun et al., 2018; Opriş et al., 2019) is linked to a reduction in photosynthetic pigments, decreased stomatal conductance to CO_2, and active photosynthetic reaction centres; however, this was not consistently observed in the present study (Figure 11). The inhibition of photosynthesis (Figure 10A) may explain the reduction of carbohydrates in roots at the 4th leaf stage (Figure 12 and 13A–B), which was not observed at the other stages (Figure 12). The effects of CBZ induced notable changes in metabolite levels (Figure 12), reducing GABA, glucose, and fructose in roots (Figure 12 and 13A–C), and 3-*O*-caffeoyl- and 3-*O*-caffeoylquinic acid in leaves (Figure 12 and 13I–J). A reduction in glucose and fructose in roots can be linked to the reduction of biosynthesis and translocation between roots and aboveground biomass. Changes in glucose, fructose, and sucrose levels were observed in tomato plants (*Solanum lycopersicum* L. cv. Daniella) for leaves and roots exposed to 500 nM (118.13 µg/L) and 2500 nM (590.67 µg/L) of CBZ (Gorovits et al., 2021). The authors observed an increase in sucrose in tomato plant roots irrigated with 2500 nM CBZ after 20 days, and an increase in glucose and fructose after 28 days of exposure to 2500 nM CBZ (Gorovits et al., 2021). In contrast to our findings, Gorovits et al. (2021) reported changes in the level of glucose, fructose, and sucrose in the leaves. These differences could be related to the different plants and C4 metabolism that characterizes *Z. mays*. The role of caffeoylquinic acids may be linked to protection against reactive oxygen species during exposure to pharmaceuticals, contributing to the maintenance of cellular redox status (Xu et al.,

2012). A similar hypothesis has been described for common reed (*Phragmites australis* (Cav.) Steud.) exposure to diclofenac, with the detection of higher quercetin levels (Wahman et al., 2020). The induction of oxidative stress due to the presence of CBZ in lettuce was described by the activation of multiple enzymes involved in quenching reactive oxygen species induced by oxidative stress (Leitão et al., 2021). Increased oxidative stress has been observed in cucumbers exposed to a mixture of pharmaceuticals and personal care products at environmentally relevant concentrations (Sun et al., 2018). In our study, an increase in carotenoids was reported in the 4th leaf stage (Figure 11A). These factors contribute to the reduction of oxidative stress in plants. In the CBZ0.1 and CBZ1 treatments for the 4th leaf phenological stage, leucine levels were reduced in the roots (Figure 12 and 13D) and isoleucine and valine levels were reduced in leaves (Figure 12 and 13E–F). However, branched-chain amino acids have shown to be important when carbohydrate availability is limited because they represent an important respiratory substrate to the tricarboxylic acid cycle and provide electrons directly to the mitochondrial electron transport chain (Kochevenko and Fernie, 2011). Valine, isoleucine, and leucine are osmoprotective amino acids whose concentrations increase in tomato plants irrigated with 500 and 2500 nM CBZ after 20 or 28 days of treatment (Gorovits et al., 2021). In the same study, an increase in GABA was observed in roots after 20 days of CBZ exposure, whereas we detected a decrease in GABA in roots (Figure 12 and 13C) 46 days after sowing in CBZ-contaminated soil at all four contamination levels investigated. GABA has been described to be involved in the defence against oxidative damage by inhibiting the formation of ROS, redox imbalance, and cell death in response to various abiotic stimuli (Rodrigues-Corrêa and Fett-Neto, 2019). Another compound known for being involved in process and pathways related to oxidative stress is maleic acid (Wang et al., 2021). This compound was highly increased in aboveground samples grown under CBZ0.1, CBZ1, and CBZ10 conditions. Additionally, maleic acid has been described as a product of CBZ degradation in wastewater (Yin et al., 2022); however, the high concentrations found in this study suggest that it originates from the plant metabolism itself. Conversely, the older plants did not show relevant metabolite changes, even though the CBZ concentration in the biomass did not decrease over time, leading to the hypothesis that older plants adapted to the environmental conditions and withstood the presence of CBZ. The yield of the crop was not affected by the CBZ treatments (Table 6), despite alterations in *A*, *E*, Fv/Fm, Fv/Fo, and carotenoids being observed (Figure 10, 11). The effect was monotonic and nonlinear with the dose and was particularly notable for the lowest concentrations (CBZ0.1 and CBZ1), which are the most relevant concentrations as these are mostly found in arable soil. The results

suggest that maize physiology is altered in the early developmental stage when exposed to CBZ, which could have potential implications for agricultural practice. These implications are likely not related to yield or production but could be associated with the plant's response to simultaneous stresses, a particular concern in today's agriculture, which is challenged by climate change. It can be hypothesised that plants grown in soil contaminated by CBZ could have a weaker response to other stresses such as flooding and heavy precipitation events commonly observed in the US (Milly et al., 2002), or warmer temperatures and reductions in annual precipitation more common in Mediterranean areas (Meza et al., 2008). Our study found that physiological and metabolic responses of maize to soil CBZ are linked to metabolites associated with oxidative stress. However, from the present study, it's not clear whether the cause of these changes could be the parent compound, or its toxic metabolites generated in the rhizosphere or inside the plant. Nevertheless, CBZ was reported as being slowly degraded in soil up to 5-30% depending on texture, microbial activity, organic matter content and aerobic condition (Li et al., 2013; Thelusmond et al., 2016). The metabolite acridone-N-carbaldehyde, which has been found to be present in a significant portion of soil and resistant to further degradation, may be a potential contributor to these changes and requires further investigation (Li et al., 2013).

Conclusion

The results of this study indicated that different CBZ concentrations in the soil results in changes in the metabolism of *Z. mays* at different phenological stages. CBZ contamination levels comparable to those found in arable soils affect the early phenological stage of *Z. mays*, while older plants adapt and only display minor effects due to the contaminant. CBZ was translocated from the soil to the plant roots and, to a lesser extent, to the aboveground biomass; CBZ accumulation corresponded well with the applied rate. The presence of CBZ in soil resulted in a decrease in net photosynthesis in all three phenological stages, but it was not directly proportional to increasing contaminant concentration. The decrease in the photosynthetic rate was not due to a decrease in stomatal conductance to CO_2. Plant photosynthetic activity and active photosynthetic reaction centres decreased in shoots grown in CBZ-contaminated soils at the 4th leaf stage, whereas both increased at the tasselling stage, even though net photosynthesis decreased.

Fv/Fm and Fv/Fo did not differ from those of the control in older plants. CBZ accumulation increased the content of carotenoids, but not chlorophylls, at the 4th leaf and dent phenological stages. The 4th leaf phenological stage displayed notable changes in the metabolites, with a reduction in GABA, glucose, and fructose in roots and leaves, but 3-*O*-caffeoyl and 5-*O*-caffeoyl quinic acid, increased significantly. The effect of CBZ concentration was nonlinear and monotonic, even at the lowest concentrations, suggesting high relevance to real-life settings. The effect of CBZ was highest in young plants and minor in older stages.

Acknowledgements

This work was supported by the European Regional Development Fund-Project (grant number CZ.02.1.01/0.0/0.0/16_019/0000845) and by the SGS CZU FAPPZ (grant number SV21-12-21310).

CHAPTER 6

Moderate salinity stress affects expression of main sugar metabolism and transport genes and soluble carbohydrate content in ripe fig fruits (*Ficus carica* L. cv. Dottato)

Based on:
Mascellani, A., Natali, L., Cavallini, A., Mascagni, F., Caruso, G., Gucci, R., Havlik, J., and Bernardi R. (2021). Moderate salinity stress affects expression of main sugar metabolism and transport genes and soluble carbohydrate content in ripe fig fruits (*Ficus carica* L. cv. Dottato). *Plants*. 10, 1861. doi:10.3390/plants10091861.

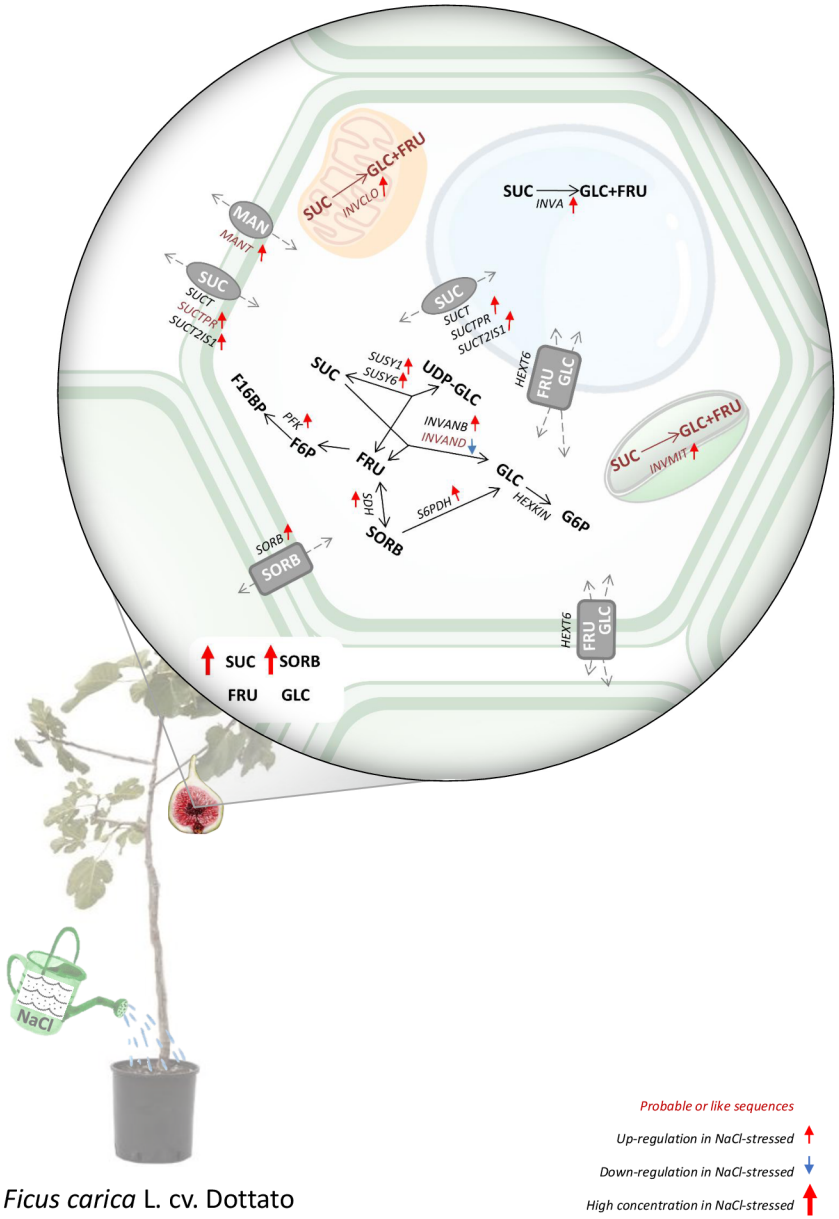

Ficus carica L. cv. Dottato

Abstract

Fig trees (*Ficus carica* L.) are commonly grown in the Mediterranean area, where salinity is an increasing problem in coastal areas. Young, fruiting plants of cv. Dottato were subjected to moderate salt stress (100 mM NaCl added to irrigation water) for 48 days before fruit sampling. To clarify the effect of salinity stress we investigated changes in the transcription of the main sugar metabolism-related genes involved in the synthesis, accumulation and transport of soluble carbohydrates in ripe fruits by quantitative real-time PCR as well as the content of soluble sugars by quantitative ^{1}H nuclear magnetic resonance spectroscopy. A general increase in the transcript levels of genes involved in the transport of soluble carbohydrates was observed. *Alkaline-neutral* and *Acid Invertases* transcripts, related to the synthesis of glucose and fructose, were up-regulated in ripe fruits of NaCl-stressed plants without a change in the content of D-glucose and D-fructose. The increases in sucrose and D-sorbitol contents were likely the result of the up-regulation of the transcription of sucrose synthase- and sorbitol dehydrogenase-encoding genes.

Keywords: *Ficus carica* L.; salinity stress; carbohydrates metabolism; RT-qPCR; qNMR; ^{1}H NMR.

Author contribution: I contributed to the current study by collecting the biological material, carrying on the qRT-PCR and NMR metabolomics analyses from extraction to raw data. I carried out the statistical analysis for all the included analyses and created the artwork. I drafted the original manuscript and curated the article until acceptance.

Introduction

Fig trees (*Ficus carica* L., Moraceae) are widely grown in the Mediterranean area for the consumption of fresh or dry fruits. In 2019, the world production of figs was about 1.3 million tonnes, with an increasing trend over the last three years. The leading country was Turkey, with a production of 310 thousand tonnes, followed by Egypt and Morocco (FAOSTAT, 2019). The consumption of fig fruits, a key component of the Mediterranean diet for millennia, is also increasing (Solomon et al., 2006; Gilani et al., 2008; Veberic et al., 2008). Fig fruits are a source of carbohydrates, vitamins, minerals, dietary fibres and amino acids, and in recent years a lot of effort and economic resources have been invested to enhance fruit quality and flavour as well as extend the storability of the highly perishable fresh fruits (Allegra et al., 2017, 2018).

Ficus carica is well known for its ability to tolerate water deficit and moderate salinity (Golombek and Lüdders, 1993; Caruso et al., 2017; Vangelisti et al., 2019; Sadder et al., 2021) that makes this species suitable to be cultivated in semi-arid environments where the use of saline or brackish water for irrigation is quite common (Tóth et al., 2008). The cultivar 'Dottato' is a bifera-type fig that is widely grown in Italy. Its 'brebas' (the first crop) are harvested between the end of June and the beginning of July, while the syconia fruit of the main crop ('fornìti') are harvested from early August to late September (Allegra et al., 2017). This cultivar showed moderate resilience to salinity (Caruso et al., 2017; Vangelisti et al., 2019).

In many species, salt stress alters leaf carbohydrate partitioning and concentration. $^{14}CO_2$ pulse-chase experiments showed an increase in mannitol and a decrease in sucrose and glucose partitioning in the leaves of salt-stressed celery and olive plants (Everard et al., 1994; Gucci et al., 1998). Salt stress also enhances fruit soluble sugar concentrations, depending on the genotype and the magnitude of stress. Salinity has been shown to reduce fruit size in many crops (Hoffman et al., 1989; Saied et al., 2005; Colla et al., 2006; Saito et al., 2008). In watermelon (Colla et al., 2006), strawberries (Saied et al., 2005) and tomato (Saito et al., 2008) salt exposure improved fruit quality by increasing dry matter, soluble solids, amino acids and soluble sugars (glucose, fructose and sucrose) concentrations. In tomato plants, salinity stress doubled starch accumulation during early developmental stages; at later stages, the complete degradation of starch to soluble sugars was responsible for the increase of sugar content in ripe red fruits (Yin et al., 2010). The main soluble carbohydrates in fig fruits are glucose and fructose, followed by sucrose (Vemmos et al., 2013). Sorbitol is present at low

concentrations and, therefore, fig is considered a sorbitol-poor species (Brown and Hu, 1996).
Many genomic tools are available for the 'Dottato' cultivar, including a haplotype phased genome sequence (Usai et al., 2020, 2021; Vangelisti et al., 2021) and a leaf transcriptome (Yin et al., 2010). Previous studies from our research group showed that the 'Dottato' transcriptome is very different from that of another fig cultivar, 'Horaishi' (Mori et al., 2017), with five hundred and thirty-four putative genes specific to the Italian cultivar (Usai et al., 2017). Some key genes involved in sugar content variability were previously identified and their expression compared between phase II (unripe fruits) and the late part of phase III (ripe fruits) of cvs. Dottato and Brogiotto (Fattorini et al., 2021). In cv. Dottato, an increased expression of a gene encoding a sucrose synthase, *SUSY1*, was shown in ripe fruits; however, another gene, *SUSY6*, showed a reduced expression. The transcripts of alkaline-neutral and acid invertases increased in the mature stages except for an *Alkaline-neutral Invertase*, *INVAND*, which decreased in ripe fruits. Sorbitol dehydrogenase (*SDH*)-encoding genes were up-regulated, as well as *Hexokinase* (*HEXKIN*) and *Phosphofructokinase* (*PFK*). Sucrose transporters-encoding genes, *SUCTPR* and *SUCT2IS1*, were up-regulated in ripe fruits compared to unripe ones; nonetheless, *SUCT* was down-regulated. Of the analysed mannitol and hexose transporter-encoding genes, *MANT* and *HEXT6*, transcript levels did not change during ripening (Fattorini et al., 2021). On the other hand, the effect of abiotic stresses on gene expression of fig fruits has not been studied so far. In the present study, we investigated the effect of short-term, moderate salinity stress on the expression of the same genes as mentioned above (Fattorini et al., 2021), involved in the synthesis, accumulation and transport of soluble carbohydrates in ripe fig fruits. The possible effect on sugar content was investigated by quantitative ^{1}H nuclear magnetic resonance (qNMR) spectroscopy.

6

Materials and Methods

Plant material and salt treatment

Sixteen plants of *F. carica* cv. Dottato (five years old), propagated by rooted cuttings from the same mother plant, were trained to a single stem and grown in a glasshouse (Fattorini et al., 2021). The substrate was a mixture of 6.4% clay,

8.6% silt and 85% sand. All plants were watered till saturation with tap water three times a week before we started the experiment. From the middle of June, half of the plants were irrigated three times a week with 700 ml of 50 mM NaCl solution for one week and then with the final 100 mM NaCl solution for the following 42 days (salt-treated plants) using distilled water. The step increment was used to alleviate the shock effect of salt and reach the final concentration gradually. The remaining eight control plants were similarly irrigated with only distilled water. The saline solution was obtained by adding NaCl (purity > 99.8%) (Sigma-Aldrich Co., St. Louis, MO, USA) to distilled water. Ripe fruits were sampled during the last part of phase III (Marei and Crane, 1971), then peeled and frozen in liquid nitrogen. The pulp (infructescence and seeds) was stored at −80°C until analysis (Fattorini et al., 2021). The sampled fruits from control and 100 mM NaCl-stressed plants were similar in morphology and colour (Supplementary Figure S1, Supplementary Table S7).

Nucleic acid isolation and analysis of gene expression

Frozen fruit pulp was ground in liquid nitrogen and 100 mg were used for the extraction of total RNA using the RNeasy® Mini Plants Kit (Qiagen, Hilden, Germany). Quantification of the total RNA samples was measured using a Qubit-iT® RNA BR Assay Kit (Life Technologies, Carlsbad, CA, USA) and the integrity was evaluated by visual observation on agarose gel electrophoresis.
The RNA samples after treatment with an Amplification Grade DNase I kit (Sigma-Aldrich Saint Louis, MO, USA) was reverse transcripted to the first-strand cDNA using a Maxima First Strand cDNA Synthesis Kit (Thermo Fisher Scientific, Waltham, MA, USA) following the manufacturer's instructions. The calibration transcription rate of the cDNA template for the following expression analysis was established by agarose gel electrophoresis of the RT-qPCR product using the primer Universal 18S ribosomal gene (QuantumRNA, universal 18S Internal Standard; Applied Biosystems/Ambion, Foster City, CA; USA).
Analysis of gene expression was carried out by RT-qPCR using Fast SYBR® Green Master Mix (Applied Biosystems, Foster City, CA, USA) with specific primers for each gene (Fattorini et al., 2021) in a StepOne® real-time PCR System (Applied Biosystems, Foster City, CA, USA) using the thermal cycling conditions reported in the use manual. The β-tubulin gene was chosen as the housekeeping gene to normalise the relative expression of each gene for both salt-stressed and control samples (Fattorini et al., 2021). The amplification of the selected genes and the

6

reference genes were run using three biological replicates and with three technical replicates each. The relative abundance of transcripts was calculated by using the $2^{-\Delta\Delta Ct}$ method (Livak and Schmittgen, 2001).

Quantitative ^{1}H NMR for the determination of free soluble carbohydrates

All chemicals and reagents used were of analytical grade. Potassium dihydrogen phosphate (99%, KH_2PO_4), deuterium oxide (99.9%, D_2O), methanol-d_4 (>99.8%, MeOD) were purchased from VWR (Radnor, PA, USA). Sodium deuteroxide 40% w/v solution in D_2O (99.5%, NaOD) was obtained from Alfa Aesar (Kandel, Germany). The 3-(trimethylsilyl) propionic-2,2,3,3-d_4 acid sodium salt (99%, TSP), D-sorbitol (≥98%), D-fructose (≥98%), D-glucose (≥98%), sucrose (≥98%) and D-mannitol (≥98%) were purchased from Sigma-Aldrich (St. Louis, MO, USA).
500 µL of MeOD and 500 µL of KH_2PO_4 buffer (90 mM, pH 6.0) in D_2O containing 0.01% TSP (w/v) were added to 50 mg of the finely ground fig pulp. The mixture was vortexed at room temperature for 1 min, ultrasonicated for 15 min and centrifuged at 24,400 × g for 10 min. An aliquot of 600 µl of the supernatant liquid was transferred to NMR tubes. The phosphate buffer was prepared by adding 90 mM of KH_2PO_4 and 0.01% of TSP. The pH was adjusted to 6.0 using 1.0 M NaOD (Kim et al., 2010).
All spectra were recorded at 298 K (25°C) on a Bruker Avance III HD spectrometer equipped with a broadband fluorine observation (BBFO) SmartProbe™ with z-axis gradients (Bruker BioSpin GmbH, Rheinstetten, Germany), operating at a ^{1}H NMR frequency of 500.23 MHz. The spectrometer transmitter was locked to MeOD, and all the spectra were recorded with the Bruker pulse sequence 'noesypr1d' for presaturation of the water signal at 4.704 ppm. Each sample was collected into 64 k data points after 128 scans and 4 dummy scans using a spectral width of 8000 Hz. The receiver gain was set to 18, the relaxation delay of 1 s, the acquisition time of 4 s and mixing time of 0.1 s. The free induction decay was multiplied by 0.3 Hz line broadening before Fourier transformation. TSP was used for calibration at 0.0 ppm.
^{1}H NMR spectra were phased and baseline corrected using Chenomx NMR suite 8.5 software, professional edition (Chenomx Inc., Edmonton, AB, Canada). The signal assignment was performed using an in-house database and spiked samples.

Experimental design and statistical analysis of data

Plants were arranged in a completely randomised experimental design in a glasshouse. Three fully-ripe fruits were sampled from three different plants for each treatment (control and salt-treated). The data for gene expression and sugar content were analysed by the Student's *t*-test using GraphPad Prism version 5.00 (GraphPad software, San Diego, CA, USA). Statistical significance was considered to occur with a p-value ≤ 0.05.
The statistical analysis for the RT-qPCR was performed by the authors from the Department of Agriculture, Food and Environment, University of Pisa. The ^{1}H NMR analysis was performed by the Department of Food Science, Czech University of Life Sciences, Prague.

Results

Salt-induced expression of genes involved in soluble carbohydrate metabolism and transport

We investigated the salinity-mediated changes in the expression of three different genes encoding sucrose transporters including *Sucrose Transporter* (*SUCT*), *Sucrose Transporter 4-Like* (*SUCTPR*) and *Sucrose Transporter 2 Isoform 1* (*SUCT2IS1*). There were no significant differences in the expression of *SUCT* (Figure 15A), whereas *SUCTPR* and *SUCT2IS1* were up-regulated in salt-treated fruits (Figure 15B–C). Moreover, we detected the transcript levels of *Sorbitol Transporter* (*SORT*) and *Probable Mannitol Transporter* (*MANT*) genes, which were higher in the pulp of the NaCl-stressed plants than in control ones (Figure 15D–E). There were no significant differences in the expression of the *Hexose Transporter 6 Like* (*HEXT6*) gene (Figure 15F).
We also analysed the expression levels of 11 key genes involved in the reversible conversion of sucrose and sorbitol into fructose and glucose. The transcript levels of *Sucrose Synthase* (*SUSY1* and *SUSY6*) genes, which catalyse the reversible conversion of sucrose into UDP-glucose and fructose (Ikegami et al., 2013; Desnoues et al., 2014), were up-regulated (Figure 16A–B). Moreover, the *Sorbitol Dehydrogenase* (*SDH*) gene, encoding the enzyme for the conversion of sorbitol into fructose (Yamaki and Moriguchi, 1989; Ikegami et al., 2013; Desnoues et

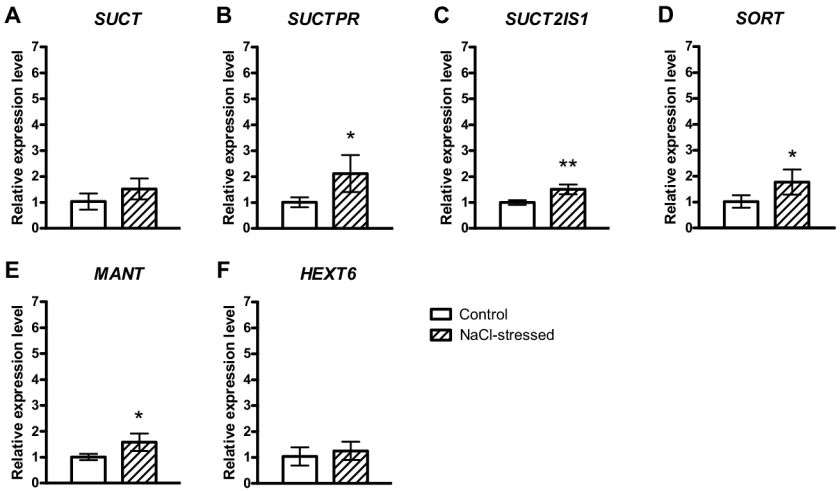

Figure 15 | Relative expression of genes encoding carbohydrate transporters in the pulp of *F. carica* (cv. Dottato) fruits harvested from control and 100 mM NaCl-stressed plants after 48 days. The values were determined with RT-qPCR. (**A**) *Sucrose Transporter* (*SUCT*); (**B**) *Sucrose Transporter 4-Like* (*SUCTPR*); (**C**) *Sucrose Transporter 2 Isoform 1* (*SUCT2IS1*); (**D**) *Sorbitol Transporter* (*SORT*); (**E**) *Probable Mannitol Transporter* (*MANT*); (**F**) *Hexose Transporter 6-Like* (*HEXT6*). Fold change values are means ± SD of three biological replicates. Asterisks indicate statistically significant differences (*$p \leq 0.05$, ** $p \leq 0.01$, *** $p \leq 0.001$).

al., 2014), was up-regulated (Figure 16C) as well as the expression of *NADP dependent D-sorbitol 6-phosphate Dehydrogenase* gene (*S6PDH*), which is related to the conversion of glucose 6-phosphate into sorbitol 6-phosphate (Yamaki and Moriguchi, 1989; Ikegami et al., 2013; Desnoues et al., 2014) in response to salinity (Figure 16D). All analysed invertase-encoding genes involved in the conversion of sucrose into glucose and fructose (Ikegami et al., 2013; Desnoues et al., 2014), were up-regulated, such as *Alkaline-neutral Invertase-Like Chloroplastic* (*INVCLO*), *Alkaline-neutral Invertase-Like Mitochondrial* (*INVMIT*), *Alkaline-neutral Invertase B* (*INVANB*) and *Acid β-fructofuranosidase* (*INVA*) but not *Probable Alkaline-neutral Invertase D* (*INVAND*), which was down-regulated (Figure 16E–I). The *Hexokinase-1* gene (*HEXKIN*) transcript level was unaffected by salinity (Figure 16J), whereas the second analysed kinase, the *ATP-dependent 6-phosphofructokinase 3* (*PFK*) was up-regulated in fruits of NaCl-stressed plants (Figure 16K).

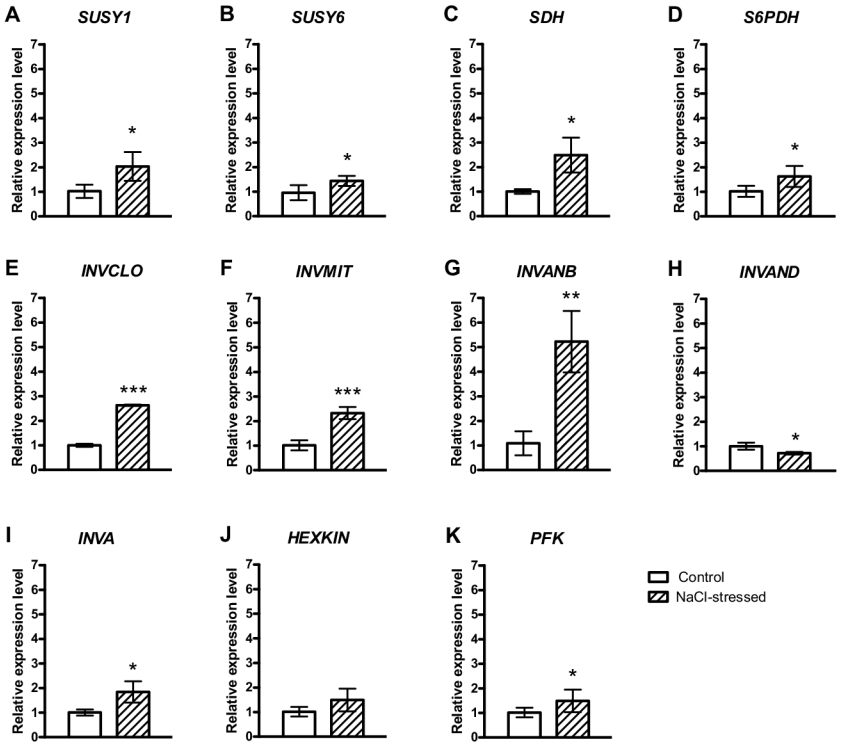

Figure 16 | Relative expression of genes encoding carbohydrate metabolism in the pulp of *F. carica* (cv. Dottato) fruits harvested from control and 100 mM NaCl-stressed plants after 48 days. The values were determined with RT-qPCR. (**A**) *Sucrose Synthases 1* (*SUSY1*); (**B**) *Sucrose Synthases 6* (*SUSY6*); (**C**) *Sorbitol Dehydrogenase* (*SDH*); (**D**) *NADP-dependent D-sorbitol 6-phosphate Dehydrogenase* (*S6PDH*); (**E**) *Alkaline-neutral Invertase-Like Chloroplastic* (*INVCLO*); (**F**) *Alkaline-neutral Invertase-Like Mitochondrial* (*INVMIT*); (**G**) *Alkaline-neutral Invertase B* (*INVANB*); (**H**) *Probable Alkaline-neutral Invertase D* (*INVAND*); (**I**) *Acid β-fructofuranosidase* (*INVA*); (**J**) *Hexokinase-1* (*HEXKIN*); (**K**) *ATP-dependent-6-phosphofructokinase 3* (*PFK*). Fold change values are means ± SD of three biological replicates. Asterisks indicate statistically significant differences (*$p \leq 0.05$, ** $p \leq 0.01$, *** $p \leq 0.001$).

Changes in main soluble carbohydrates contents in response to salinity

The D-glucose, D-fructose, D-sorbitol, D-mannitol and sucrose concentrations in the fruit pulp were determined by NMR quantitative analysis to investigate whether the differences in key soluble carbohydrates pathway-related genes could affect the soluble carbohydrate contents of NaCl-stressed plants. The spin systems

of D-mannitol were not unequivocally identified (Figure 17).
Total soluble carbohydrate, glucose and fructose concentrations were unaffected by salinity, but those of sucrose and D-sorbitol were higher in NaCl-stressed fruits than in control fruits (Table 7). The ratios between soluble sugars reported in Table 7 were generally higher in the stressed treatment, except for glucose/fructose. The ratios of sucrose/fructose+glucose and D-sorbitol/fructose+glucose were significantly higher in the fruits of NaCl-stressed plants than in the control fruits (Table 7).

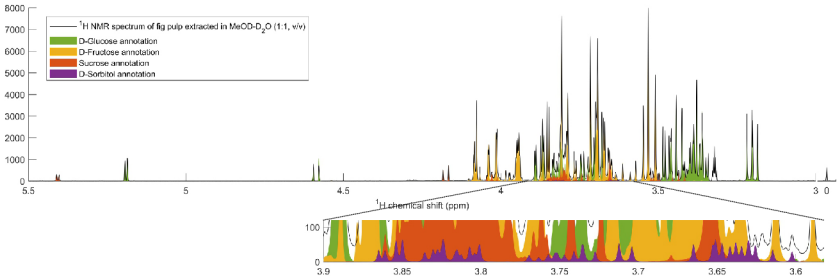

Figure 17 | Representative annotated ^{1}H NMR spectrum of fig pulp extracted in MeOD-D$_2$O (1:1, v/v).

Table 7 | Concentrations of D-fructose, D-glucose, sucrose and D-sorbitol and their ratios in *F. carica* cv. Dottato fruits from control and 100 mM NaCl-stressed plants for 48 days. Values are means ± S.D. of three replicate fruits expressed as mg g^{-1} of fruit dry pulp. $p \leq 0.05$ is in bold font.

Soluble carbohydrates	Control	100 mM NaCl-stressed	*p*-value
D-Fructose	242.68 ± 7.73	235.87 ± 3.64	0.24
D-Glucose	240.92 ± 15.71	219.30 ± 5.29	0.09
Sucrose	27.9 ± 0.3	34.31 ± 3.51	**0.03**
D-Sorbitol	0.99 ± 0.23	1.48 ± 0.15	**0.04**
Total	511.68 ± 23.04	490.97 ± 2.14	0.18
Ratio (*100)			
Glucose/Fructose	99.22 ± 3.76	92.99 ± 3.04	0.09
Sucrose/Fructose	11.5 ± 0.25	14.55 ± 1.55	**0.03**
Sucrose/Glucose	11.61 ± 0.64	15.68 ± 1.95	**0.03**
Sucrose/Glucose+Fructose	5.78 ± 0.22	7.55 ± 0.87	**0.03**
Sorbitol/Sucrose	3.55 ± 0.82	4.35 ± 0.69	0.26
Sorbitol/Glucose	0.42 ± 0.12	0.68 ± 0.08	**0.03**
Sorbitol/Fructose	0.41 ± 0.10	0.63 ± 0.06	**0.03**
Sorbitol/Glucose+Fructose	0.21 ± 0.05	0.33 ± 0.03	**0.03**

Discussion

Fig plants show several adaptive responses to salinity, which makes this species suitable for cultivation in moderately saline soils (Caruso et al., 2017; Vangelisti et al., 2019). However, there is no information on the effect of salt stress on soluble sugar concentrations, a key attribute of fruit quality. Fig fruits can accumulate high amounts of soluble sugars, up to 50% of dry weight at ripening (Vemmos et al., 2013). Therefore, we investigated how salinity affected carbohydrate metabolism by comparing the transcript level of the main genes involved in the synthesis, accumulation and transport of soluble carbohydrates in ripe fruits of cv. Dottato plants grown under saline conditions.
The genes encoding sugar transporters analysed in this study showed a significant increase in the transcript levels in the fruit pulp of NaCl-stressed plants compared to controls, except *SUCT* and *HEXT6*, whose transcript level increases were not significant (Figure 15). We found that salt stress induced a general increase in the expression of genes related to carbohydrate transport, similar to results obtained in tomato fruits (Yin et al., 2010). The expression of *MANT* was also higher in salt- stressed fruits (Figure 15E), but it has to be considered that we were unable to quantify the mannitol concentration by qNMR. This might be due to the low sensitivity of qNMR for the detection of mannitol in the dry fig matrix or to the absence of mannitol. To the best of our knowledge, mannitol has not been quantified in *Ficus* spp. tissue so far. Mannitol is a polyol that can confer resistance to oxidative stress (Smirnoff and Cumbes, 1989; Williamson et al., 1995; Jennings et al., 1998) and salt tolerance (Conde et al., 2007) because it may play multiple roles as a compatible solute, a low molecular weight chaperone, a reactive oxygen species scavenging compound, an osmolyte and an osmoprotectant (Gupta and Huang, 2014). In our experiment, fig *MANT* transcript levels increased in the mature fruits of NaCl-stressed plants (Figure 15E), as already observed in olive fruits, in which the *OeMaT1* transcripts increased throughout salinity stress, suggesting that this gene was involved in the accumulation of mannitol for salt tolerance (Conde et al., 2008).
Among the analysed genes encoding enzymes of carbohydrate metabolism, it should be noted that the expression level of both sucrose synthase-encoding genes increased under salinity stress, with a major expression level for *SUSY1* (Figure 16A). In NaCl-stressed tomato plants, an increased expression of a gene encoding a *Sucrose Synthase*, *SUS3*, was shown; however, another gene, *SUS2*, showed a reduced expression (Lu et al., 2010). Salinity stress promoted sucrose translocation into the fruit (Saito et al., 2009) increasing its concentration (Saito et al., 2008)

and increased sucrose synthase activity in tomato fruits (Saito et al., 2008, 2009). This is consistent with a higher concentration of sucrose in fig fruits grown under salinity conditions compared to control fruits.

The *INVAND* gene was the only gene whose transcript levels decreased in fruits of NaCl-stressed plants (Figure 16H), while the transcripts of other invertase encoding genes increased (Figure 16E–G, I). Similar differences among invertase encoding genes were reported in tomato fruits in response to salinity (Lu et al., 2010), where salinity increased the expression levels of the *Tiv-1* gene and reduced those of *Lin5* (Lu et al., 2010).

In addition, the *PFK* transcript levels increased in mature fig fruits of salt-treated plants (Figure 16K). It has been evidenced that phosphofructokinase-encoding genes play diverse functional roles in different tissues (Lü et al., 2019) including stress responses, as observed in rice seedlings (Mustroph et al., 2013).

In many species, salt stress affects carbohydrate contents in the fruit, depending on the genotype and the magnitude of stress. For example, a difference in the partitioning of assimilates in salinity stress conditions has been reported in tomato fruits (Gao et al., 1998; Lu et al., 2010; Yin et al., 2010; Moles et al., 2019). Few studies have investigated changes in soluble carbohydrates in fig fruits. Despite differences among cultivars, fructose and glucose are the most abundant sugars reported in *F. carica*, followed by sucrose (Ersoy, 2007; Slatnar et al., 2011; Sedaghat and Rahemi, 2018; Fattorini et al., 2021). In this work, we confirm that major soluble carbohydrates in fig fruit were fructose, glucose and sucrose (Table 7). The D-glucose/D-fructose content ratio was about 1:1 and remained fairly constant under saline conditions. On the other hand, sucrose and sorbitol were significantly higher in the fruits of salt-stressed plants (Table 7), which suggests a different partitioning towards translocatable sugars in the fruit. In salt-stressed tomato fruit, the sucrose content rose, whereas the glucose and fructose contents were unaffected by salinity (Saito et al., 2008), despite glucose and fructose increasing in watermelon cultivated under salinity (Colla et al., 2006). Nevertheless, in strawberry, glucose, fructose, sucrose and starch content reduced in all plant organs, including the fruits, due to NaCl salinity (Saied et al., 2005).

D-sorbitol is a well-known osmolyte that plays various roles in responses to salinity stress (Gupta and Huang, 2014). Sorbitol has also been implicated in drought mitigation in sink organs of peach (Lo Bianco et al., 2000). Higher concentrations of sorbitol in the fruits of plants grown in stressed conditions also suggest a possible key role for sorbitol in fig. Recent studies have reported the advantages of having sorbitol in addition to sucrose as the main translocatable sugars in apple trees to maintain the glucose and fructose levels to near homeostasis (Li et al., 2018b).

Conclusion

In conclusion, we showed that salinity affected the expression of main sugar metabolism and transport genes in fig fruits. A general increase in the transcript levels of genes involved in transport was observed. The increase of the transcripts encoding the enzymes involved in the synthesis of glucose and fructose did not increase the content of D-glucose and D-fructose, which are the most readily metabolised sugars. Perhaps an up-regulation of *Sorbitol Dehydrogenases* could lead to the accumulation of D-sorbitol using glucose and fructose since there was an increase of D-sorbitol.

Acknowledgements

This research was funded by University of Pisa, Italy, project "Progetto di Ricerca di Ateneo 2020: Risposta a stress ambientali e controllo ecosostenibile dei parassiti di *Ficus carica*", by FIGGEN/PRIMA19_00197 project, that is part of the PRIMA Programme supported by the European Union through a national MIUR (Italy) grant, and by METROFOOD-CZ research infrastructure project (MEYS Grant No: LM2018100) including access to its facilities.

CHAPTER 7

General discussion and conclusion

Unlocking the potentials

With its exceptional versatility, quantifiability and ability to probe molecular structure in mixtures, NMR spectroscopy emerges as a powerful tool capable of detecting and elucidating changes associated with both biotic and abiotic stress. Its broad range of applicability renders it invaluable for investigating diverse biological questions targeted at different plant organs (roots, fruits, leaves and flowers). Throughout this thesis, the versatility of NMR spectroscopy in exploring different biological questions, solidifying its significance in the field, is presented. The NMR method served as the connection between the three research chapters and the review chapter within this thesis. During this comprehensive discussion, particular emphasis will be placed on NMR and the knowledge we acquired from its practical application in studying plant metabolism and physiology.

Here we have shown that NMR is highly versatile as a screening tool for powdery mildew constitutive resistance in gerbera. The NMR analysis not only pointed at the most significant molecules the plant produces to protect itself against mildew, but by applying state-of-the-art statistical methods, such as a decision tree, it became clear how these molecules are ranked in their importance. Classification decision trees are constructed by recursive binary splitting; the prediction is obtained by starting at the root node and following a set of logical rules, for instance, metabolite concentration cut-off values, until a terminal node is reached (Debik et al., 2022). In constitutive defence, plants choose several chemical or physiological strategies to increase the survival and reduce the damage from pathogen or herbivore. Unlike in classical statistics, decision trees can show as a more complex insight into the plant defence mechanisms. Individual plants or breeding lines show slightly different strategies and alterations in synthetic pathways to produce these defence chemicals. The plant can for instance produce either less of one more active metabolite or more of another with slightly lower biological activity, but the effect will be the same. Some constitutive defensive compounds can be almost equally important for the plant, and different varieties can use them interchangeably. These trends can only be seen when using the metabolomics approach and are not visible from the commonly applied approach when compounds are first separated and later tested for their activities in bioassays. The results highlight the significance of polyketides in gerbera as biomarkers for detecting resistance against powdery mildew. Among these polyketides, gerberinside emerged as a key compound associated with resistance, with higher levels indicating higher resistance. Additionally, when this was low, higher levels of gerberin and parasorboside were also observed to contribute to resistance. Moreo-

ver, a newly identified compound, 5-hydroxyhexanoic acid 3-*O*-*β*-D-glucoside, is potentially involved in resistance mechanisms. Interestingly, in the chromatographic system, gerberine and parasorboside elute at the same retention time and are often reported as an inseparable mixture (Yrjönen et al., 2002), but in the NMR spectrum, they can be easily identified and quantified due to their distinct and prominent signals. Different varieties have different strategies of resistance, which was indicated when the resistance model was tested on other 27 varieties, and the model performance decreased.

The advantages of LC-MS over NMR are frequently highlighted. Nevertheless, our research yielded a contradictory experience. A well-curated set of 30–60 molecules with high physiological relevance, providing a reasonable data size for practical data mining and capturing the major metabolic trends, can overcome the limitations of datasets obtained through MS, which often comprise thousands of provisionally identified features with limited information about the structure, posing challenges for data interpretation. The study investigating the effect of carbamazepine soil contamination on maize, where key metabolic trends were identified and integrated with physiological parameters, exemplifies the power of a precisely annotated molecular set. Plants possess an impressive capacity to adjust to environmental challenges. Through the use of NMR spectroscopy, it was shown that whilst carbamazepine soil contamination and plant accumulation did not directly impact crop yields, it significantly influenced multiple metabolic functions at the early phenological stage, but older plants were able to compensate and adapt. Notably, alterations at the early phenological stage in the photosystems and photosynthesis were linked to decreased levels of sugars (glucose and fructose) in the roots. Furthermore, aboveground biomass exhibited an increase in the levels of carotenoids and phenylpropanoids, such as chlorogenic acid and its isomer, 5-*O*-caffeoylquinic acid, known for their ability to balance oxidative stress.

Metabolomics is complementary to other omics disciplines such as transcriptomics and proteomics. Being a „downstream“ consequence of gene expression, changes in the metabolome are widely regarded as the most accurate reflection of cellular activities at a functional level (Putri et al., 2013). In our study on the effect of salinity stress on the quality of fig fruits, we integrated NMR-based metabolomics within a multidisciplinary framework. We specifically focused on the expression of crucial sugar metabolism and transport genes, as well as the soluble carbohydrate content of fig fruits. Interestingly, changes in gene transcript levels did not directly correlate with alterations in the sugar content. Although there was a general increase in the transcript levels of genes involved in the transport of soluble carbohydrates, the up-regulation of *Alkaline-neutral* and *Acid Invertase*

transcripts, responsible for glucose and fructose synthesis, did not result in corresponding changes in the glucose and fructose contents in ripe fruits of NaCl-stressed plants. Instead, the higher levels of sucrose and D-sorbitol were likely attributable to the up-regulation of genes encoding sucrose synthase and sorbitol dehydrogenase, respectively. Here, NMR spectroscopy played a crucial role in rapidly screening and quantifying major sugars, providing valuable quantitative data. We uncovered the intricate connections between gene regulation and metabolic responses by coupling NMR spectroscopy with gene expression analysis. This integrative approach deepens our understanding of the molecular mechanisms underlying complex biological phenomena and elucidates how changes in gene expression contribute to alterations in metabolic pathways. The importance of the integration of the omics technology in research was pointed out for abiotic and biotic stress responses and tolerance in plants (Meena et al., 2017; Sheikh et al., 2020; Jamla et al., 2021; Raza et al., 2022).

All three self-containing studies mentioned above pointed out the capability of NMR metabolomics to provide the simultaneous quantification of primary and secondary metabolites. Although secondary metabolites are often the target of interest because of their role in plant interactions with other organisms, the primary metabolism regulates the vital functions of the plant.

Although NMR spectroscopy has been applied for approximately two decades, constant efforts are required to fully exploit its vast potential. Future advancements should focus on establishing freely available databases to ensure the annotation of taxonomically restricted secondary metabolites. The initial and essential progress towards advancement lies in the establishment of databases consisting of real (non-simulated) standard compounds, isolated compounds from mixtures and matrix spectra under well-defined standard conditions. This crucial step aims to facilitate the annotation process for the vast array of compounds that plants have the capacity to synthetise. By providing a comprehensive compound annotation reference, researchers can more effectively identify and characterise these compounds, accelerating our understanding of the plant metabolome.

The greatest and unique benefit of NMR spectroscopy is the robustness of the method, which enables the exchange of spectra and the combination of spectrum collections among research teams. Ensuring the comparability of data sets, such as using standard operating procedures and possibly buying ready-to-use extraction kits or buffering solutions, can be crucial to facilitate the spectrum exchange among laboratories. The standardisation of extraction methods towards methanolic solutions, which gives a broader overview of secondary metabolism along with primary metabolites, enhances the holistic overview of NMR-based plant metabolomics.

Advances are needed in spectral processing. The use of 0.01- and 0.04-ppm bins is a common practice for data reduction (Kim et al., 2010); although it is a relatively easy process, it has the disadvantage that deconvolution is not applied, and concentrations related to a single compound are often left behind. The development of semi- or fully-automated advanced fittings created ad-hoc for plant metabolites is another important advancement. Nowadays, multiple attempts are available, but they were mainly developed for the clinical investigation of biofluids or foodomics (Hao et al., 2014; Howarth et al., 2020; Khakimov et al., 2020; Wenk et al., 2023).

Due to its low sensitivity, NMR spectroscopy is often overlooked in the field of plant metabolomics (Patel et al., 2021; Katam et al., 2022). Simultaneously, it is known for its easy sample preparation procedure. It may be interesting to include multiple steps for metabolite concentration in sample preparation, such as solid-phase extraction methods. This would target the analysis in a range of metabolites, increase the concentration and overcome the limit in the detection level of NMR spectroscopy.

Nevertheless, the application of NMR spectroscopy in multi-omics research, advancement toward single-cell metabolomics and root exudates in environmental responses and the interactions with symbiotic organisms could be the new frontiers for a comprehensive understanding in plant responses to abiotic and biotic stresses. These developments could facilitate the wider use of NMR spectroscopy, enabling researchers to maximise its capabilities and accelerate progress in various fields. However, enhancing the availability of NMR instruments for metabolomics studies is crucial, enabling researchers to freely choose the technique that best suits their research questions. Each analytical method offers unique advantages tailored to address specific research inquiries.

Conclusion

NMR spectroscopy stands as an indispensable tool for probing the impacts of biotic and abiotic stresses on plants. Its applicability relies on the robustness of the technique, allowing spectrum collection exchange between laboratories; it should be chosen as a preferred method as it can provide an overview of the key metabolite changes for further investigations. Its ability to detect metabolite changes in plants offers a comprehensive overview of metabolic pathways and

provides a comprehensive understanding of stress responses allocated at the levels of primary and secondary metabolism. Additionally, the accuracy in the annotation and the size of the collected data provides the possibility to target metabolic pathways. This gives invaluable insights into multiple biological concerns, serving as a fundamental screening method in multiple studies. Consequently, this facilitates the identification of specific metabolic pathways for crop improvement in the context of global yield losses caused by a multitude of abiotic and biotic factors. Its broad applicability solidifies its status as a potential cornerstone technique in pursuing sustainable agriculture, disease management and fundamental biological research. Therefore, NMR spectroscopy emerges as a valuable tool for multi-omics investigations, providing insights into the functioning of metabolic networks.

Supplementary tables

Supplementary Table S1 | Strategy for literature search.

Criterium	Details
Used databases	Scopus (https://www.scopus.com) Web of Science (https://www.webofknowledge.com)
Search keywords (Boolean operators) included in article title, abstract, and keywords.	Nuclear magnetic resonance spectroscopy (NMR OR 1HNMR OR "1H-NMR" OR "nuclear magnetic resonance"), metabolomics (metabolomics OR "metabol* profil*") and biotic stress (biotic OR pathogen OR insect OR fungi OR caterpillar OR herbivor* OR resistanc* OR susceptib* OR pest OR nematod* OR "defen?e mechanism" OR "plant defen*" OR "resistance against" OR "insect resistance" OR virus OR insect OR infected).
Inclusion criteria	^{1}H NMR spectroscopy was used as an analytical technique for metabolomics studies in plants to investigate biochemical processes related to plant resistance to biotic stress by pathogenic organisms and herbivores, post-infection stress response, and plant-host interactions. Studies in which elicitors were used, in which the effect was investigated during the application of a treatment, or in which simulated stressors (e.g., wounding) were used were excluded. Reviews, book chapters and conference abstracts were not included.
Extracted data	Publication (authors, year of publication, title), information about the type of the stress (scientific name of the organism), study design, scientific name of the stressed plant and resistance and susceptibility traits if specified, organ, chemical responses of the host, spectra acquisition specifications (proton frequency, pulse sequence), extraction method (type of solvent and use published standard protocols), annotation method (spiking with standard compounds, in-house database, acquisition of 2D NMR spectra, comparison with database, annotation and structural elucidation), integration with other type of analysis and the statistical approaches used. Only metabolites that were significantly modulated by the host-plant interaction (increase or decrease in concentration) and by resistance traits (increase or decrease in concentration) ($p < 0.05$) were extracted from the eligible publications; in case multivariate methods were included the compounds mentioned in the result section as of interest were included.
Number of total records screened after duplicate removal	2700
Number of records excluded	2606
Number of records included	94

Supplementary Table S2 | Description of the independent validation dataset.

Variety	Type	Resistance definition according to the breeder	Location
Clasico	Standard	Susceptible	Breeder D
Cream Beach	Standard	Susceptible	Breeder D
Dark Diamond	Standard	Resistant	Breeder D
Don Leo	Standard	Resistant	Breeder D
Evi	Standard	Susceptible	Breeder D
Full moon	Standard	Resistant	Breeder D
Mandarina	Standard	Susceptible	Breeder D
Peptalk	Standard	Susceptible	Breeder D
Mango	Standard	Susceptible	Breeder D
Red Explosion	Standard	Resistant	Breeder D

Supplementary Table S2 | Continued.

Variety	Type	Resistance definition according to the breeder	Location
Rodeo	Standard	Resistant	Breeder D
Romance	Standard	Susceptible	Breeder D
Submarine	Standard	Resistant	Breeder D
White House	Standard	Susceptible	Breeder D
Albino	Mini	Resistant	Breeder D
Allure	Mini	Susceptible	Breeder D
Banana	Mini	Susceptible	Breeder D
Cafe	Mini	Resistant	Breeder D
Cassis	Mini	Resistant	Breeder D
Delmonte	Mini	Resistant	Breeder D
Noud	Mini	Susceptible	Breeder D
Dorito	Mini	Susceptible	Breeder D
Kimsey	Mini	Resistant	Breeder D
Suri	Mini	Susceptible	Breeder D
Navelino	Mini	Resistant	Breeder D
Delphi	Mini	Resistant	Breeder A
Kimsey	Standard	Susceptible	Breeder A
Jumbo	Mini	Resistant	Breeder A
Mokka	Mini	Susceptible	Breeder A
Passoa	Standard	Resistant	Breeder A
Madeira	Standard	Susceptible	Breeder A
Flamenco	Standard	Susceptible	Breeder A
Contigo	Standard	Susceptible	Breeder A
Betty Boop	Mini	Susceptible	Breeder A
Lido	Mini	Susceptible	Breeder A
Cafe del mar	Standard	Resistant	Breeder A
Monza	Mini	Resistant	Breeder A
Bravia	Mini	Resistant	Breeder A
Petticoat	Mini	Resistant	Breeder A
Franky	Mini	Resistant	Breeder A
Suri	Standard	Susceptible	Breeder E
Cafe	Standard	Resistant	Breeder E
Prosseco	Mini	Susceptible	Breeder E
Caramba	Standard	Resistant	Breeder E
Nirvana	Mini	Resistant	Breeder E
Maserati	Mini	Susceptible	Breeder E
Dixon	Standard	Resistant	Breeder E
Caprise	Standard	Susceptible	Breeder E

Supplementary Table S3 | Description of the acquisition of the 2D NMR experiments.

2D experiment	Description
DQF-COSY	A phase-sensitive 2D correlation spectroscopy (DQF-COSY) with Double Quantum Filter and presaturation (Bruker pulse sequence *cosydfphpr*) was obtained with 1.0 s relaxation delay, 6510 Hz spectral width in both dimensions (^{1}H chemical shift axes). Twenty-four scans were acquired per 521 increments for an overall experimental time of 5hr and 56 min. Zero filled data to 4,096 × 4,096 points and a sine2 bell-shaped window function shifted by /2 in the F1 and /4 in the F2 dimension was applied. Automatically phased and calibrated to the internal standard (TSP = 0.0 ppm).
HMBC	A phase-sensitive ge-2D heteronuclear multiple bond correlation (HMBC) (Bruker pulse sequence *hmbcetgpl3nd*) was acquired using 512 and 4,096 complex points in F1 and F2, respectively. Spectral widths of 6510 Hz in F2 (^{1}H chemical shift axis) and 27675 Hz in F1 (^{13}C chemical shift axis) yielding t1 and t2 acquisition times of 4 and 314 ms, respectively. 240 scans were acquired for an overall experimental time of 23 hr and 51 min. A sine2 bell-shaped window function shifted by /2 in the F1 and /6 in the F2 dimension was applied. The spectrum was calibrated according to the internal standard (^{1}H: TSP = 0 ppm; ^{13}C: methanol = 16.7 ppm).
HSQC	A phase-sensitive ge-2D heteronuclear single quantum coherence spectroscopy (HSQC) (Bruker pulse sequence *hsqcgpph*) was acquired using 256 and 1,024 complex points in F1 and F2, respectively. Spectral widths of 6510 Hz in F2 (^{1}H chemical shift axis) and 27675 Hz in F1 (^{13}C chemical shift axis) yielding t1 and t2 acquisition times of 4 and 314 ms, respectively. 240 scans were acquired for an overall experimental time of 1d 3 hr and 13 min. A sine2 bell-shaped window function shifted by /2 in the F1 and /6 in the F2 dimension was applied. The spectrum was calibrated according to the internal standard (^{1}H: TSP = 0 ppm; ^{13}C: methanol = 49.0 ppm).

Supplementary Table S4 | Parameters of the liquid chromatography separation and the mass spectrometer settings.

	Parameter	Settings	
Liquid chromatography separations	Column	Acclaim™ RSLC 120 C18 column (2.2 µm, 120Å 2.1 × 100 mm; Thermo Fisher Scientific, Waltham, MA, USA), coupled with an Acquity UPLC BEH C18 VanGuard pre-column (Waters, Milford, MA, USA)	
	Temperature	35°C	
	Mobile phase	5 mM ammonium formate or 0.2% formic acid in water (phase A) and methanol (phase B)	
	Gradient elution program	5% B isocratically for 1.5 min, then from 5% to 70% B over the next 8.5 min, from 70% to 100% B during the next 3 min, held constant for 4 minutes, and then returned to the initial conditions	
	Flow rate	0.25 mL/min	
	Injection volume	5 µL	
Mass spectrometer	Ion source settings:	End plate offset:	500 V
		Capillary voltage:	3500 V
		Nebulizer gas:	2.0 Bar
		Drying gas (N_2):	8.0 L/min
		Drying temperature:	250°C
	Mass Range:	50-1500 m/z	
	Scan rate:	3x1sec	
	Calibration mixture:	Na^+ formate clusters	
	collision energy	The MS/MS fragmentation spectra collected at three discrete levels of collision energy 20, 40, and 60 eV for each precursor ion	

Supplementary Table S5 | Pairwise analysis of 5-hydroxyhexanoic acid 3-*O*-*β*-D-glucoside, gerberin, parasorboside, and gerberinside of young and old leaves of varieties resistant and susceptible to powdery mildew extracted in MeOD-D_2O (1:1, v/v).

	5-hydroxyhexanoic acid 3-*O*-*β*-D-glucoside			Gerberin			Parasorboside			Gerberinside		
Class	**$\bar{x}$***	**±SD**	***p*-value**	**$\bar{x}$***	**±SD**	***p*-value**	**$\bar{x}$***	**±SD**	***p*-value**	**$\bar{x}$***	**±SD**	***p*-value**
Resistant[a]	12.58	9.09	0.63	73.72	47.47	0.31	39.69	12.62	8.60 e-04	11.36	5.46	6.05 e-08
Susceptible[a]	11.71	10.16		65.84	36.61		32.56	10.07		6.88	2.44	
Young resistant[b]	13.78	10.58	0.95	74.16	43.78	0.69	43.65	11.95	0.02	13.48	6.03	5.80 e-05
Young susceptible[b]	13.99	12.54		69.89	39.26		37.56	7.82		8.46	1.95	
Old resistant[b]	11.38	7.30	0.28	73.29	51.65	0.31	35.72	12.20	0.01	9.23	3.89	5.16 e-06
Old susceptible[b]	9.45	6.51		61.81	33.93		27.56	9.67		5.31	1.79	
Resistant young[b]	13.78	10.58	0.31	74.16	43.78	0.94	43.65	11.95	0.01	13.48	6.03	1.96 e-03
Resistant old[b]	11.38	7.30		73.29	51.65		35.72	12.20		9.23	3.89	
Susceptible young[b]	13.99	12.54	0.08	69.89	39.26	0.40	37.56	7.82	4.63 e-05	8.46	1.95	1.93 e-08
Susceptible old[b]	9.45	6.51		61.81	33.93		27.56	9.67		5.31	1.79	
Mini resistant[b]	12.51	9.60	0.56	34.31	25.48	0.19	35.09	9.47	0.94	14.92	5.43	3.53 e-09
Mini susceptible[b]	11.22	7.55		40.83	8.04		35.32	11.99		7.48	2.19	
Standard resistant[b]	12.65	8.72	0.88	113.13	26.87	0.01	44.28	13.82	3.30 e-06	7.79	2.22	0.02
Standard susceptible[b]	12.22	12.35		90.87	36.97		29.80	6.83		6.28	2.57	
Resistant mini[b]	12.51	9.60	0.95	34.31	25.48	7.79 e-17	35.09	9.47	3.91 e-03	14.92	5.43	1.11 e-08
Resistant standard[b]	12.65	8.72		113.13	26.87		44.28	13.82		7.79	2.22	
Susceptible mini[b]	11.22	7.55	0.70	40.83	8.04	1.13 e-09	35.32	11.99	0.03	7.48	2.19	0.06
Susceptible standard[b]	12.22	12.35		90.87	36.97		29.80	6.83		6.28	2.57	

*average concentration expressed as mg/g dry leaves. [a]N=60, [b]N=30.

Supplementary Table S6 | Performance of the analytical methods.

Matrix	**Method (variants)**	**Absolute Recovery (%)***	**RSD (%)****	**MLOQ (ng/g dw.)*****
Roots	Protein precipitation (CBZ10, CBZ1000)	89	2	1
Aboveground biomass	Protein precipitation (CBZ10, CBZ1000)	87	4	1
Roots	SPE (CBZ0.1, CBZ1)	100	5	0.02
Aboveground biomass	SPE (CBZ0.1, CBZ1)	99	8	0.02

MLOQ: method limits of quantification; RSD: relative standard deviation, dw.: dry weight.
* Calculated as pre-extract spike peak area/post-extract spike peak area × 100.
** Relative standard deviation calculated from 4 independent extractions.
*** Method limit of quantification.

Supplementary Table S7 | Fruit fresh weight of control and 100 mM NaCl-stressed plants for 48 days. Values are means ± standard deviations (SD) of three replicate fruits expressed as g of fresh fruit. *p*-value was calculated by Student's *t*-test.

	Control	**100 mM NaCl-stressed**	***p*-value**
Replicate 1	40.56	24.75	-
Replicate 2	53.19	30.37	-
Replicate 3	29.41	23.22	-
Mean ± SD	41.05 ± 11.90	26.11 ± 3.76	0.11

Supplementary figures

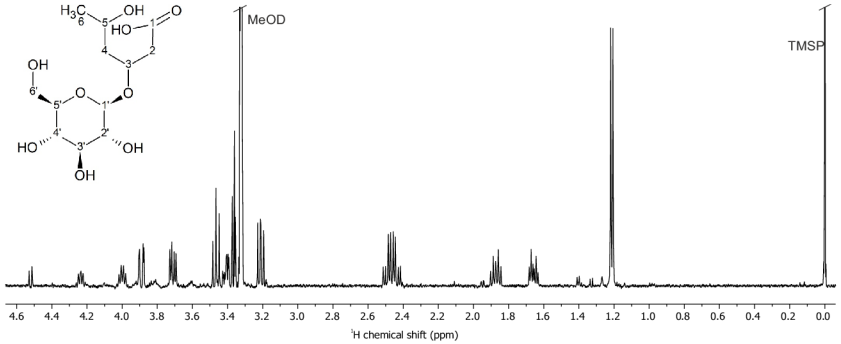

Supplementary Figure S1 | ^{1}H NMR spectrum of 5-hydroxyhexanoic acid 3-*O*-*β*-D-glucoside in MeOD-D_2O (1:1, v/v) (500MHz).

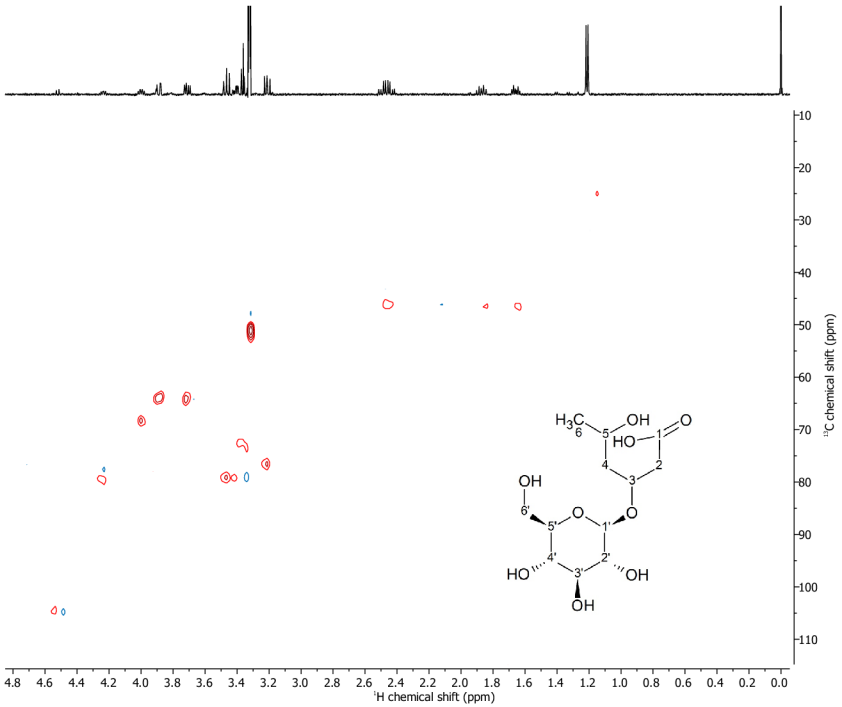

Supplementary Figure S2 | HSQC spectrum of 5-hydroxyhexanoic acid 3-*O*-*β*-D-glucoside in MeOD-D_2O (1:1, v/v).

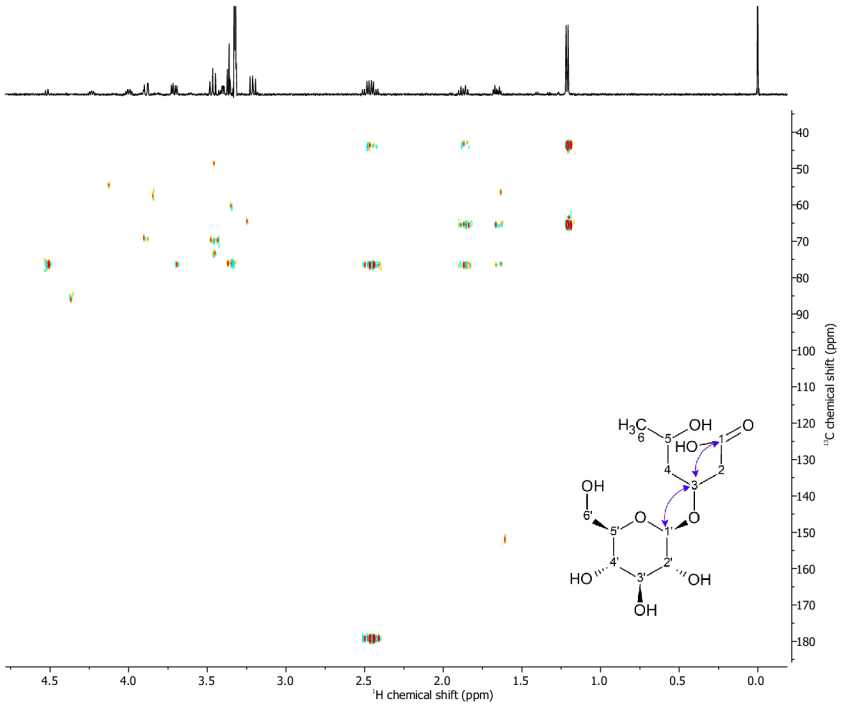

Supplementary Figure S3 | HMBC spectrum and key correlations of 5-hydroxyhexanoic acid 3-*O*-*β*-D-glucoside in MeOD-D_2O (1:1, v/v).

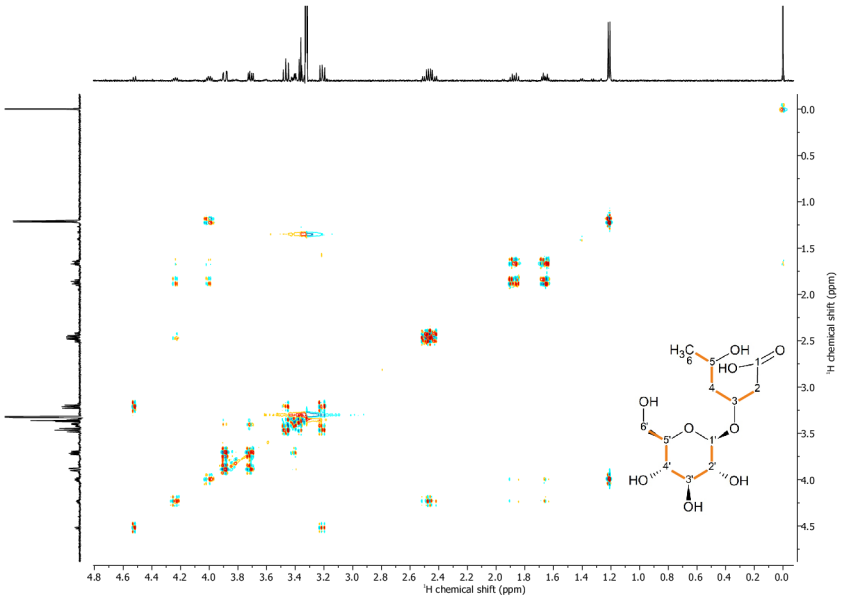

Supplementary Figure S4 | DQF-COSY spectrum and key correlations of 5-hydroxyhexanoic acid 3-*O*-*β*-D-glucoside in MeOD-D_2O (1:1, v/v).

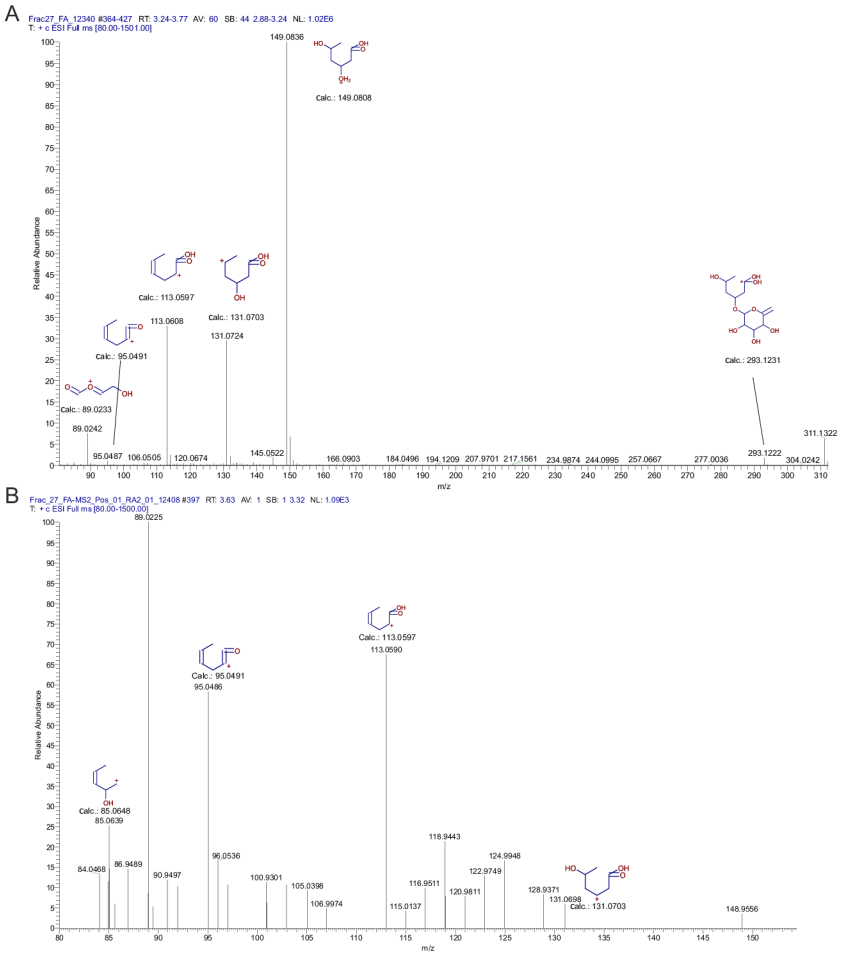

Supplementary Figure S5 | (**A**) MS spectrum (in-source fragmentation) and proposed fragments of 5-hydroxyhexanoic acid 3-*O*-*β*-D-glucoside at *m/z* 311.1336 $[M+H]^+$ and (**B**) MS/MS spectrum of the aglycone at *m/z* 149.0808 $[M+H]^+$ (positive mode, 0.2% formic acid and methanol).

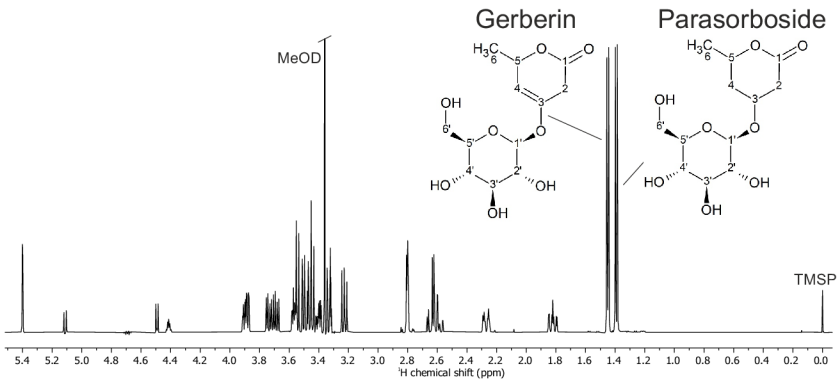

Supplementary Figure S6 | ^{1}H NMR spectrum of gerberin and parasorboside in MeOD-D_2O (1:1, v/v) (500MHz).

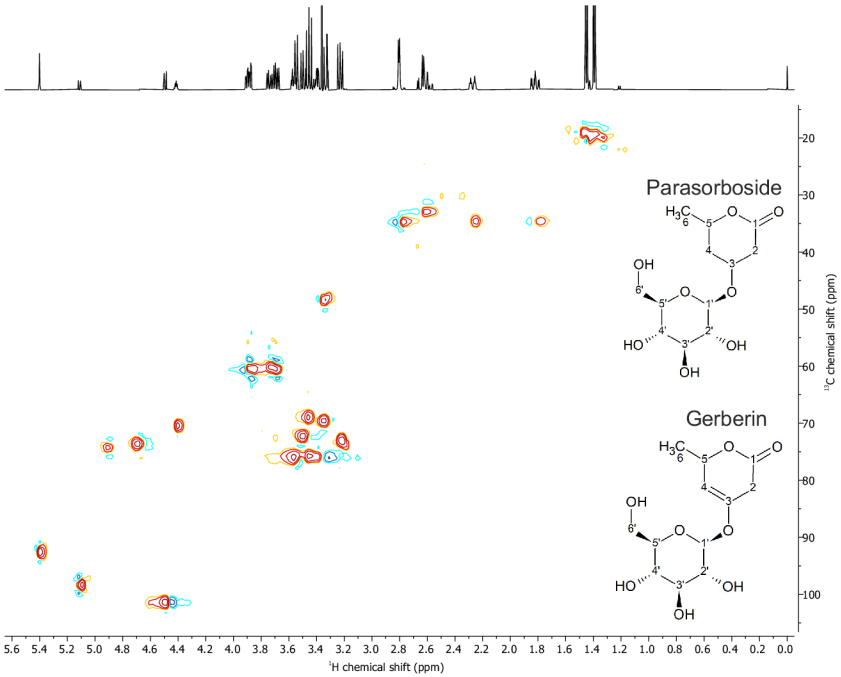

Supplementary Figure S7 | HSQC spectrum of gerberin and parasorboside in MeOD-D_2O (1:1, v/v).

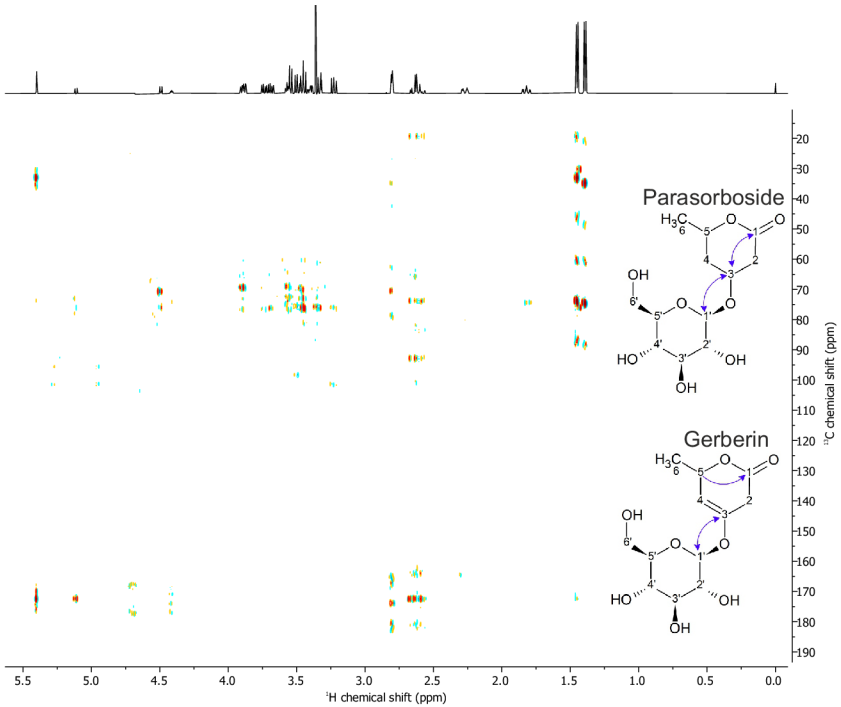

Supplementary Figure S8 | HMBC spectrum and key correlations of gerberin and parasorboside in MeOD-D_2O (1:1, v/v).

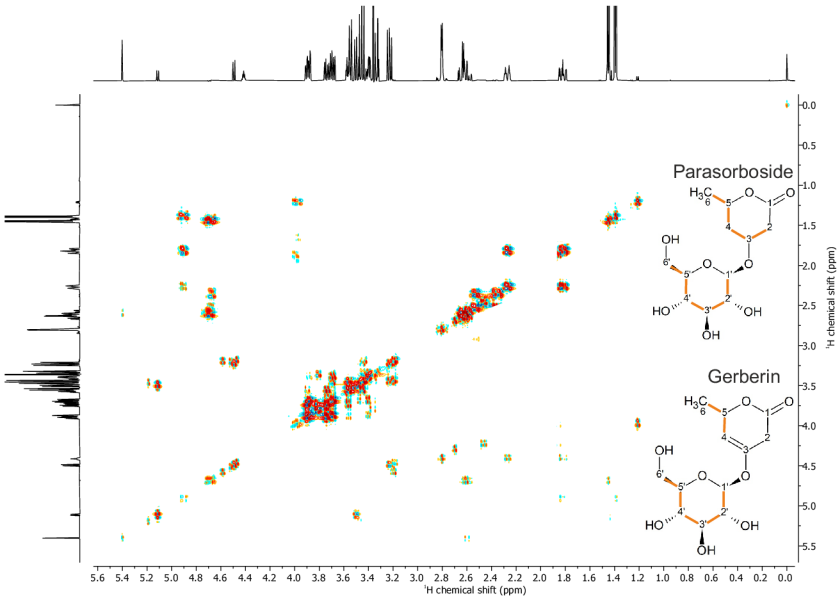

Supplementary Figure S9 | DQF-COSY spectrum and key correlations of gerberin and parasorboside in MeOD-D_2O (1:1, v/v).

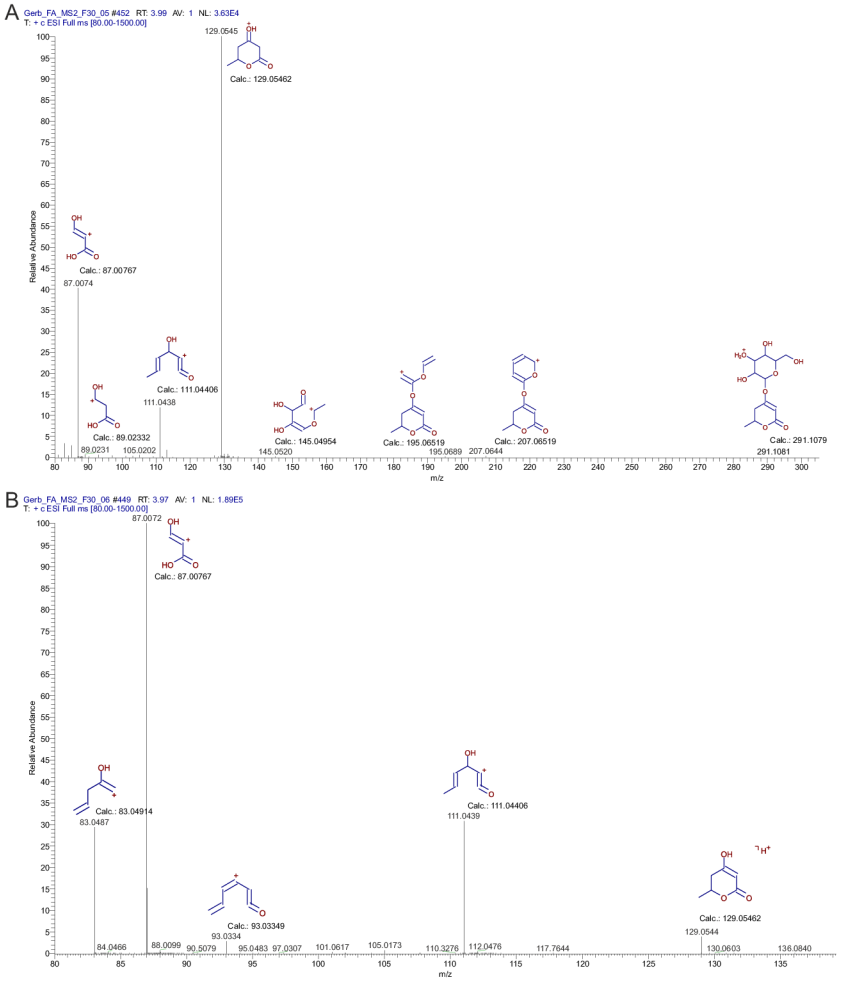

Supplementary Figure S10 | MS/MS spectrum and proposed fragmentation of (**A**) gerberin at *m/z* 291.1071 $[M+H]^+$ and (**B**) geberin aglycone at *m/z* 129.0546 $[M+H]^+$ (positive mode, 0.2% formic acid and methanol).

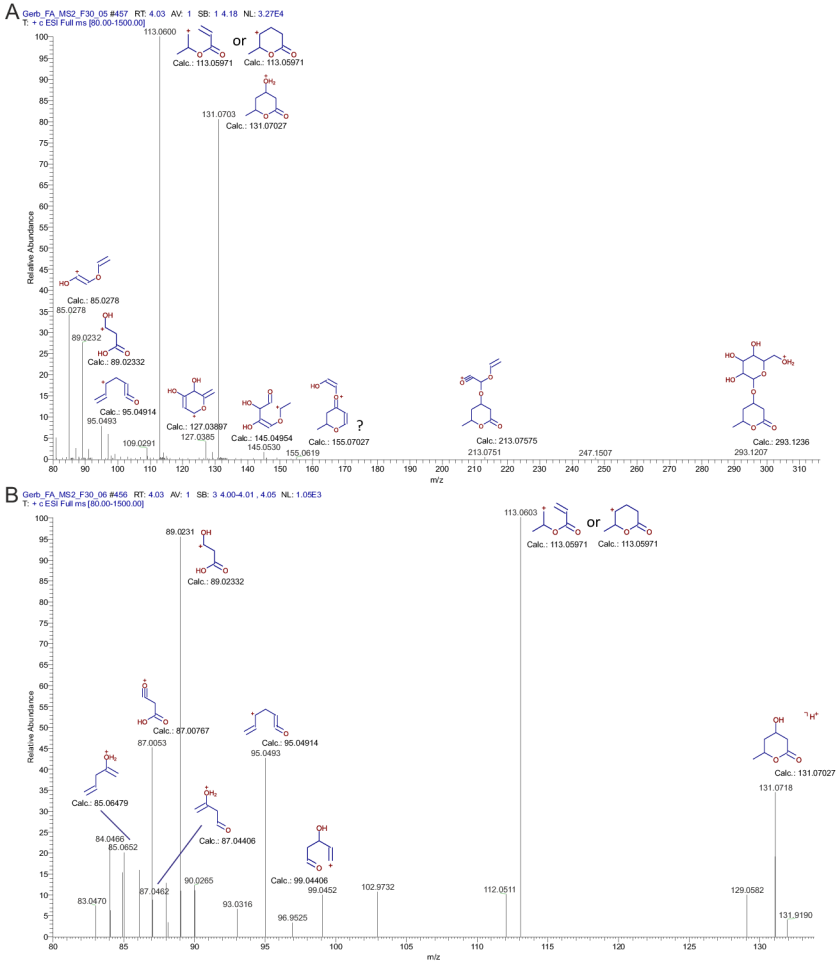

Supplementary Figure S11 | MS/MS spectrum and proposed fragmentation of (**A**) parasorboside at *m/z* 293.1207 $[M+H]^+$ and (**B**) parasorboside aglycone at *m/z* 131.0718 $[M+H]^+$ (positive mode, 0.2% formic acid and methanol).

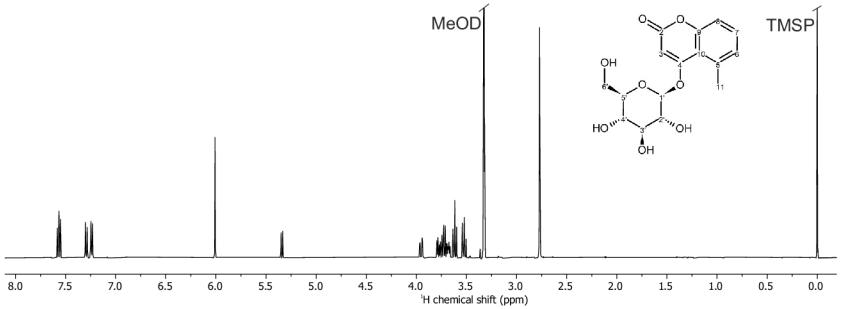

Supplementary Figure S12 | ^{1}H NMR spectrum of gerberinside in MeOD-D_2O (1:1, v/v) (500MHz).

Supplementary Figure S13 | HSQC spectrum of gerberinside in MeOD-D_2O (1:1, v/v).

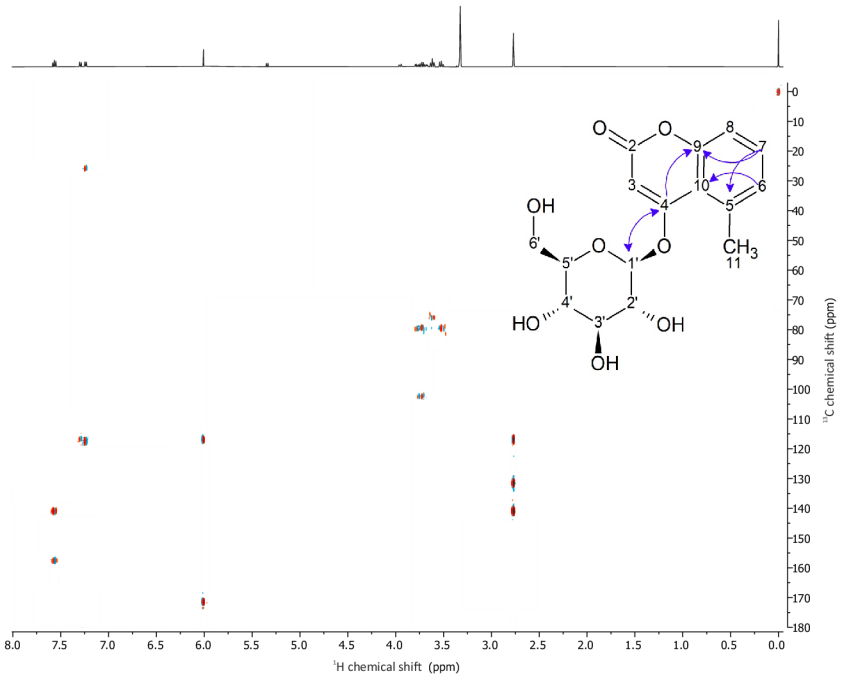

Supplementary Figure S14 | HMBC spectrum and key correlations of gerberinside in MeOD-D_2O (1:1, v/v).

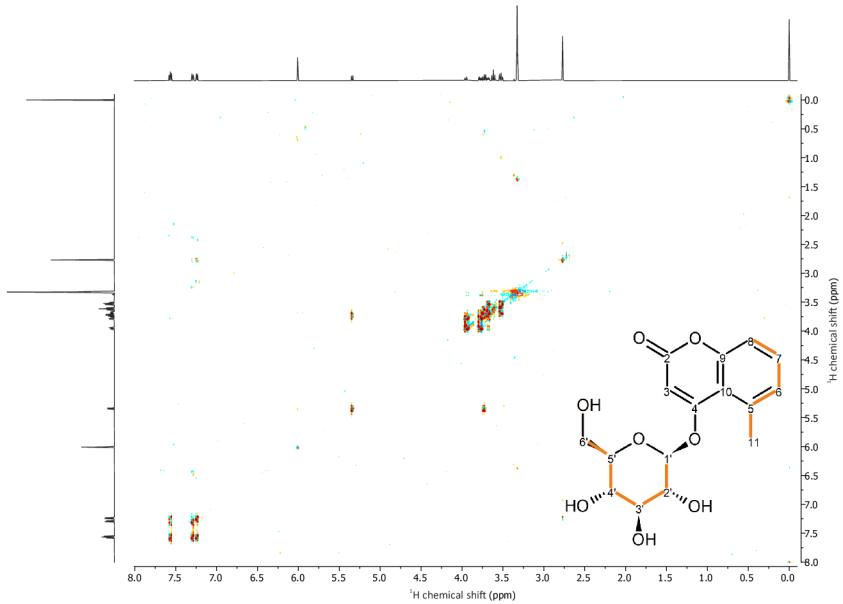

Supplementary Figure S15 | DQF-COSY spectrum and key correlations of gerberinside in MeOD-D_2O (1:1, v/v).

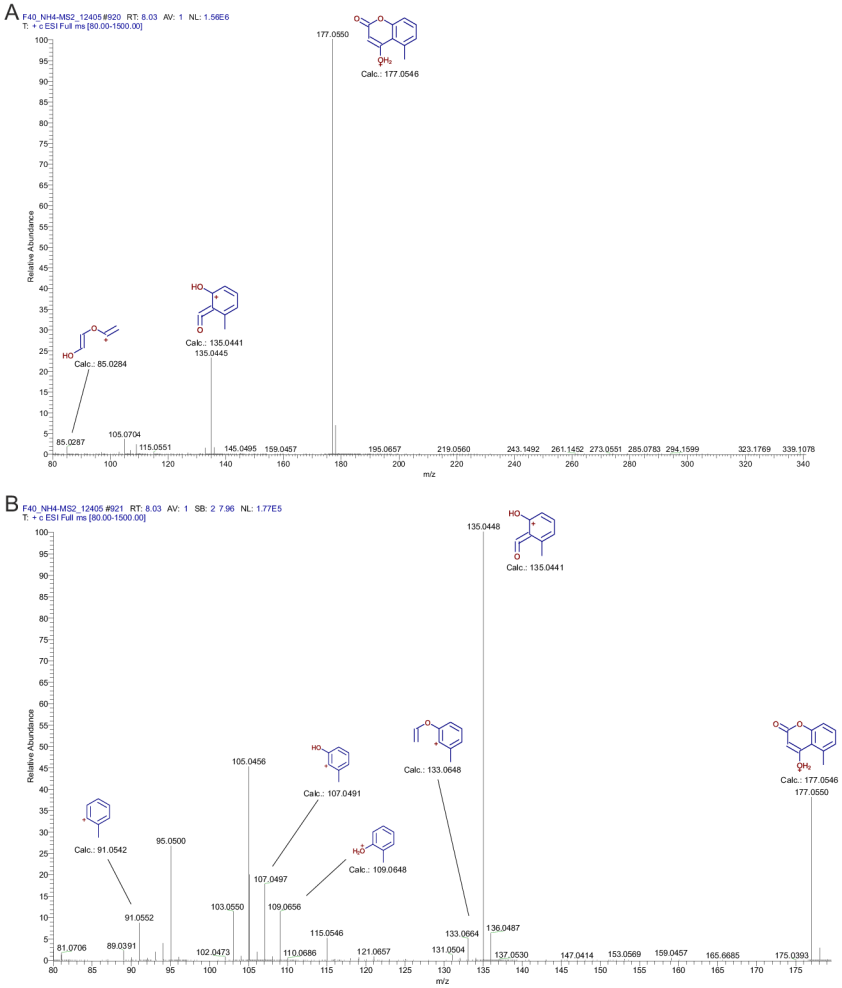

Supplementary Figure S16 | MS/MS spectrum and proposed fragmentation of (**A**) gerberinside at *m/z* 339.1070 $[M+H]^+$ and (**B**) gerberinside aglycone at *m/z* 177.0545 $[M+H]^+$ (positive mode, 5mM ammonium formate).

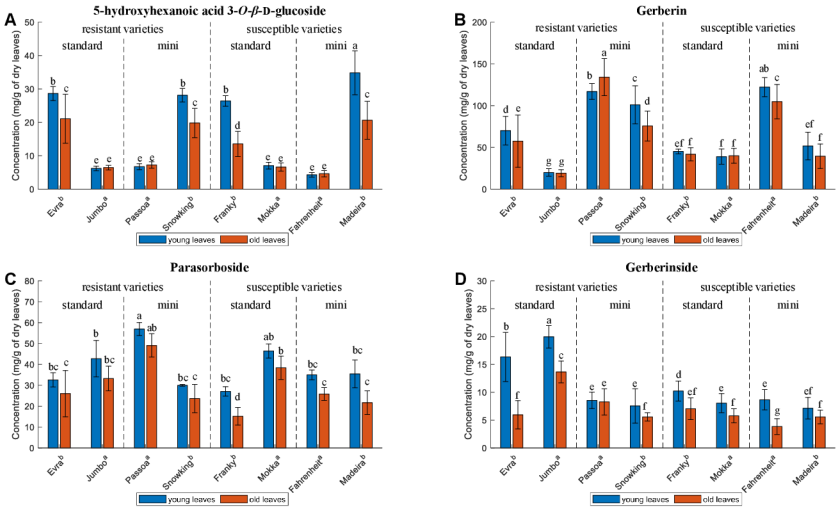

Supplementary Figure S17 | Quantitative ^{1}H NMR analysis in the leaves of varieties resistant and susceptible to powdery mildew extracted in MeOD-D_2O (1:1, v/v). (**A**) Quantitative ^{1}H NMR analysis of 5-hydroxyhexanoic acid 3-*O*-*β*-D-glucoside. (**B**) Quantitative ^{1}H NMR analysis of gerberin. (**C**) Quantitative ^{1}H NMR analysis of parasorboside. (**D**) Quantitative ^{1}H NMR analysis of gerberinside. Error bars refer to the standard deviation (^{a}N=10, ^{b}N=5). Different letters on the vertical bars indicate similarities on the mean among groups. If a letter is shared, the mean is similar.

Supplementary Figure S18 | Ripe fruit of *Ficus carica* cv. Dottato during the salinity experiment.

References

Abdel-Farid, I. B., Jahangir, M., van den Hondel, C. A. M. J. J., Kim, H. K., Choi, Y. H., and Verpoorte, R. (2009). Fungal infection-induced metabolites in *Brassica rapa. Plant Sci.* 176, 608–615. doi:10.1016/j.plantsci.2009.01.017.

Afifah, E. N., Murti, R. H., and Nuringtyas, T. R. (2019). Metabolomics approach for the analysis of resistance of four tomato genotypes (*Solanum lycopersicum* L.) to root-knot nematodes (*Meloidogyne incognita*). *Open Life Sci.* 14, 141–149. doi:10.1515/biol-2019-0016.

Afifah, E. N., Murti, R. H., and Nuringtyas, T. R. (2020). Comparison of metabolomics expressionin the root and leaf of resistance and susceptible tomato against root-knot nematode. *Agrivita* 42, 563–571. doi:10.17503/agrivita.v42i3.2440.

Ahuja, I., de Vos, R. C. H., Bones, A. M., and Hall, R. D. (2010). Plant molecular stress responses face climate change. *Trends Plant Sci.* 15, 664–674. doi:10.1016/j.tplants.2010.08.002.

Ali, K., Maltese, F., Figueiredo, A., Rex, M., Fortes, A. M., Zyprian, E., et al. (2012). Alterations in grapevine leaf metabolism upon inoculation with *Plasmopara viticola* in different time-points. *Plant Sci.* 191–192, 100–107. doi:10.1016/j.plantsci.2012.04.014.

Allegra, A., Gallotta, A., Carimi, F., Mercati, F., Inglese, P., and Martinelli, F. (2018). Metabolic profiling and post-harvest behavior of "Dottato" fig (*Ficus carica* L.) fruit covered with an edible coating from *Opuntia ficus-indica. Front. Plant Sci.* 9, 1–10. doi:10.3389/fpls.2018.01321.

Allegra, A., Sortino, G., Inglese, P., Settanni, L., Todaro, A., and Gallotta, A. (2017). The effectiveness of *Opuntia ficus-indica* mucilage edible coating on post-harvest maintenance of 'Dottato' fig (*Ficus carica* L.) fruit. *Food Packag. Shelf Life* 12, 135–141. doi:10.1016/j.fpsl.2017.04.010.

Allwood, J. W., Ellis, D. I., and Goodacre, R. (2008). Metabolomic technologies and their application to the study of plants and plant-host interactions. *Physiol. Plant.* 132, 117–135. doi:10.1111/j.1399-3054.2007.01001.x.

Arye, G., Dror, I., and Berkowitz, B. (2011). Fate and transport of carbamazepine in soil aquifer treatment (SAT) infiltration basin soils. *Chemosphere* 82, 244–252. doi:10.1016/j.chemosphere.2010.09.062.

Aznar, R., Sánchez-Brunete, C., Albero, B., Rodríguez, J. A., and Tadeo, J. L. (2014). Occurrence and analysis of selected pharmaceutical compounds in soil from Spanish agricultura fields. *Environ. Sci. Pollut. Res.* 21, 4772–4782. doi:10.1007/s11356-013-2438-7.

Bailey, N. J. C., Oven, M., Holmes, E., Nicholson, J. K., and Zenk, M. H. (2003). Metabolomic analysis of the consequences of cadmium exposure in *Silene cucubalus* cell cultures via

[1]H NMR spectroscopy and chemometrics. *Phytochemistry* 62, 851–858. doi:10.1016/S0031- 9422(02)00719-7.

Baldacci-Cresp, F., Maucourt, M., Deborde, C., Pierre, O., Moing, A., Brouquisse, R., et al. (2015). Maturation of nematode-induced galls in *Medicago truncatula* is related to water status and primary metabolism modifications. *Plant Sci.* 232, 77–85. doi:10.1016/j.plantsci.2014.12.019.

Bashandy, H., Pietiäinen, M., Carvalho, E., Lim, K. J., Elomaa, P., Martens, S., et al. (2015). Anthocyanin biosynthesis in gerbera cultivar 'Estelle' and its acyanic sport 'Ivory.' *Planta* 242, 601–611. doi:10.1007/s00425-015-2349-6.

Beltrán, E. M., Pablos, M. V., Fernández Torija, C., Porcel, M. Á., and González-Doncel, M. (2020). Uptake of atenolol, carbamazepine and triclosan by crops irrigated with reclaimed water in a Mediterranean scenario. *Ecotoxicol. Environ. Saf.* 191, 110171. doi:10.1016/j.ecoenv.2020.110171.

Benheim, D., Rochfort, S., Korosi, G. A., Powell, K. S., Robertson, E., and Potter, I. D. (2014). Nuclear magnetic resonance metabolic profiling of leaves from *Vitis vinifera* infested with root-feeding grape phylloxera (*Daktulosphaira vitifoliae* Fitch) under field conditions. *Acta Hortic.* 1045, 59–66. doi:10.17660/ActaHortic.2014.1045.8.

Bhattarai, K., Conesa, A., Xiao, S., Peres, N. A., Clark, D. G., Parajuli, S., et al. (2020). Sequencing and analysis of gerbera daisy leaf transcriptomes reveal disease resistance and susceptibility genes differentially expressed and associated with powdery mildew resistance. *BMC Plant Biol.* 20, 1–17. doi:10.1186/s12870-020-02742-4.

Blanchet, L., and Smolinska, A. (2016). "Data fusion in metabolomics and proteomics for biomarker discovery" in *Statistical Analysis in Proteomics. Methods in Molecular Biology, vol 1362*, ed. K. Jung (Humana Press, New York, NY). doi:https://doi.org/10.1007/978-1-4939-3106-4_14.

Bohlmann, F., Zdero, C., and Heinrich, F. (1973). Über die Inhaltsstoffe der Gattung Gerbera. *Chern. Ber.* 106, 382–387. doi:10.1017/CBO9781107415324.004.

Boughton, B. A., Thinagaran, D., Sarabia, D., Bacic, A., and Roessner, U. (2016). Mass spectrometry imaging for plant biology: a review. *Phytochem.* Rev. 15, 445–488. doi:10.1007/s11101-015- 9440-2.

Bourgaud, F., Hehn, A., Larbat, R., Doerper, S., Gontier, E., Kellner, S., et al. (2006). Biosynthesis of coumarins in plants: A major pathway still to be unravelled for cytochrome P450 enzymes. *Phytochem. Rev.* 5, 293–308. doi:10.1007/s11101-006-9040-2.

Broholm, S. K., Pöllänen, E., Ruokolainen, S., Tähtiharju, S., Kotilainen, M., Albert, V. A., et al. (2010). Functional characterization of B class *MADS*-box transcription factors in *Gerbera hybrida*. *J. Exp. Bot.* 61, 75–85. doi:10.1093/jxb/erp279.

Brown, P. H., and Hu, H. (1996). Phloem mobility of boron is species dependent: Evidence for phloem mobility in sorbitol-rich species. *Ann. Bot.* 77, 497–506. doi:10.1006/anbo.1996.0060.

Browne, R. A., and Brindle, K. M. (2007). [1]H NMR-based metabolite profiling as a potential selection tool for breeding passive resistance against *Fusarium* head blight (FHB) in wheat. *Mol. Plant Pathol.* 8, 401–410. doi:10.1111/j.1364-3703.2007.00400.x.

Calderón-Preciado, D., Jiménez-Cartagena, C., Matamoros, V., and Bayona, J. M. (2011). Screening of 47 organic microcontaminants in agricultural irrigation waters and their soil loading. *Water Res.* 45, 221–231. doi:10.1016/j.watres.2010.07.050.

Capitani, D., Sobolev, A. P., Tomassini, A., Sciubba, F., De Salvador, F. R., Mannina, L., et al. (2013). Peach fruit: Metabolic comparative analysis of two varieties with different resistances to insect attacks by NMR spectroscopy. *J. Agric. Food Chem.* 61, 1718–1726. doi:10.1021/jf303248z.

Carter, L. J., Williams, M., Böttcher, C., and Kookana, R. S. (2015). Uptake of pharmaceuticals influences plant development and affects nutrient and hormone homeostases. *Environ. Sci. Technol.* 49, 12509–12518. doi:10.1021/acs.est.5b03468.

Caruso, G., Gennai, C., Ugolini, F., Marchini, F., Quartacci, M. F., and Gucci, R. (2017). Tolerance and physiological response of young *Ficus carica* L. plants irrigated with saline water. *Acta Hortic.* 1173, 137–141. doi: 10.17660/ActaHortic.2017.1173.23

Chen, F., Ma, R., and Chen, X. L. (2019). Advances of metabolomics in fungal pathogen–plant interactions. *Metabolites* 9,169. doi:10.3390/metabo9080169.

Chen, Z. H., and Soltis, D. E. (2020). Evolution of environmental stress responses in plants. *Plant Cell Environ.* 43, 2827–2831. doi:10.1111/pce.13922.

Chin, E. L., Mishchuk, D. O., Breksa, A. P., and Slupsky, C. M. (2014). Metabolite signature of *Candidatus Liberibacter asiaticus* infection in two *Citrus* varieties. *J. Agric. Food Chem.* 62, 6585–6591. doi:10.1021/jf5017434.

Chin, E. L., Ramsey, J. S., Mishchuk, D. O., Saha, S., Foster, E., Chavez, J. D., et al. (2020). Longitudinal transcriptomic, proteomic, and metabolomic analyses of *Citrus sinensis* (L.) Osbeck graft-inoculated with *Candidatus Liberibacter asiaticus*. *J. Proteome Res.* 19, 719–732. doi:10.1021/acs.jproteome.9b00616.

Choi, H. K., Choi, Y. H., Verberne, M., Lefeber, A. W. M., Erkelens, C., and Verpoorte, R. (2004a). Metabolic fingerprinting of wild type and transgenic tobacco plants by [1]H NMR and multivariate analysis technique. *Phytochemistry* 65, 857–864. doi:10.1016/j.phytochem.2004.01.019.

Choi, Y. H., Casas Tapias, E., Kim, H. K., Lefeber, A. W. M., Erkelens, C., Verhoeven, J. T. J., et al. (2004b). Metabolic discrimination of *Catharanthus roseus* leaves infected by phytoplasma using [1]H-NMR spectroscopy and multivariate data analysis. *Plant Physiol.* 135, 2398–2410. doi:10.1104/pp.104.041012.

Choi, Y. H., Kim, H. K., Linthorst, H. J. M., Hollander, J. G., Lefeber, A. W. M., Erkelens, C., et al. (2006). NMR metabolomics to revisit the tobacco mosaic virus infection in *Nicotiana tabacum* leaves. *J. Nat. Prod.* 69, 742–748. doi:10.1021/np050535b.

Colla, G., Rouphael, Y., Cardarelli, M., and Rea, E. (2006). Effect of salinity on yield, fruit quality, leaf gas exchange, and mineral composition of grafted watermelon plants. *HortScience* 41, 622– 627. doi:10.21273/hortsci.41.3.622.

Conde, C., Delrot, S., and Gerós, H. (2008). Physiological, biochemical and molecular changes occurring during olive development and ripening. *J. Plant Physiol.* 165, 1545–1562. doi:10.1016/j.jplph.2008.04.018.

Conde, C., Silva, P., Agasse, A., Lemoine, R., Delrot, S., Tavares, R., et al. (2007). Utilization and transport of mannitol in *Olea europaea* and implications for salt stress tolerance. *Plant Cell Physiol.* 48, 42–53. doi:10.1093/pcp/pcl035.

Copley, T. R., Aliferis, K. A., Kliebenstein, D. J., and Jabaji, S. H. (2017). An integrated RNA seq-^{1}H NMR metabolomics approach to understand soybean primary metabolism regulation in response to *Rhizoctonia* foliar blight disease. *BMC Plant Biol.* 17, 1–18. doi:10.1186/s12870- 017-1020-8.

Crandall, S. G., Gold, K. M., Del Mar Jiménez-Gasco, M., Camila, Filgueiras, C., and Willett, D. S. (2020). A multi-omics approach to solving problems in plant disease ecology. *PLoS One* 15, 1– 23. doi:10.1371/journal.pone.0237975.

Cuperlovic-Culf, M., Wang, L., Forseille, L., Boyle, K., Merkley, N., Burton, I., et al. (2016). Metabolic biomarker panels of response to *Fusarium* head blight infection in different wheat varieties. *PLoS One* 11, 1–16. doi:10.1371/journal.pone.0153642.

Dalkmann, P., Broszat, M., Siebe, C., Willaschek, E., Sakinc, T., Huebner, J., et al. (2012). Accumulation of pharmaceuticals, enterococcus, and resistance genes in soils irrigated with wastewater for zero to 100 years in central Mexico. *PLoS One* 7, e45397. doi:10.1371/journal.pone.0045397.

de Falco, B., Manzo, D., Incerti, G., Garonna, A. P., Ercolano, M., and Lanzotti, V. (2019). Metabolomics approach based on NMR spectroscopy and multivariate data analysis to explore the interaction between the leafminer *Tuta absoluta* and tomato (*Solanum lycopersicum*). *Phytochem. Anal.* 30, 556–563. doi:10.1002/pca.2850.

Debik, J., Sangermani, M., Wang, F., Madssen, T. S., and Giskeødegård, G. F. (2022). Multivariate analysis of NMR-based metabolomic data. *NMR Biomed.* 35, 1–21. doi:10.1002/nbm.4638.

Deng, Z., and Harbaugh, B. K. (2010). UFGE 4141, UFGE 7014, UFGE 7015, UFGE 7023, UFGE 7032, and UFGE 7034: Six new gerbera cultivars for marketing flowering plants in large containers. *HortScience* 45, 971–974. doi:10.21273/hortsci.45.6.971.

Desnoues, E., Gibon, Y., Baldazzi, V., Signoret, V., Génard, M., and Quilot-Turion, B. (2014). Profiling sugar metabolism during fruit development in a peach progeny with different fructose-to-glucose ratios. *BMC Plant Biol.* 14, 12–14. doi:10.1186/s12870-014-0336-x.

Dietze, M. C., Sala, A., Carbone, M. S., Czimczik, C. I., Mantooth, J. A., Richardson, A. D., et al. (2014). Nonstructural carbon in woody plants. *Annu. Rev. Plant Biol.* 65, 667–687. doi:10.1146/annurev-arplant-050213-040054.

do Prado Apparecido, R., Carlos, E. F., Lião, L. M., Vieira, L. G. E., and Alcantara, G. B. (2017). NMR-based metabolomics of transgenic and non-transgenic sweet orange reveals different responses in primary metabolism during citrus canker development. *Metabolomics* 13, 1–12. doi:10.1007/s11306-017-1163-5.

Dona, A. C., Kyriakides, M., Scott, F., Shephard, E. A., Varshavi, D., Veselkov, K., et al. (2016). A guide to the identification of metabolites in NMR-based metabonomics/metabolomics experiments. *Comput. Struct. Biotechnol. J.* 14, 135–153. doi:10.1016/j.csbj.2016.02.005.

Dordio, A. V., Belo, M., Martins Teixeira, D., Palace Carvalho, A. J., Dias, C. M. B., Picó, Y., et al. (2011). Evaluation of carbamazepine uptake and metabolization by *Typha* spp., a plant with potential use in phytotreatment. *Bioresour. Technol.* 102, 7827–7834. doi:10.1016/j.biortech.2011.06.050.

Dueñas, M. E., Larson, E. A., and Lee, Y. J. (2019). Toward mass spectrometry imaging in the metabolomics scale: Increasing metabolic coverage through multiple on-tissue chemical modifications. *Front. Plant Sci.* 10, 860. doi:10.3389/fpls.2019.00860.

Dunn, W. B., Bailey, N. J. C., and Johnson, H. E. (2005). Measuring the metabolome: Current analytical technologies. *Analyst* 130, 606–625. doi:10.1039/b418288j.

Eckermann, S., Schröder, G., Schmidt, J., Streck, D., Edrada, R. A., Helariutta, Y., et al. (1998). New pathway to polyketides in plants. *Nature* 396, 387–90. doi:10.1038/24652.

Edison, A. S., Colonna, M., Gouveia, G. J., Holderman, N. R., Judge, M. T., Shen, X., et al. (2021). NMR: Unique strengths that enhance modern metabolomics research. *Anal. Chem.* 93, 478–499. doi:10.1021/acs.analchem.0c04414.

Ersoy, N. (2007). Changes in sugar contents of fig fruit (*Ficus carica* L. cv. Bursa Siyahı) during development. *SDÜ Ziraat Fakültesi Derg.* 2, 22–26. ISSN 1304-9984

Everard, J. D., Gucci, R., Kann, S. C., Flore, J. A., and Loescher, W. H. (1994). Gas exchange and carbon partitioning in the leaves of celery (*Apium graveolens* L.) at various levels of root zone salinity. *Plant Physiol.* 106, 281–292. doi:10.1104/pp.106.1.281.

FAOSTAT (2019). Statistical databases, food and agriculture organization of the United Nations. *2019*. Available at: http://www.fao.org/faostat/en/#home [Accessed March 6, 2021].

Fattorini, C., Bernardi, R., Quartacci, M. F., Mascgni, F., Caruso, G., Cavallini, A., et al. (2021).

Expression of genes involved in metabolism and transport of soluble carbohydrates during fruit ripening in two cultivars of *Ficus carica* L. *Agrochimica* 65, 117–136. doi:10.12871/00021857202122.

Fenet, H., Mathieu, O., Mahjoub, O., Li, Z., Hillaire-Buys, D., Casellas, C., et al. (2012). Carbamazepine, carbamazepine epoxide and dihydroxycarbamazepine sorption to soil and occurrence in a wastewater reuse site in Tunisia. *Chemosphere* 88, 49–54. doi:10.1016/j.chemosphere.2012.02.050.

Fernandes, H. P., Salomé-Abarca, L. F., Gonçalves Pereira, R., Brandão Seibert, J., Silva-Junior, G. J., Das Graças Fernandes da Silva, M. F., et al. (2022). Metabolomic investigation of *Citrus latifolia* and the putative role of coumarins in resistance to black spot disease. *Front. Mol. Biosci.* 9, 1–13. doi:10.3389/fmolb.2022.934401.

Fiehn, O. (2002). Metabolomics - The link between genotypes and phenotypes. *Plant Mol. Biol.* 48, 155–171. doi:10.1023/A:1013713905833.

Figueiredo, A., Fortes, A. M., Ferreira, S., Sebastiana, M., Choi, Y. H., Sousa, L., et al. (2008). Transcriptional and metabolic profiling of grape (*Vitis vinifera* L.) leaves unravel possible innate resistance against pathogenic fungi. *J. Exp. Bot.* 59, 3371–3381. doi:10.1093/jxb/ern187.

Forsman, A. (2014). Effects of genotypic and phenotypic variation on establishment are important for conservation, invasion, and infection biology. *Proc. Natl. Acad. Sci. U. S. A.* 111, 302–307. doi:10.1073/pnas.1317745111.

Frost, C. J., Mescher, M. C., Carlson, J. E., and De Moraes, C. M. (2008). Plant defense priming against herbivores: Getting ready for a different battle. *Plant Physiol.* 146, 818–824. doi:10.1104/pp.107.113027.

Gachon, C. M. M., Langlois-Meurinne, M., and Saindrenan, P. (2005). Plant secondary metabolism glycosyltransferases: The emerging functional analysis. *Trends Plant Sci.* 10, 542–549. doi:10.1016/j.tplants.2005.09.007.

Gao, F., Chao, J., Zhao, L., Zhao, L., and Tian, H. (2021). ^{1}H NMR-based metabolomics to identify resistance-related metabolites in *Astragalus membranaceus* var. Mongholicus against *Fusarium* root rot. *Int. J. Agric. Biol.* 26, 69–78. doi:10.17957/IJAB/15.1810.

Gao, Z., Sagi, M., and Lips, S. H. (1998). Carbohydrate metabolism in leaves and assimilate partitioning in fruits of tomato (*Lycopersicon esculentum* L.) as affected by salinity. *Plant Sci.* 135, 149–159. doi:10.1016/S0168-9452(98)00085-5.

Garcia-Perez, I., Posma, J. M., Serrano-Contreras, J. I., Boulangé, C. L., Chan, Q., Frost, G., et al. (2020). Identifying unknown metabolites using NMR-based metabolic profiling techniques. *Nat. Protoc.* 15, 2538–2567. doi:10.1038/s41596-020-0343-3.

Ghani, M., and Sharma, S. K. (2019). Induction of powdery mildew resistance in gerbera (*Gerbera jamesonii*) through gamma irradiation. *Physiol. Mol. Biol. Plants* 25, 159–166. doi:10.1007/s12298-018-0613-5.

Gilani, A. H., Mehmood, M. H., Janbaz, K. H., Khan, A., and Saeed, S. A. (2008). Ethnopharmacological studies on antispasmodic and antiplatelet activities of *Ficus carica*. *J. Ethnopharmacol.* 119, 1–5. doi:10.1016/j.jep.2008.05.040.

Goldstein, M., Shenker, M., and Chefetz, B. (2014). Insights into the uptake processes of wastewater-borne pharmaceuticals by vegetables. *Environ. Sci. Technol.* 48, 5593–5600. doi:10.1021/es5008615.

Golombek, S. D., and Lüdders, P. (1993). Effects of short-term salinity on leaf gas exchange of the fig (*Ficus carica* L.). *Plant Soil* 148, 21–27. doi:10.1007/BF02185381.

Gorovits, R., Shteinberg, M., Mishra, R., Ari, J. Ben, Malchi, T., Chefetz, B., et al. (2021). Interplay of stress responses to carbamazepine treatment, whitefly infestation and virus infection in tomato plants. *Plant Stress* 1, 100009. doi:10.1016/j.stress.2021.100009.

Gray, S. B., and Brady, S. M. (2016). Plant developmental responses to climate change. *Dev. Biol.* 419, 64–77. doi:10.1016/j.ydbio.2016.07.023.

Greco, M., Chiappetta, A., Bruno, L., and Bitonti, M. B. (2012). In *Posidonia oceanica* cadmium induces changes in DNA methylation and chromatin patterning. *J. Exp. Bot.* 63, 695–709. doi:10.1093/jxb/err313.

Gucci, R., Moing, A., Gravano, E., and Gaudillere, J. (1998). Partitioning of photosynthetic carbohydrates in leaves of salt-stressed olive plants. *Aust. J. Plant Physiol.* 25, 571–579. doi:10.1071/PP98003.

Gupta, B., and Huang, B. (2014). Mechanism of salinity tolerance in plants: Physiological, biochemical, and molecular characterization. *Int. J. Genomics* 2014, 701596. doi: 10.1155/2014/701596.

Halabalaki, M., Bertrand, S., Stefanou, A., Gindro, K., Kostidis, S., Mikros, E., et al. (2014). Sample preparation issues in NMR-based plant metabolomics: Optimisation for *Vitis* wood samples. *Phytochem. Anal.* 25, 350–356. doi:10.1002/pca.2497.

Hall, C. R., Robertson, L. P., Carroll, A. R., and Kitching, R. L. (2018). The effect of *Psephodiplosis rubi* (Diptera: Cecidomyiidae) leaf galls on the secondary metabolite profiles of two congeneric host plants. *Austral Entomol.* 57, 228–237. doi:10.1111/aen.12338.

Hao, J., Liebeke, M., Astle, W., De Iorio, M., Bundy, J. G., and Ebbels, T. M. D. (2014). Bayesian deconvolution and quantification of metabolites in complex 1D NMR spectra using BATMAN. *Nat. Protoc.* 9, 1416–1427. doi:10.1038/nprot.2014.090.

He, F., Wang, M., Gao, M., Zhao, M., Bai, Y., and Zhao, C. (2014). Chemical composition and biological activities of *Gerbera anandria*. *Molecules* 19, 4046–4057. doi:10.3390/molecules19044046.

Helariutta, Y., Kotilainen, M., Elomaa, P., Kalkkinen, N., Bremer, K., Teeri, T. H., et al. (1996). Duplication and functional divergence in the chalcone synthase gene family of Asteraceae: Evolution with substrate change and catalytic simplification. *Proc. Natl. Acad. Sci. U. S. A.* 93, 9033–9038. doi:10.1073/pnas.93.17.9033.

Heyman, H. M., and Dubery, I. A. (2016). The potential of mass spectrometry imaging in plant metabolomics: a review. *Phytochem. Rev.* 15, 297–316. doi:10.1007/s11101-015-9416-2.

Hodge, S., Ward, J. L., Beale, M. H., Bennett, M., Mansfield, J. W., and Powell, G. (2013). Aphid-induced accumulation of trehalose in *Arabidopsis thaliana* is systemic and dependent upon aphid density. *Planta* 237, 1057–1064. doi:10.1007/s00425-012-1826-4.

Hoffman, G. J., Catlin, P. B., Mead, R. M., Johnson, R. S., Francois, L. E., and Goldhamer, D. (1989). Yield and foliar injury responses of mature plum trees to salinity. *Irrig. Sci.* 10, 215–229. doi:10.1007/BF00257954.

Hothorn, T., Hornik, K., and Zeileis, A. (2006). Unbiased recursive partitioning: A conditional inference framework. *J. Comput. Graph. Stat.* 15, 651–674. doi:10.1198/106186006X 133933.

Howarth, A., Ermanis, K., and Goodman, J. M. (2020). DP4-AI automated NMR data analysis: straight from spectrometer to structure. *Chem. Sci.* 11, 4351–4359. doi:10.1039/d0sc00442a.

Hurtado, C., Parastar, H., Matamoros, V., Piña, B., Tauler, R., and Bayona, J. M. (2017). Linking the morphological and metabolomic response of *Lactuca sativa* L. exposed to emerging contaminants using GC × GC-MS and chemometric tools. *Sci. Rep.* 7, 18–26. doi:10.1038/s41598-017-06773-0.

Ikegami, H., Habu, T., Mori, K., Nogata, H., Hirata, C., Hirashima, K., et al. (2013). *De novo* sequencing and comparative analysis of expressed sequence tags from gynodioecious fig (*Ficus carica* L.) fruits: Caprifig and common fig. *Tree Genet. Genomes* 9, 1075–1088. doi:10.1007/s11295-013-0622-z.

Inoue, T., Toyonaga, T., Nagumo, S., and Nagai, M. (1989). Biosynthesis of 4-hydroxy-5- methylcoumarin in a *Gerbera jamesonii* hybrid. *Phytochemistry* 28, 2329–2330. doi:10.1016/S0031-9422(00)97977-9.

Isha, A., Akanbi, F. S., Yusof, N. A., Osman, R., Mui-Yun, W., and Abdullah, S. N. A. (2019). An NMR metabolomics approach and detection of *Ganoderma boninense*-infected oil palm leaves using MWCNT-based electrochemical sensor. *J. Nanomater.* 2019, 1–12. doi:10.1155/2019/4729706.

Isha, A., Yusof, N. A., Osman, R., Wong, M. Y., and Abdullah, S. N. A. (2020). NMR-based metabolomics reveals effect of *Ganoderma boninense* infection on oil palm leaf at 30 days post-infection. *Plant Omics* 13, 15–20. doi:10.21475/POJ.13.01.20.P2071.

Jamil, I. N., Remali, J., Azizan, K. A., Nor Muhammad, N. A., Arita, M., Goh, H. H., et al. (2020). Systematic multi-omics integration (MOI) approach in plant systems biology. *Front. Plant Sci.* 11. doi:10.3389/fpls.2020.00944.

Jamla, M., Khare, T., Joshi, S., Patil, S., Penna, S., and Kumar, V. (2021). Omics approaches for understanding heavy metal responses and tolerance in plants. *Curr. Plant Biol.* 27, 100213. doi:10.1016/j.cpb.2021.100213.

Jamwal, K., Bhattacharya, S., and Puri, S. (2018). Plant growth regulator mediated consequences of secondary metabolites in medicinal plants. *J. Appl. Res. Med. Aromat. Plants* 9, 26–38. doi:10.1016/j.jarmap.2017.12.003.

Jendoubi, T. (2021). Approaches to integrating metabolomics and multi-omics data: A primer. *Metabolites* 11, 184. doi:10.3390/metabo11030184.

Jennings, D. B., Ehrenshaft, M., Mason Pharr, D., and Williamson, J. D. (1998). Roles for mannitol and mannitol dehydrogenase in active oxygen-mediated plant defense. *Proc. Natl. Acad. Sci. U. S. A.* 95, 15129–15133. doi:10.1073/pnas.95.25.15129.

Jlilat, A., Ragone, R., Gualano, S., Santoro, F., Gallo, V., Varvaro, L., et al. (2021). A non-targeted metabolomics study on *Xylella fastidiosa* infected olive plants grown under controlled conditions. *Sci. Rep.* 11, 1–11. doi:10.1038/s41598-020-80090-x.

Jones, O. A. H., Maguire, M. L., Griffin, J. L., Jung, Y. H., Shibato, J., Rakwal, R., et al. (2011). Using metabolic profiling to assess plant-pathogen interactions: An example using rice (*Oryza sativa*) and the blast pathogen *Magnaporthe grisea*. *Eur. J. Plant Pathol.* 129, 539–554. doi:10.1007/s10658-010-9718-6.

Jones, P., and Vogt, T. (2001). Glycosyltransferases in secondary plant metabolism: Tranquilizers and stimulant controllers. *Planta* 213, 164–174. doi:10.1007/s004250000492.

Kalisz, S., and Kramer, E. M. (2008). Variation and constraint in plant evolution and development. *Heredity* 100, 171–177. doi:10.1038/sj.hdy.6800939.

Kantor, M., Levi, A., Thies, J., Guner, N., Kantor, C., Parnham, S., et al. (2018). NMR analysis reveals a wealth of metabolites in root-knot nematode resistant roots of *Citrullus amarus* watermelon plants. *J. Nematol.* 50, 303–316. doi:10.21307/jofnem-2018-030.

Karban, R., and Myers, J. H. (1989). Induced plant responses to herbivory. *Annu. Rev. Ecol. Syst.* 20, 331–348. doi:10.1146/annurev.es.20.110189.001555.

Kashif, A., Federica, M., Eva, Z., Martina, R., Young, H. C., and Robert, V. (2009). NMR metabolic fingerprinting based identification of grapevine metabolites associated with downy mildew resistance. *J. Agric. Food Chem.* 57, 9599–9606. doi:10.1021/jf902069f.

Katam, R., Lin, C., Grant, K., Katam, C. S., and Chen, S. (2022). Advances in plant metabolomics and its applications in stress and single-cell biology. *Int. J. Mol. Sci.* 23. doi:10.3390/ijms23136985.

Keeler, J. (2002). *Understanding NMR spectroscopy.* Second Edition, Wiley, Hoboken. doi:https://doi.org/10.17863/CAM.968.

Khakimov, B., Mobaraki, N., Trimigno, A., Aru, V., and Engelsen, S. B. (2020). Signature Mapping (SigMa): An efficient approach for processing complex human urine ^{1}H NMR metabolomics data. *Anal. Chim. Acta* 1108, 142–151. doi:10.1016/j.aca.2020.02.025.

Khare, S., Singh, N. B., Singh, A., Hussain, I., Niharika, K., Yadav, V., et al. (2020). Plant secondary metabolites synthesis and their regulations under biotic and abiotic constraints. *J. Plant Biol.* 63, 203–216. doi:10.1007/s12374-020-09245-7.

Kim, H. K., Choi, Y. H., and Verpoorte, R. (2010). NMR-based metabolomic analysis of plants. *Nat. Protoc.* 5, 536–549. doi:10.1038/nprot.2009.237.

Kim, H. K., Choi, Y. H., and Verpoorte, R. (2011). NMR-based plant metabolomics: Where do we stand, where do we go? *Trends Biotechnol.* 29, 267–275. doi:10.1016/j.tibtech.2011.02.001.

Kim, H. K., and Verpoorte, R. (2010). Sample preparation for plant metabolomics. *Phytochem. Anal.* 21, 4–13. doi:10.1002/pca.1188.

Kloos, W. E., George, C. G., and Sorge, L. K. (2005a). Dark disk color in the flower of *Gerbera hybrida* is determined by a dominant gene, *Dc. HortScience* 40, 1992–1994. doi:10.21273/hortsci.40.7.1992.

Kloos, W. E., George, C. G., and Sorge, L. K. (2005b). Inheritance of powdery mildew resistance and leaf macrohair density in *Gerbera hybrida*. *HortScience* 40, 1246–1251. doi:10.21273/hortsci.40.5.1246.

Knight, E. R., Carter, L. J., and McLaughlin, M. J. (2018). Bioaccumulation, uptake, and toxicity of carbamazepine in soil–plant systems. *Environ. Toxicol. Chem.* 37, 1122–1130. doi:10.1002/etc.4053.

Kochevenko, A., and Fernie, A. R. (2011). The genetic architecture of branched-chain amino acid accumulation in tomato fruits. *J. Exp. Bot.* 62, 3895–3906. doi:10.1093/jxb/err091.

Kodešová, R., Klement, A., Golovko, O., Fér, M., Nikodem, A., Kočárek, M., et al. (2019). Root uptake of atenolol, sulfamethoxazole and carbamazepine, and their transformation in three soils and four plants. *Environ. Sci. Pollut. Res.* 26, 9876–9891. doi:10.1007/s11356-019-04333-9.

Koskela, S., Elomaa, P., Helariutta, Y., Kilpeläinen, I., Harjunpää, T., Teeri, T. H., et al. (2001). Two bioactive compounds and a novel chalcone synthase-like enzyme identified in *Gerbera hybrida*. *Acta Hortic.* 560, 271–274. doi:10.17660/ActaHortic.2001.560.52.

Koskela, S., Söderholm, P. P., Ainasoja, M., Wennberg, T., Klika, K. D., Ovcharenko, V. V., et al. (2011). Polyketide derivatives active against *Botrytis cinerea* in *Gerbera hybrida*. *Planta* 233, 37–48. doi:10.1007/s00425-010-1277-8.

Kotsiantis, S. B. (2013). Decision trees: A recent overview. *Artif. Intell. Rev.* 39, 261–283. doi:10.1007/s10462-011-9272-4.

Krishnan, P., Kruger, N. J., and Ratcliffe, R. G. (2005). Metabolite fingerprinting and profiling in plants using NMR. *J. Exp. Bot.* 56, 255–265. doi:10.1093/jxb/eri010.

Krstić, G., Anđelković, B., Choi, Y. H., Vajs, V., Stević, T., Tešević, V., et al. (2016). Metabolic changes in *Euphorbia palusrtis* latex after fungal infection. *Phytochemistry* 131, 17–25. doi:10.1016/j.phytochem.2016.08.005.

Kulhánek, M., Balík, J., Černý, J., Sedlář, O., and Vašák, F. (2016). Evaluating of soil sulfur forms changes under different fertilizing systems during long-term field experiments. *Plant, Soil Environ.* 62, 408–415. doi:10.17221/236/2016-PSE.

Kumar, R., Bohra, A., Pandey, A. K., Pandey, M. K., and Kumar, A. (2017). Metabolomics for plant improvement: Status and prospects. *Front. Plant Sci.* 8, 1–27. doi:10.3389/fpls.2017.01302.

Kumar, Y., Zhang, L., Panigrahi, P., Dholakia, B. B., Dewangan, V., Chavan, S. G., et al. (2016). *Fusarium oxysporum* mediates systems metabolic reprogramming of chickpea roots as revealed by a combination of proteomics and metabolomics. *Plant Biotechnol. J.* 14, 1589–1603. doi:10.1111/pbi.12522.

Lankadurai, B. P., Nagato, E. G., and Simpson, M. J. (2013). Environmental metabolomics: An emerging approach to study organism responses to environmental stressors. *Environ. Rev.* 21, 180–205. doi:10.1139/er-2013-0011.

Le Guennec, A., Tayyari, F., and Edison, A. S. (2017). Alternatives to nuclear overhauser enhancement spectroscopy presat and Carr-Purcell-Meiboom-Gill presat for NMR-based metabolomics. *Anal. Chem.* 89, 8582–8588. doi:10.1021/acs.analchem.7b02354.

Leiss, K. A., Choi, Y. H., Abdel-Farid, I. B., Verpoorte, R., and Klinkhamer, P. G. L. (2009a). NMR metabolomics of thrips (*Frankliniella occidentalis*) resistance in senecio hybrids. *J. Chem. Ecol.* 35, 219–229. doi:10.1007/s10886-008-9586-0.

Leiss, K. A., Choi, Y. H., Verpoorte, R., and Klinkhamer, P. G. L. (2011). An overview of NMR-based metabolomics to identify secondary plant compounds involved in host plant resistance. *Phytochem. Rev.* 10, 205–216. doi:10.1007/s11101-010-9175-z.

Leiss, K. A., Cristofori, G., Van Steenis, R., Verpoorte, R., and Klinkhamer, P. G. L. (2013). An eco-metabolomic study of host plant resistance to western flower thrips in cultivated, biofortified and wild carrots. *Phytochemistry* 93, 63–70. doi:10.1016/j.phytochem.2013.03.011.

Leiss, K. A., Maltese, F., Choi, Y. H., Verpoorte, R., and Klinkhamer, P. G. L. (2009b). Identification of chlorogenic acid as a resistance factor for thrips in chrysanthemum. *Plant Physiol.* 150, 1567– 1575. doi:10.1104/pp.109.138131.

Leitão, I., Mourato, M. P., Carvalho, L., Oliveira, M. C., Marques, M. M., and Martins, L. L. (2021). Antioxidative response of lettuce (*Lactuca sativa*) to carbamazepine-induced stress. *Environ. Sci. Pollut. Res.* 28, 45920–45932. doi:10.1007/s11356-021-13979-3.

Li, J., Dodgen, L., Ye, Q., and Gan, J. (2013). Degradation kinetics and metabolites of carbamazepine in soil. *Environ. Sci. Technol.* 47, 3678–3684. doi:10.1021/es304944c.

Li, J., Yan, G., Duan, X., Zhang, K., Zhang, X., Zhou, Y., et al. (2022). Research progress and trends in metabolomics of fruit trees. *Front. Plant Sci.* 13, 881856. doi:10.3389/fpls.2022.881856.

Li, M., Ding, T., Wang, H., Wang, W., Li, J., and Ye, Q. (2018a). Uptake and translocation of ^{14}C-Carbamazepine in soil-plant systems. *Environ. Pollut.* 243, 1352–1359. doi:10.1016/j.envpol.2018.09.079.

Li, M., Li, P., Ma, F., Dandekar, A. M., and Cheng, L. (2018b). Sugar metabolism and accumulation in the fruit of transgenic apple trees with decreased sorbitol synthesis. *Hortic. Res.* 5, 60. doi:10.1038/s41438-018-0064-8.

Li, Y., Kong, D., Fu, Y., Sussman, M. R., and Wu, H. (2020). The effect of developmental and environmental factors on secondary metabolites in medicinal plants. *Plant Physiol. Biochem.* 148, 80–89. doi:10.1016/j.plaphy.2020.01.006.

Lima, C., Muhamadali, H., and Goodacre, R. (2021). The role of Raman spectroscopy within quantitative metabolomics. *Annu. Rev. Anal. Chem.* 14, 323–345. doi:10.1146/annurev-anchem-091420-092323.

Lima, M. R. M., Felgueiras, M. L., Graça, G., Rodrigues, J. E. A., Barros, A., Gil, A. M., et al. (2010). NMR metabolomics of esca disease-affected *Vitis vinifera* cv. Alvarinho leaves. *J. Exp. Bot.* 61, 4033–4042. doi:10.1093/jxb/erq214.

Litvinov, D. Y., Karlov, G. I., and Divashuk, M. G. (2021). Metabolomics for crop breeding: General considerations. *Genes (Basel).* 12, 1602. doi:10.3390/genes12101602.

Liu, C., Chen, F., Liu, L., Fan, X., Liu, H., Zeng, D., et al. (2022). The different metabolic responses of resistant and susceptible wheats to *Fusarium graminearum* inoculation. *Metabolites* 12. doi:10.3390/metabo12080727.

Liu, C., Hao, F., Hu, J., Zhang, W., Wan, L., Zhu, L., et al. (2010). Revealing different systems responses to brown planthopper infestation for pest susceptible and resistant rice plants with the combined metabonomic and gene-expression analysis. *J. Proteome Res.* 9, 6774–6785. doi:10.1021/pr100970q.

Livak, K. J., and Schmittgen, T. D. (2001). Analysis of relative gene expression data using real-time quantitative PCR and the $2^{-\Delta\Delta Ct}$ method. *Methods* 25, 402–408. doi:10.1006/meth.2001.1262.

Lo Bianco, R., Rieger, M., and Sung, S. J. S. (2000). Effect of drought on sorbitol and sucrose metabolism in sinks and sources of peach. *Physiol. Plant.* 108, 71–78. doi:10.1034/j.1399-3054.2000.108001071.x.

López-Gresa, M. P., Lisón, P., Kim, H. K., Choi, Y. H., Verpoorte, R., Rodrigo, I., et al. (2012). Metabolic fingerprinting of tomato mosaic virus infected *Solanum lycopersicum*. *J. Plant Physiol.* 169, 1586–1596. doi:10.1016/j.jplph.2012.05.021.

López-Gresa, M. P., Maltese, F., Bellés, J. M., Conejero, V., Kim, H. K., Choi, Y. H., et al. (2010). Metabolic response of tomato leaves upon different plant-pathogen interactions. *Phytochem. Anal.* 21, 89–94. doi:10.1002/pca.1179.

Lü, H., Li, J., Huang, Y., Zhang, M., Zhang, S., and Wu, J. (2019). Genome-wide identification, expression and functional analysis of the phosphofructokinase gene family in chinese white pear (*Pyrus bretschneideri*). *Gene* 702, 133–142. doi:10.1016/j.gene.2019.03.005.

Lu, S., Li, T., and Jiang, J. (2010). Effects of salinity on sucrose metabolism during tomato fruit development. *African J. Biotechnol.* 9, 842–849.

Maag, D., Erb, M., and Glauser, G. (2015). Metabolomics in plant-herbivore interactions: Challenges and applications. *Entomol. Exp. Appl.* 157, 18–29. doi:10.1111/eea.12336.

Machado, A. R. T., Campos, V. A. C., da Silva, W. J. R., Campos, V. P., Zeri, A. C. de M., and Oliveira, D. F. (2012). Metabolic profiling in the roots of coffee plants exposed to the coffee root-knot nematode, *Meloidogyne exigua*. *Eur. J. Plant Pathol.* 134, 431–441. doi:10.1007/s10658-012-0008-3.

Machado, A. R. T., Medeiros, F. S., De Souza Filho, J. D., Sena, M. M., Terra, W. C., and Pimenta, L. P. S. (2019). NMR-based metabolomic screening for metabolites associated with resistance to *Meloidogyne javanica* in *Annona muricata* roots. *J. Braz. Chem. Soc.* 30, 1276–1283. doi:10.21577/0103-5053.20190022.

Maravi, D. K., Kumar, S., and Sahoo, L. (2022). NMR-based metabolomic profiling of mungbean infected with mungbean yellow mosaic india virus. *Appl. Biochem. Biotechnol.* 194, 5808–5826. doi:10.1007/s12010-022-04074-5.

Marei, N., and Crane, J. C. (1971). Growth and respiratory response of fig (*Ficus carica* L. cv. Mission) fruits to ethylene. *Plant Physiol.* 48, 249–254. doi:10.1104/pp.48.3.249.

Marsoni, M., De Mattia, F., Labra, M., Bruno, A., Bracale, M., and Vannini, C. (2014). Uptake and effects of a mixture of widely used therapeutic drugs in *Eruca sativa* L. and *Zea mays* L. plants. *Ecotoxicol. Environ. Saf.* 108, 52–57. doi:10.1016/j.ecoenv.2014.05.029.

Martins, M. C. M., Caldana, C., Wolf, L. D., and de Abreu, L. G. F. (2018). "The importance of experimental design, quality assurance, and control in plant metabolomics experiments," in *Plant Metabolomics. Methods in Molecular Biology, vol 1778*, ed. C. António (Humana Press, New York, NY). doi:https://doi.org/10.1007/978-1-4939-7819-9_1.

Mascellani, A., Leiss, K., Bac-Molenaar, J., Malanik, M., Marsik, P., Hernandez Olesinski, E., et

al. (2022). Polyketide derivatives in the resistance of *Gerbera hybrida* to powdery mildew. *Front. Plant Sci.* 12, 790907. doi:10.3389/fpls.2021.790907.

Mascellani, A., Natali, L., Cavallini, A., Mascagni, F., Caruso, G., Gucci, R., et al. (2021). Moderate salinity stress affects expression of main sugar metabolism and transport genes and soluble carbohydrate content in ripe fig fruits (*Ficus carica* L. cv. Dottato). *Plants* 10, 1861. doi:10.3390/plants10091861.

McDowell, N. G. (2011). Mechanisms linking drought, hydraulics, carbon metabolism, and vegetation mortality. *Plant Physiol.* 155, 1051–1059. doi:10.1104/pp.110.170704.

Mckay, R. T. (2011). How the 1D-NOESY suppresses solvent signal in metabonomics NMR spectroscopy: An examination of the pulse sequence components and evolution. *Concepts Magn. Reson. Part A Bridg. Educ. Res.* 38 A, 197–220. doi:10.1002/cmr.a.20223.

Medeiros Selegato, D., Cesar Pilon, A., and Carnevale Neto, F. (2019). "Plant metabolomics using NMR spectroscopy," in *NMR-Based Metabolomics* (New York: Springer Science+Business Media, LLC), 345–363.

Medina-Melchor, D. L., Zapata-Sarmiento, D. H., Becerra-Martínez, E., Rodríguez-Monroy, M., Vallejo, L. G. Z., and Sepúlveda-Jiménez, G. (2022). Changes in the metabolomic profiling of *Allium cepa* L. (onion) plants infected with *Stemphylium vesicarium*. *Eur. J. Plant Pathol.* 162, 557–573. doi:10.1007/s10658-021-02421-6.

Meena, K. K., Sorty, A. M., Bitla, U. M., Choudhary, K., Gupta, P., Pareek, A., et al. (2017). Abiotic stress responses and microbe-mediated mitigation in plants: The omics strategies. *Front. Plant Sci.* 8, 1–25. doi:10.3389/fpls.2017.00172.

Mejías, C., Martín, J., Santos, J. L., Aparicio, I., and Alonso, E. (2021). Occurrence of pharmaceuticals and their metabolites in sewage sludge and soil: A review on their distribution and environmental risk assessment. *Trends Environ. Anal. Chem.* 30, e00125. doi:10.1016/j.teac.2021.e00125.

Mercl, F., Košnář, Z., Maršík, P., Vojtíšek, M., Dušek, J., Száková, J., et al. (2021). Pyrolysis of biosolids as an effective tool to reduce the uptake of pharmaceuticals by plants. *J. Hazard. Mater.* 405. doi:10.1016/j.jhazmat.2020.124278.

Meza, F. J., Silva, D., and Vigil, H. (2008). Climate change impacts on irrigated maize in Mediterranean climates: Evaluation of double cropping as an emerging adaptation alternative. *Agric. Syst.* 98, 21–30. doi:10.1016/j.agsy.2008.03.005.

Miège, C., Choubert, J. M., Ribeiro, L., Eusèbe, M., and Coquery, M. (2009). Fate of pharmaceuticals and personal care products in wastewater treatment plants - conception of a database and first results. *Environ. Pollut.* 157, 1721–1726. doi:10.1016/j.envpol.2008.11.045.

Mielko, K. A., Pudełko-Malik, N., Tarczewska, A., and Młynarz, P. (2021). NMR spectroscopy as a "green analytical method" in metabolomics and proteomics studies. *Sustain. Chem. Pharm.* 22, 100474. doi:10.1016/j.scp.2021.100474.

Milly, P. C. D., Wetherald, R. T., Dunne, K. A., and Delworth, T. L. (2002). Increasing risk of great floods in a changing climate. *Nature* 415, 514–517. doi:https://doi.org/10.1038/415514a.

Minic, Z. (2008). Physiological roles of plant glycoside hydrolases. *Planta* 227, 723–740. doi:10.1007/s00425-007-0668-y.

Mirnezhad, M., Romero-González, R. R., Leiss, K. A., Choi, Y. H., Verpoorte, R., and Klinkhamera, P. G. L. (2010). Metabolomic analysis of host plant resistance to thrips in wild and cultivated tomatoes. *Phytochem. Anal.* 21, 110–117. doi:10.1002/pca.1182.

Moles, T. M., de Brito Francisco, R., Mariotti, L., Pompeiano, A., Lupini, A., Incrocci, L., et al. (2019). Salinity in autumn-winter season and fruit quality of tomato landraces. *Front. Plant Sci.* 10, 1–15. doi:10.3389/fpls.2019.01078.

Mori, K., Shirasawa, K., Nogata, H., Hirata, C., Tashiro, K., Habu, T., et al. (2017). Identification of *RAN1* orthologue associated with sex determination through whole genome sequencing analysis in fig (*Ficus carica* L.). *Sci. Rep.* 7, 41124. doi:10.1038/srep41124.

Morkunas, I., and Ratajczak, L. (2014). The role of sugar signaling in plant defense responses against fungal pathogens. *Acta Physiol. Plant.* 36, 1607–1619. doi:10.1007/s11738-014-1559-z.

Mosa, K. A., Ismail, A., and Helmy, M. (2017). "Omics and system biology approaches in plant stress research," in *Plant Stress Tolerance. SpringerBriefs in Systems Biology* (Springer, Cham). doi:https://doi.org/10.1007/978-3-319-59379-1_2.

Murphy, C., Powlowski, J., Wu, M., Butler, G., and Tsang, A. (2011). Curation of characterized glycoside hydrolases of fungal origin. *Database* 2011, 1–14. doi:10.1093/database/bar020.

Murti, R. H., Afifah, E. N., and Nuringtyas, T. R. (2021). Metabolomic response of tomatoes (*Solanum lycopersicum* L.) against bacterial wilt (*Ralstonia solanacearum*) using ^{1}H-NMR spectroscopy. *Plants* 10, 1143. doi: 10.3390/plants10061143

Mustroph, A., Stock, J., Hess, N., Aldous, S., Dreilich, A., and Grimm, B. (2013). Characterization of the phosphofructokinase gene family in rice and its expression under oxygen deficiency stress. *Front. Plant Sci.* 4, 1–16. doi:10.3389/fpls.2013.00125.

Nagumo, S., Toyonaga, T., Inoue, T., and Masahiro, N. (1989). New glucosides of a 4-hydroxy-5-methylcoumarin and a dihydro-α-pyrone from *Gerbera jamesonii* hybrida. *Chem. Pharm. Bull.* 10, 2621–2623. doi: 10.1248/cpb.37.2621

Nicholson, J. K., Lindon, J. C., and Holmes, E. (1999). "Metabonomics": Understanding the metabolic responses of living systems to pathophysiological stimuli via multivariate statistical analysis of biological NMR spectroscopic data. *Xenobiotica* 29, 1181–1189.

doi:10.1080/004982599238047.

Nicotra, A. B., Atkin, O. K., Bonser, S. P., Davidson, A. M., Finnegan, E. J., Mathesius, U., et al. (2010). Plant phenotypic plasticity in a changing climate. *Trends Plant Sci.* 15, 684–692. doi:10.1016/j.tplants.2010.09.008.

Numata, A., Takahashi, C., Fujiki, R., Kitano, E., Kitajima, A., and T, T. (1990). Plant constitutents biologically active to insects. VI. Antifeedants for larvae of the yellow butterfly *Eurema hecabe mandarina* in *Osmunda japonica. Chem. Pharm. Bull.* 38, 2862–2865. doi: 10.1248/cpb.38.2862

Oliver, S. G., Winson, M. K., Kell, D. B., and Baganz, F. (1998). Systematic functional analysis of the yeast genome. *Trends Biotechnol.* 16, 373–378. doi:10.1016/S0167-7799(98) 01214-1.

Olivieri, P., and Farina, M. (2012). "Data analysis and chemometrics," in *Chemical Analysis of Food: Techniques and Applications* doi:10.1016/B978-0-12-384862-8.00002-9.

Opriş, O., Ciorîţă, A., Soran, M. L., Lung, I., Copolovici, D., and Copolovici, L. (2019). Evaluation of the photosynthetic parameters, emission of volatile organic compounds and ultrastructure of common green leafy vegetables after exposure to non-steroidal anti-inflammatory drugs (NSAIDs). *Ecotoxicology* 28, 631–642. doi:10.1007/s10646-019-02059-5.

Osbourn, A. E. (1996). Preformed antimicrobial compounds and plant defense against fungal attack. *Plant Cell* 8, 1821–1831. doi:10.1105/tpc.8.10.1821.

Paknikar, S. K., Pai Fondekar, K. P., Kirtany, J. K., and Natori, S. (1996). 4-hydroxy-5-methylcoumarin derivatives from *Diospyros kaki* thunb and D. kaki var. Sylvestris makino; structure and synthesis of 11-methylgerberinol. *Phytochemistry* 41, 931–933. doi:10. 1016/0031- 9422(95)00698-2.

Palama, T. L., Grisoni, M., Fock-Bastide, I., Jade, K., Bartet, L., Choi, Y. H., et al. (2012). Metabolome of *Vanilla planifolia* (Orchidaceae) and related species under cymbidium mosaic virus (CymMV) infection. *Plant Physiol. Biochem.* 60, 25–34. doi:10.1016/j.plaphy. 2012.07.015.

Panchal, P., Miller, A. J., and Giri, J. (2021). Organic acids: Versatile stress-response roles in plants. *J. Exp. Bot.* 72, 4038–4052. doi:10.1093/jxb/erab019.

Pang, Z., Chong, J., Li, S., and Xia, J. (2020). Metaboanalystr 3.0: Toward an optimized workflow for global metabolomics. *Metabolites* 10. doi:10.3390/metabo10050186.

Patel, M. K., Pandey, S., Kumar, M., Haque, M. I., Pal, S., and Yadav, N. S. (2021). Plants metabolome study: Emerging tools and techniques. *Plants* 10, 2409. doi:10.3390/plants 10112409.

Paz, A., Tadmor, G., Malchi, T., Blotevogel, J., Borch, T., Polubesova, T., et al. (2016). Fate of

carbamazepine, its metabolites, and lamotrigine in soils irrigated with reclaimed wastewater: Sorption, leaching and plant uptake. *Chemosphere* 160, 22–29. doi:10.1016/j. chemosphere.2016.06.048.

Pereira, A. (2016). Plant abiotic stress challenges from the changing environment. *Front. Plant Sci.* 7, 2013–2015. doi:10.3389/fpls.2016.01123.

Pereira, G. E., Padhi, E. M. T., Sudarshana, M. R., Fialho, F. B., Medina-Plaza, C., Girardello, R. C., et al. (2021). Impact of grapevine red blotch disease on primary and secondary metabolites in 'Cabernet Sauvignon' grape tissues. *Food Chem.* 342, 128312. doi:10.1016/ j.foodchem.2020.128312.

Pérez, D. J., Doucette, W. J., and Moore, M. T. (2022). Contaminants of emerging concern (CECs) in *Zea mays*: Uptake, translocation and distribution tissue patterns over the time and its relation with physicochemical properties and plant transpiration rate. *Chemosphere* 288, 132480. doi:10.1016/j.chemosphere.2021.132480.

Pichersky, E., and Gang, D. R. (2000). Genetics and biochemistry of secondary metabolites in plants: An evolutionary perspective. *Trends Plant Sci.* 5, 439–445. doi:10.1016/S1360-1385(00)01741- 6.

Pietiäinen, M., Kontturi, J., Paasela, T., Deng, X., Ainasoja, M., Nyberg, P., et al. (2016). Two polyketide synthases are necessary for 4-hydroxy-5-methylcoumarin biosynthesis in *Gerbera hybrida. Plant J.* 87, 548–558. doi:10.1111/tpj.13216.

Plischke, A., Choi, Y. H., Brakefield, P. M., Klinkhamer, P. G. L., and Bruinsma, M. (2012). Metabolomic plasticity in GM and non-GM potato leaves in response to aphid herbivory and virus infection. *J. Agric. Food Chem.* 60, 1488–1493. doi:10.1021/jf204864y.

Pokala, N. (2012). dunnett.m. Available at: https://www.mathworks.com/matlabcentral/fileexchange/38157-dunnett-m.

Pontes, J. G. M., Ohashi, W. Y., Brasil, A. J. M., Filgueiras, P. R., Espíndola, A. P. D. M., Silva, J. S., et al. (2016). Metabolomics by NMR spectroscopy in plant disease diagnostic: Huanglongbing as a case study. *ChemistrySelect* 1, 1176–1178. doi:10.1002/slct. 201600064.

Putri, S. P., Nakayama, Y., Matsuda, F., Uchikata, T., Kobayashi, S., Matsubara, A., et al. (2013). Current metabolomics: Practical applications. *J. Biosci. Bioeng.* 115, 579–589. doi: 10.1016/j.jbiosc.2012.12.007.

R Core Team (2020). R: A language and environment for statistical computing. Available at: https://www.r-project.org/.

Ramakrishna, A., and Ravishankar, G. A. (2011). Influence of abiotic stress signals on secondary metabolites in plants. *Plant Signal. Behav.* 6, 1720–1731. doi:10.4161/psb.6.11.17613.

Ramaroson, M. L., Koutouan, C., Helesbeux, J. J., Le Clerc, V., Hamama, L., Geoffriau, E., et al.

(2022). Role of phenylpropanoids and flavonoids in plant resistance to pests and diseases. *Molecules* 27. doi:10.3390/molecules27238371.

Ramsey, J. S., Chin, E. L., Chavez, J. D., Saha, S., Mischuk, D., Mahoney, J., et al. (2020). Longitudinal transcriptomic, proteomic, and metabolomic analysis of *Citrus limon* response to graft inoculation by *Candidatus Liberibacter asiaticus*. *J. Proteome Res.* 19, 2247–2263. doi:10.1021/acs.jproteome.9b00802.

Raza, A., Tabassum, J., Zahid, Z., Charagh, S., Bashir, S., Barmukh, R., et al. (2022). Advances in "omics" approaches for improving toxic metals/metalloids tolerance in plants. *Front. Plant Sci.* 12, 1–28. doi:10.3389/fpls.2021.794373.

Riemenschneider, C., Seiwert, B., Moeder, M., Schwarz, D., and Reemtsma, T. (2017). Extensive transformation of the pharmaceutical carbamazepine following uptake into intact tomato plants. *Environ. Sci. Technol.* 51, 6100–6109. doi:10.1021/acs.est.6b06485.

Rivas-Ubach, A., Pérez-Trujillo, M., Sardans, J., Gargallo-Garriga, A., Parella, T., and Peñuelas, J. (2013). Ecometabolomics: Optimized NMR-based method. *Methods Ecol. Evol.* 4, 464–473. doi:10.1111/2041-210X.12028.

Rodrigues-Corrêa, K. C. da S., and Fett-Neto, A. G. (2019). Abiotic stresses and non-protein amino acids in plants. *CRC. Crit. Rev. Plant Sci.* 38, 411–430. doi:10.1080/07352689.2019.1707944.

Rodrigues, A. M., Ribeiro-Barros, A. I., and António, C. (2019). Experimental design and sample preparation in forest tree metabolomics. *Metabolites* 9, 5–7. doi:10.3390/metabo9120285.

Ruokolainen, S., Ng, Y. P., Broholm, S. K., Albert, V. A., Elomaa, P., and Teeri, T. H. (2010). Characterization of SQUAMOSA-like genes in *Gerbera hybrida*, including one involved in reproductive transition. *BMC Plant Biol.* 10, 75–85. doi:10.1186/1471-2229-10-128.

Ryšlavá, H., Pomeislová, A., Pšondrová, Š., Hýsková, V., and Smrček, S. (2015). Phytoremediation of carbamazepine and its metabolite 10,11-epoxycarbamazepine by C3 and C4 plants. *Environ. Sci. Pollut. Res.* 22, 20271–20282. doi:10.1007/s11356-015-5190-3.

Sabino, A. R., Tavares, S. S., Riffel, A., Li, J. V., Oliveira, D. J. A., Feres, C. I. M. A., et al. (2019). ^{1}H NMR metabolomic approach reveals chlorogenic acid as a response of sugarcane induced by exposure to *Diatraea saccharalis*. *Ind. Crops Prod.* 140, 111651. doi:10.1016/j.indcrop.2019.111651.

Sadder, M. T., Alshomali, I., Ateyyeh, A., and Musallam, A. (2021). Physiological and molecular responses for long term salinity stress in common fig (*Ficus carica* L.). *Physiol. Mol. Biol. Plants* 27, 107–117. doi:10.1007/s12298-020-00921-z.

Saied, A. S., Keutgen, A. J., and Noga, G. (2005). The influence of NaCl salinity on growth, yield and fruit quality of strawberry cvs. "Elsanta" and "Korona." *Sci. Hortic.* 103, 289–303. doi:10.1016/j.scienta.2004.06.015.

Saito, T., Fukuda, N., Matsukura, C., and Nishimura, S. (2009). Effects of salinity on distribution of photosynthates and carbohydrate metabolism in tomato grown using nutrient film technique. *J. Japanese Soc. Hortic. Sci.* 78, 90–96. doi:10.2503/jjshs1.78.90.

Saito, T., Matsukura, C., Ban, Y., Shoji, K., Sugiyama, M., Fukuda, N., et al. (2008). Salinity stress affects assimilate metabolism at the gene-expression level during fruit development and improves fruit quality in tomato (*Solanum lycopersicum* L.). *J. Japanese Soc. Hortic. Sci.* 77, 61–68. doi:10.2503/jjshs1.77.61.

Santamaria, M. E., Martínez, M., Cambra, I., Grbic, V., and Diaz, I. (2013). Understanding plant defence responses against herbivore attacks: An essential first step towards the development of sustainable resistance against pests. *Transgenic Res.* 22, 697–708. doi:10.1007/s11248-013- 9725-4.

Sardari, S., Nishibe, S., and Daneshtalab, M. (2000). Coumarins, the bioactive structures with antifungal property. *Stud. Nat. Prod. Chem.* 23, 335–393. doi:10.1016/S1572-5995(00)80133- 7.

Schripsema, J. (2010). Application of NMR in plant metabolomics: Techniques, problems and prospects. *Phytochem. Anal.* 21, 14–21. doi:10.1002/pca.1185.

Sciubba, F., Di Cocco, M. E., Angori, G., Spagnoli, M., De Salvador, F. R., Engel, P., et al. (2020). NMR-based metabolic study of leaves of three species of *Actinidia* with different degrees of susceptibility to P*seudomonas syringae* pv. actinidiae. *Nat. Prod. Res.* 34, 2043–2050. doi:10.1080/14786419.2019.1574784.

Sedaghat, S., and Rahemi, M. (2018). Enzyme activity regarding sugar and organic acid changes during developmental stages in rainfed fig (*Ficus carica* L. cv Sabz). *Int. J. Fruit Sci.* 18, 14–28. doi:10.1080/15538362.2017.1367984.

Sekiyama, Y., Okazaki, K., Kikuchi, J., and Ikeda, S. (2017). NMR-based metabolic profiling of field-grown leaves from sugar beet plants harbouring different levels of resistance to *Cercospora* leaf spot disease. *Metabolites* 7, 4. doi:10.3390/metabo7010004.

Shao, Y., Yang, K., Jia, R., Tian, C., and Zhu, Y. (2018). Degradation of triclosan and carbamazepine in two agricultural and garden soils with different textures amended with composted sewage sludge. *Int. J. Environ. Res. Public Health* 15, 1–14. doi:10.3390/ijerph15112557.

Sheikh, N., Barman, D., and Bhattacharjee, K. (2020). "Abiotic and biotic stress research in plants: A gizmatic approach of modern omics technologies," in *Sustainable Agriculture in the Era of Climate Change*, eds. R. Roychowdhury, S. Choudhury, M. Hasanuzzaman, and S. Srivastava (Cham: Springer). doi:https://doi.org/10.1007/978-3-030-45669-6_19.

Shenker, M., Harush, D., Ben-Ari, J., and Chefetz, B. (2011). Uptake of carbamazepine by cucumber plants - A case study related to irrigation with reclaimed wastewater. *Chemosphere* 82, 905– 910. doi:10.1016/j.chemosphere.2010.10.052.

Shulaev, V., Cortes, D., Miller, G., and Mittler, R. (2008). Metabolomics for plant stress response.

Physiol. Plant. 132, 199–208. doi:10.1111/j.1399-3054.2007.01025.x.

Simoh, S., Quintana, N., Kim, H. K., Choi, Y. H., and Verpoorte, R. (2009). Metabolic changes in *Agrobacterium tumefaciens*-infected *Brassica rapa. J. Plant Physiol.* 166, 1005–1014. doi:10.1016/j.jplph.2008.11.015.

Sirikantaramas, S., Yamazaki, M., and Saito, K. (2008). Mechanisms of resistance to self-produced toxic secondary metabolites in plants. *Phytochem. Rev.* 7, 467–477. doi:10.1007/s11101-007- 9080-2.

Slatnar, A., Klancar, U., Stampar, F., and Veberic, R. (2011). Effect of drying of figs (*Ficus carica* L.) on the contents of sugars, organic acids, and phenolic compounds. *J. Agric. Food Chem.* 59, 11696–11702. doi:10.1021/jf202707y.

Slisz, A. M., Breksa, A. P., Mishchuk, D. O., Mc Collum, G., and Slupsky, C. M. (2012). Metabolomic analysis of *Citrus* infection by *Candidatus Liberibacter* reveals insight into pathogenicity. *J. Proteome Res.* 11, 4223–4230. doi:10.1021/pr300350x.

Smirnoff, N., and Cumbes, Q. J. (1989). Hydroxyl radical scavenging activity of compatible solutes. *Phytochemistry* 28, 1057–1060. doi:10.1016/0031-9422(89)80182-7.

Solomon, A., Golubowicz, S., Yablowicz, Z., Grossman, S., Bergman, M., Gottlieb, H. E., et al. (2006). Antioxidant activities and anthocyanin content of fresh fruits of common fig (*Ficus carica* L.). *J. Agric. Food Chem.* 54, 7717–7723. doi:10.1021/jf060497h.

Song, X., and Deng, Z. (2013). Powdery mildew resistance in gerbera: Mode of inheritance, quantitative trait locus identification, and resistance responses. *J. Am. Soc. Hortic. Sci.* 138, 470– 478. doi:10.21273/jashs.138.6.470.

Song, X., Deng, Z., Gong, L., Hu, J., and Ma, Q. (2012). Cloning and characterization of resistance gene candidate sequences and molecular marker development in gerbera (*Gerbera hybrida*). *Sci. Hortic.* 145, 68–75. doi:10.1016/j.scienta.2012.07.027.

Srivastava, S., Bisht, H., Sidhu, O. P., Srivastava, A., Singh, P. C., Pandey, R. M., et al. (2012). Changes in the metabolome and histopathology of *Amaranthus hypochondriacus* L. in response to *Ageratum enation virus* infection. *Phytochemistry* 80, 8–16. doi:10.1016/j.phytochem.2012.05.007.

Su, X., Lu, G., Guo, H., Zhang, K., Li, X., and Cheng, H. (2018). The dynamic transcriptome and metabolomics profiling in *Verticillium dahliae* inoculated *Arabidopsis thaliana. Sci. Rep.* 8, 1−11. doi:10.1038/s41598-018-33743-x.

Sumner, L. W., Amberg, A., Barrett, D., Beale, M. H., Beger, R., Daykin, C. A., et al. (2007). Proposed minimum reporting standards for chemical analysis. *Metabolomics* 3, 211–221. doi:10.1007/s11306-007-0082-2.

Sun, C., Dudley, S., Trumble, J., and Gan, J. (2018). Pharmaceutical and personal care products-induced stress symptoms and detoxification mechanisms in cucumber plants. *Environ.*

Pollut. 234, 39–47. doi:10.1016/j.envpol.2017.11.041.

Taiz, L., and Zeiger, E. (1991). *Plant physiology.* 6th ed. Redwood City, California: Benjamin/Cummings Pub. Co.

Teeri, T. H., Elomaa, P., Kotilainen, M., and Albert, V. A. (2006). Mining plant diversity: Gerbera as a model system for plant developmental and biosynthetic research. *BioEssays* 28, 756–767. doi:10.1002/bies.20439.

Thelusmond, J. R., Strathmann, T. J., and Cupples, A. M. (2016). The identification of carbamazepine biodegrading phylotypes and phylotypes sensitive to carbamazepine exposure in two soil microbial communities. *Sci. Total Environ.* 571, 1241–1252. doi:10.1016/j.scitotenv.2016.07.154.

Tomita, S., Ikeda, S., Tsuda, S., Someya, N., Asano, K., Kikuchi, J., et al. (2017). A survey of metabolic changes in potato leaves by NMR-based metabolic profiling in relation to resistance to late blight disease under field conditions. *Magn. Reson. Chem.* 55, 120–127. doi:10.1002/mrc.4506.

Tóth, G., Adhikari, K., Várallyay, G., Tóth, T., Bódis, K., and Stolbovoy, V. (2008). "Update map of salt affected soils in the European Union," in *Threats to soil quality in Europe* (Luxemburg: Office for Official Publications of the European Communities), 67–77.

Trouvelot, S., Héloir, M. C., Poinssot, B., Gauthier, A., Paris, F., Guillier, C., et al. (2014). Carbohydrates in plant immunity and plant protection: Roles and potential application as foliar sprays. *Front. Plant Sci.* 5, 1–14. doi:10.3389/fpls.2014.00592.

Tschesche, R., Hoppe, H., Snatzke, G., Walff, G., and Fehlhaber, H.-W. (1971). Über Glykoside mit lacton-bildendem Aglykon, III. Über Parasorbosid, den glykosidischen Vorläufer der Parasorbinsäure, aus Vogelbeeren. *Chem. Ber.* 104, 1420–1428. doi: 10.1002/cber.19711040510

Uawisetwathana, U., Graham, S. F., Kamolsukyunyong, W., Sukhaket, W., Klanchui, A., Toojinda, T., et al. (2015). Quantitative ^{1}H NMR metabolome profiling of thai jasmine rice (*Oryza sativa*) reveals primary metabolic response during brown planthopper infestation. *Metabolomics* 11, 1640–1655. doi:10.1007/s11306-015-0817-4.

Usai, G., Mascagni, F., Giordani, T., Vangelisti, A., Bosi, E., Zuccolo, A., et al. (2020). Epigenetic patterns within the haplotype phased fig (*Ficus carica* L.) genome. *Plant J.* 102, 600–614. doi:10.1111/tpj.14635.

Usai, G., Vangelisti, A., Simoni, S., Giordani, T., Natali, L., Cavallini, A., et al. (2021). DNA modification patterns within the transposable elements of the fig (*Ficus carica* L.) genome. *Plants* 10, 451. doi:10.3390/plants10030451.

Usai, G., Vangelisti, A., Solorzano-Zambrano, L., Mascagni, F., Giordani, T., Cavallini, A., et al. (2017). Transcriptome comparison between two fig (*Ficus carica* L.) cultivars. *Agrochimica* 61, 340–354. doi:10.12871/00021857201735.

USDA (2019). Floriculture crops 2018 summary. *Natl. Agric. Stat. Serv.*

Uthe, H., van Dam, N. M., Hervé, M. R., Sorokina, M., Peters, K., and Weinhold, A. (2021). *A practical guide to implementing metabolomics in plant ecology and biodiversity research.* First ed. Elsevier Ltd. doi:10.1016/bs.abr.2020.09.019.

Vangelisti, A., Simoni, S., Usai, G., Ventimiglia, M., Natali, L., Cavallini, A., et al. (2021). LTR-retrotransposon dynamics in common fig (*Ficus carica* L.) genome. *BMC Plant Biol.* 21, 221. doi: 10.1186/s12870-021-02991-x.

Vangelisti, A., Zambrano, L. S., Caruso, G., Macheda, D., Bernardi, R., Usai, G., et al. (2019). How an ancient, salt-tolerant fruit crop, *Ficus carica* L., copes with salinity: a transcriptome analysis. *Sci. Rep.* 9, 1–13. doi:10.1038/s41598-019-39114-4.

Vasmatkar, P., Kaur, K., Pannu, P. P. S., Kaur, G., and Kaur, H. (2019). Unraveling the metabolite signatures of maize genotypes showing differential response towards southern corn leaf blight by ^{1}H-NMR and FT-IR spectroscopy. *Physiol. Mol. Plant Pathol.* 108, 101441. doi:10.1016/j.pmpp.2019.101441.

Veberic, R., Colaric, M., and Stampar, F. (2008). Phenolic acids and flavonoids of fig fruit (*Ficus carica* L.) in the northern Mediterranean region. *Food Chem.* 106, 153–157. doi:10.1016/j.foodchem.2007.05.061.

Vemmos, S. N., Petri, E., and Stournaras, V. (2013). Seasonal changes in photosynthetic activity and carbohydrate content in leaves and fruit of three fig cultivars (*Ficus carica* L.). *Sci. Hortic.* 160, 198–207. doi:10.1016/j.scienta.2013.05.036.

Verpoorte, R., Choi, Y. H., and Kim, H. K. (2007). NMR-based metabolomics at work in phytochemistry. *Phytochem. Rev.* 6, 3–14. doi:10.1007/s11101-006-9031-3.

Verpoorte, R., Choi, Y. H., Mustafa, N. R., and Kim, H. K. (2008). Metabolomics: Back to basics. *Phytochem. Rev.* 7, 525–537. doi:10.1007/s11101-008-9091-7.

Verpoorte, R., Kim, H. K., and Choi, Y. H. (2022). Trivialities in metabolomics: Artifacts in extraction and analysis. *Front. Mol. Biosci.* 9, 1–11. doi:10.3389/fmolb.2022.972190.

Vignoli, A., Ghini, V., Meoni, G., Licari, C., Takis, P. G., Tenori, L., et al. (2019). High-throughput metabolomics by 1D NMR. *Angew. Chemie - Int. Ed.* 58, 968–994. doi:10.1002/anie.201804736.

Vinci, G., Cozzolino, V., Mazzei, P., Monda, H., Spaccini, R., and Piccolo, A. (2018). An alternative to mineral phosphorus fertilizers: the combined effects of *Trichoderma harzianum* and compost on *Zea mays*, as revealed by ^{1}H NMR and GC-MS metabolomics. *PLoS One* 13, e0209664. doi:10.1371/journal.pone.0209664.

Wahman, R., Sauvêtre, A., Schröder, P., Moser, S., and Letzel, T. (2020). Untargeted metabolomics studies on drug-incubated *Phragmites australis* profiles. *Metabolites* 11, 2. doi:10.3390/metabo11010002.

Wahyuni, D. S. C., Choi, Y. H., Leiss, K. A., and Klinkhamer, P. G. L. (2021). Morphological and chemical factors related to western flower thrips resistance in the ornamental gladiolus. *Plants* 10, 1384. doi:10.3390/plants10071384.

Wang, R., Lin, K., Chen, H., Qi, Z., Liu, B., Cao, F., et al. (2021). Metabolome analysis revealed the mechanism of exogenous glutathione to alleviate cadmium stress in maize (*Zea mays* L.) seedlings. *Plants* 10, 105. doi:10.3390/plants10010105.

Ward, J. L., Baker, J. M., Miller, S. J., Deborde, C., Maucourt, M., Biais, B., et al. (2010a). An inter-laboratory comparison demonstrates that [^{1}H]-NMR metabolite fingerprinting is a robust technique for collaborative plant metabolomic data collection. *Metabolomics* 6, 263–273. doi:10.1007/s11306-010-0200-4.

Ward, J. L., Forcat, S., Beckmann, M., Bennett, M., Miller, S. J., Baker, J. M., et al. (2010b). The metabolic transition during disease following infection of *Arabidopsis thaliana* by *Pseudo monas syringae* pv. tomato. *Plant J.* 63, 443–457. doi:10.1111/j.1365-313X.2010.04254.x.

Wenk, M., Nuzillard, J. M., and Steinbeck, C. (2023). Sherlock—A free and open-source system for the computer-assisted structure elucidation of organic compounds from NMR data. *Molecules* 28, 1448. doi:10.3390/molecules28031448.

Westad, F., and Marini, F. (2015). Validation of chemometric models - A tutorial. *Anal. Chim. Acta* 893, 14–24. doi:10.1016/j.aca.2015.06.056.

Wickham, H. (2016). ggplot2: *Elegant Graphics for Data Analysis.* Verlag New York: Springer.

Widarto, H. T., Van Der Meijden, E., Lefeber, A. W. M., Erkelens, C., Kim, H. K., Choi, Y. H., et al. (2006). Metabolomic differentiation of *Brassica rapa* following herbivory by different insect instars using two-dimensional nuclear magnetic resonance spectroscopy. *J. Chem. Ecol.* 32, 2417–2428. doi:10.1007/s10886-006-9152-6.

Williams, C. F., Williams, C. F., and Adamsen, F. J. (2006). Sorption-desorption of carbamazepine from irrigated soils. *J. Environ. Qual.* 35, 1779–1783. doi:10.2134/jeq2005.0345.

Williamson, J. D., Stoop, J. M. H., Massel, M. O., Conkling, M. A., and Pharr, D. M. (1995). Sequence analysis of a mannitol dehydrogenase cDNA from plants reveals a function for the pathogenesis-related protein ELI3. *Proc. Natl. Acad. Sci. U. S. A.* 92, 7148–7152. doi:10.1073/pnas.92.16.7148.

Wink, M. (2003). Evolution of secondary metabolites from an ecological and molecular phylogenetic perspective. *Phytochemistry* 64, 3–19. doi:10.1016/S0031-9422(03)00300-5.

Winning, H., Larsen, F. H., Bro, R., and Engelsen, S. B. (2008). Quantitative analysis of NMR spectra with chemometrics. *J. Magn. Reson.* 190, 26–32. doi:10.1016/j.jmr.2007.10.005.

Wishart, D. S., Sayeeda, Z., Budinski, Z., Guo, A., Lee, B. L., Berjanskii, M., et al. (2022). NP-MRD: the natural products magnetic resonance database. *Nucleic Acids Res.* 50, D665–D677.

doi:10.1093/nar/gkab1052.

Wold, S. (1972). Spline functions, a new tool in data-analysis. *Kem. Tidskr.* 3, 34–37.

Wolfender, J. L., Ndjoko, K., and Hostettmann, K. (2003). Liquid chromatography with ultraviolet absorbance-mass spectrometric detection and with nuclear magnetic resonance spectroscopy: A powerful combination for the on-line structural investigation of plant metabolites. *J. Chromatogr. A* 1000, 437–455. doi:10.1016/S0021-9673(03)00303-0.

Wu, X., Ernst, F., Conkle, J. L., and Gan, J. (2013). Comparative uptake and translocation of pharmaceutical and personal care products (PPCPs) by common vegetables. *Environ. Int.* 60, 15–22. doi:10.1016/j.envint.2013.07.015.

Xu, J. G., Hu, Q. P., and Liu, Y. (2012). Antioxidant and DNA-protective activities of chlorogenic acid isomers. *J. Agric. Food Chem.* 60, 11625–11630. doi:10.1021/jf303771s.

Yadav, B., Jogawat, A., Rahman, M. S., and Narayan, O. P. (2021). Secondary metabolites in the drought stress tolerance of crop plants: A review. *Gene Reports* 23, 101040. doi:10.1016/j.genrep.2021.101040.

Yamaki, S., and Moriguchi, T. (1989). Seasonal fluctuation of sorbitol-related enzymes and invertase activities accompanying maturation of japanese pear (*Pyrus serotina* Rehder var. culta Rehder) fruit. *J. Japanese Soc. Hortic. Sci.* 57, 602–607. doi:10.2503/jjshs.57.602.

Yin, H., Zhang, Q., Jing, J., Wang, X., Yin, X., and Zhou, M. (2022). An efficient Fe^{2+} assisted UV/electrogenerated-chlorine process for carbamazepine degradation: The role of Fe(IV). *Chemosphere* 307, 136168. doi:10.1016/j.chemosphere.2022.136168.

Yin, Y. G., Kobayashi, Y., Sanuki, A., Kondo, S., Fukuda, N., Ezura, H., et al. (2010). Salinity induces carbohydrate accumulation and sugar-regulated starch biosynthetic genes in tomato (*Solanum lycopersicum* L. cv. 'Micro-Tom') fruits in an ABA- and osmotic stress-independent manner. *J. Exp. Bot.* 61, 563–574. doi:10.1093/jxb/erp333.

Yrjönen, T., Vuorela, P., Klika, K. D., Pihlaja, K., Teeri, T. H., and Vuorela, H. (2002). Application of centrifugal force to the extraction and separation of parasorboside and gerberin from *Gerbera hybrida*. *Phytochem. Anal.* 13, 349–353. doi:10.1002/pca.665.

Zdero, C., Bohlmann, F., and Solomon, J. (1988). Further 5-methylcoumarin derivatives from *Mutisia orbignyana*. *Phytochemistry* 27, 891–897. doi: 10.1016/0031-9422(88)84114-1.

Zeier, J. (2013). New insights into the regulation of plant immunity by amino acid metabolic pathways. *Plant, Cell Environ.* 36, 2085–2103. doi:10.1111/pce.12122.

Zemanová, V., Popov, M., Pavlíková, D., Kotrba, P., Hnilička, F., Česká, J., et al. (2020). Effect of arsenic stress on 5-methylcytosine, photosynthetic parameters and nutrient content in arsenic hyperaccumulator *Pteris cretica* (L.) var. Albo-lineata. *BMC Plant Biol.* 20, 1–10. doi:10.1186/s12870-020-2325-6.

ABOUT ME

My research focus is NMR-based metabolomic approach, chemometrics and data integration to extract information for plant responses to environments stress. Although, I extend the skills in clinical, ecological and food quality studies.

I participated in groundbreaking multidisciplinary research with international collaborators. I am a dedicated and reliable team member. I particularly enjoy collaborating with researchers from different disciplines to develop new skills and take on new challenges.

RESEARCH FOCUS

- Analytical chemistry (NMR, LC-MS)
- Agriculture and plant science
- NMR Metabolomics
- Chemometrics and data integration
- Structural annotation
- Environmental metabolomics
- Foodomics

CONTACTS

a.mascellani14@gmail.com

Anna Mascellani Bergo

Date of birth: 20/07/1995

WORK EXPERIENCE

Junior Scientist

Czech University of Life Sciences, Prague | Sep 2019 - present

- Application of NMR metabolomics for wine quality assessment: from sample preparation to data interpretation.
- Analysis of NMR metabolomics data for clinical studies.

EDUCATION

Doctoral candidate

Czech University of Life Sciences, Prague | Oct 2019 - present

- Title of the thesis: Insights from NMR metabolomics into plant responses to environmental stress.

MSc degree

University of Pisa | 2017-2019

- Laurea magistrale (equivalent to MSc degree) in Plant and Microbe Biotechnologies (mark 110/110 *cum laude*).
- Title of the thesis: "Differential expression gene analysis on sugar pathway in ripe *Ficus carica* L. cv. Dottato fruits under salinity stress".

BSc degree

University of Padova | 2015-2017

- Laurea triennale (equivalent to BSc degree) in Applied Pharmaceutical Science (mark 110/110 *cum laude*).
- Title of the thesis: "Perspectives of biofumigation in medicinal plants' crops".

INTERNSHIPS ABROAD

- 2023: German Centre for Integrative Biodiversity Research (DE) for 5 months, topic: **LC-MS platform for plant metabolomics** (Dr. Stefanie Döll)
- 2022: University of Minnesota (MN, USA) for 1 month, topic: **multi-omics in biology research** (Dr. Andres Gomez)
- 2022: Wageningen University & Research (NL) for 3 months, topic: **plant resilience bio-assays** (Dr. Kirsten Leiss)
- 2021: University of Copenhagen (DK) for 5 months, topic: **utilization of high-field NMR spectroscopy on wine** (Prof. Søren Balling-Engelsen and Dr. Bekzod Khakimov)
- 2019: Czech University of Life Sciences Prague (CZ) for 5 months, topic: **utilization of quantitative high-field NMR spectroscopy in food quality** (Dr. Jaroslav Havlik)

SKILLS

- Programming (MATLAB, R)
- I work independently and in team settings
- Good written and verbal communication
- Critical and creative thinking

LANGUAGES

- English (full professional proficiency)
- Italian (native)
- Czech (beginner)

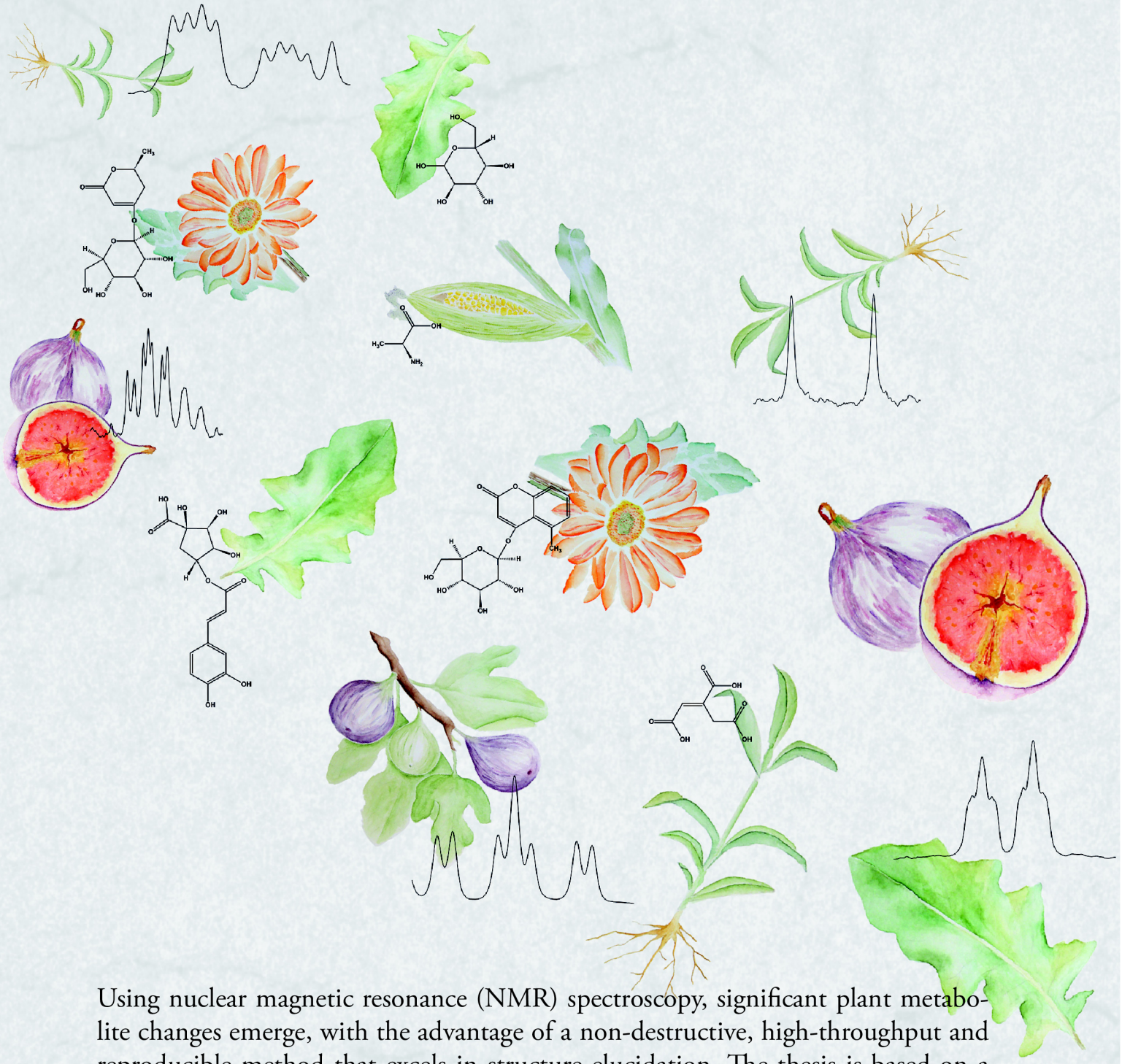

Using nuclear magnetic resonance (NMR) spectroscopy, significant plant metabolite changes emerge, with the advantage of a non-destructive, high-throughput and reproducible method that excels in structure elucidation. The thesis is based on a review and three studies, in which NMR was applied to monitor metabolic changes related to biotic and abiotic stress. In the last two decades, NMR metabolomics was limitedly chosen for accessing plant responses to biotic stress, although resistance mechanisms are detectable and clear. We show that polyketides in gerbera are biomarkers of resistance to powdery mildew. Maize overcomes the stress caused by accumulation of carbamazepine with notable metabolic changes at the early phenological stage; while older plants adapt and only display minor effects. Salinity stress affects the expression of key sugar metabolism and transport genes, as well as the soluble carbohydrate content of fig fruits. The thesis concludes by pointing out the peculiarities NMR-based metabolomics in plant science and presenting prospects for the technique.

Česká
zemědělská
univerzita
v Praze